

University of Milano-Bicocca
School of Medicine and Surgery
PhD Program in Translational and Molecular Medicine
XXIX PhD course

Relevance of electrolytic balance in channelopathies.

Dr. Anna BINDA

Matr. 708721

Tutor: Dr.ssa Ilaria RIVOLTA

Coordinator: prof. Andrea BIONDI

Academic year 2015-2016

Table of contents

Chapter 1: introduction

Channelopathies.....	p. 7
Skeletal muscle channelopathies.....	p. 10
Neuromuscular junction channelopathies.....	p. 16
Neurological channelopathies.....	p. 17
Cardiac channelopathies.....	p. 26
Channelopathies of non-excitabile tissue.....	p. 35
Scope of the thesis.....	p. 44
References.....	p. 45

Chapter 2: SCN4A mutation as modifying factor of Myotonic Dystrophy Type 2 phenotype.....p. 51

Chapter 3: Functional characterization of a novel KCNJ2 mutation identified in an Autistic proband.....p. 79

Chapter 4: A Novel Copy Number Variant of GSTM3 in Patients with Brugada Syndrome.....p. 105

Chapter 5: Functional characterization of a mutation in KCNT1 gene related to non-familial Brugada Syndrome.....p. 143

Chapter 6: summary, conclusions and future perspectives....p.175

Chapter 1: introduction

Channelopathies.

The term “electrolyte” defines every substance that dissociates into ions in an aqueous solution and acquires the capacity to conduct electricity. Electrolytes have a central role in cellular physiology, in particular their correct balance between the intracellular compartment and the extracellular environment regulates physiological functions of both excitable and non-excitable cells, acting on cellular excitability, muscle contraction, neurotransmission and hormone release, signal transduction, ion and water homeostasis [1]. The most important electrolytes in the human organism are sodium, potassium, magnesium, phosphate, calcium and chloride. Every cells is able to control electrolytic balance thanks to specific ion channel proteins that selectively regulate electrolytes fluxes across cells membrane. While only a few ion channels are single protein, the majority of them are coassembly of homomeric or heteromeric subunits. Mechanisms as multiple promoters, alternative splicing, posttranslational modification and interaction with accessory proteins increase ion channel diversity. Electrolytic flux depends on ion channel conformation, that could typically switch, passing from an open to an inactivated closed (indicate also as “refractory period”) and a resting closed state (fig. 1) [2]. Gating mechanisms (opening and closing) of these membrane proteins differ based on the stimuli to which they respond, indeed ion channel conformational state could be modulated by changes in membrane voltage, by the binding of a ligand (hormones, neurotransmitters), by the activity of a second messenger (calcium,

cyclic nucleotides) or as a consequence of a physical (temperature, light) or a mechanical stimuli [1; 2].

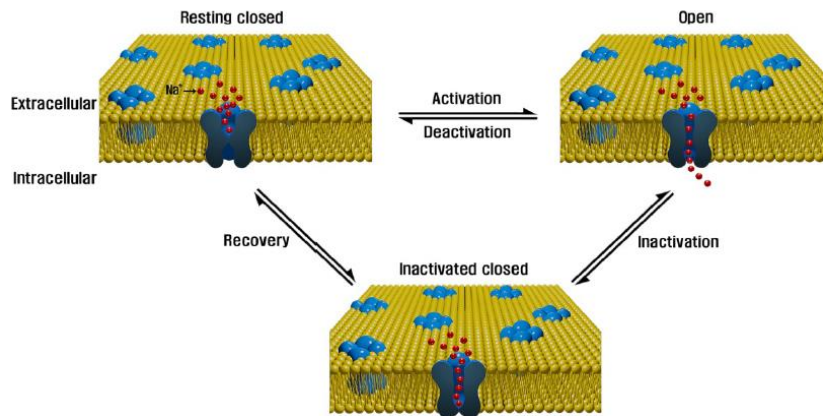


Fig. 1. Voltage-gated sodium channel is a typical channel whose conformation could fluctuate between three different states [2]. The activation process occurs in response to depolarization: the voltage across the plasma membrane becoming less negative inside respect to the outside of the cell, this leads to the opening of the channel and, consequently, let sodium ions enter the intracellular environment. Deactivation is the opposite process of the activation gate closing in response to the inside of the membrane becoming more negative. Inactivation happens when the inactivation gate closes during depolarization, so the open channel becomes non-conducting and ions passage is prevented. Finally, recovery is the opposite process of inactivation and it restores the channel in its close non-conducting state.

Disorders affecting ion channels resulting from genetic mutations are usually referred as “channelopathies” [3]. Considering that ion channels are expressed both on the plasma membrane and on the membrane of different organelles of all cells and that their activity is finely regulated by several interacting proteins, channelopathies are a huge group of heterogeneous diseases [2] ranging from relatively common to very rare ones [1]. Different factors, such as the type of

mutation and its functional consequences on channel activity, the cellular and subcellular localization of the channel isoform and channel oligomeric assembly, contribute to determine the symptoms of each channelopathy [4]. Furthermore, the range of clinical manifestations is complicated by the fact that some disease modifiers (age of the patient, life conditions, interplay of different genes, comorbidity) could interfere. All these aspects lead to both a genetic and a clinical variability that complicate a clear genotype-phenotype correlation, which is worsen by the fact that affected patients are overall rare [1]. Several authors struggled with channelopathies heterogeneity in order to identify criteria to improve classification. On the basis of their cause, channelopathies could be easily categorized as genetic type, a group assembling familiar forms, or acquired type, in which the disease could be a result of idiopathic disorders (auto antibodies), drugs or toxins administration [5]. Another possibility is to discriminate between “primary channelopathy”, if a mutation affects directly an ion channel, and “secondary channelopathy”, whether an ion channel interacting protein is mutated [3]. In the first case, the primary determinants of membrane excitability are directly involved in the pathogenesis of the disease because a loss- or a gain-of-function mutation in an ion channel subunit induces an alteration of the biophysical properties of the channel in terms of conductance, gating or ionic selectivity [6]. In the second case, ion channel activity is indirectly affected by defects in their transcriptional regulation, in their posttranslational modifications, in their trafficking and localization or in interacting proteins that regulate their functions [3].

Finally, channelopathies could also be divided considering the organ or the system in which pathophysiological clinical symptoms are prevalent.

Skeletal muscle channelopathies.

Skeletal muscle channelopathies were the first human pathologies linked to ion channel mutations [7]. Furthermore they were also the first diseases identified in the literature with the definition of “channelopathies” [8]. Since then, skeletal muscle channelopathies have been studied in depth, discovering a wide spectrum of various disorders compromising tissue physiological functions as the fidelity of neuromuscular transmission, the correct excitability of the muscle fiber (sarcolemma), the proper excitation-contraction coupling and calcium homeostasis [9]. The correct physiological functions of the skeletal muscle is ensured by the relationship between a motor neuron and its innervated muscle fiber. Resting membrane potential of the sarcolemma (approximately -80 mV) [5] is maintained at a constant voltage thanks to the balance of inward and outward transmembrane currents. The motor neuron activates the muscle fiber through the release of acetylcholine (ACh) that triggers an influx of cations (fig. 2). The following depolarization opens voltage-gated sodium channels carrying sodium inside the cytoplasm; as Na^+ ions continue to enter, cell membrane depolarizes till the “threshold potential” is reached and an action potential is generated [10]. Consequently, membrane rapidly depolarizes from its resting potential value to approximately +25 mV.

Voltage-gated sodium channels quickly inactivate while delayed rectifier potassium channels and high-chloride conductance channels open and repolarize membrane. The kinetics of recovery from inactivation of sodium channels defines the refractory period subsequent an action potential: a short period in which cell membrane is unexcitable [5].

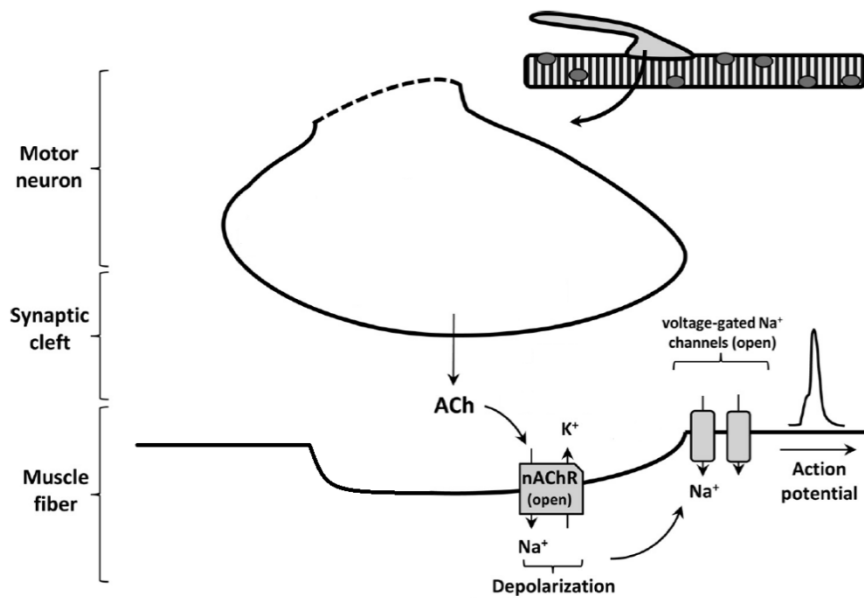


Fig. 2. Neuromuscular junction activation. Acetylcholine molecules released by the motor neuron bind their nicotinic receptors (nAChRs) on the sarcolemma. The opening of nAChRs allows cytoplasmic cations entry, which induces a membrane depolarization finally generating an action potential [adapted from 11].

Action potential propagation is bidirectionally, both axially along the surface of the sarcolemma and radially inward the interior of the fiber along the T-tubule system [10]. Radial propagation of the depolarization activates a signaling cascade starting with the change of calcium channels conformation and following with the activation of ryanodine receptors that release calcium from the sarcoplasmic reticulum. Increased cytoplasmic calcium concentration finally leads to sarcolemma contraction (fig. 3) [9].

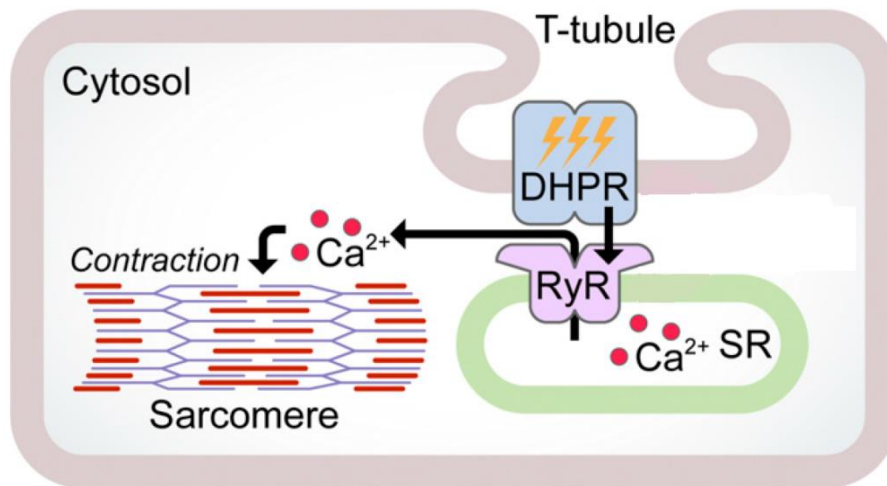


Fig. 3. Cytoplasmic signaling cascade of sarcolemma contraction. Following depolarization triggered by an action potential, the conformation of dihydropyridine receptors (DHPRs, calcium channels located in the plasma membrane) changes activating ryanodine receptors (RyRs) on the sarcoplasmic reticulum (SR). As a consequence, calcium passes from SR to the cytoplasm and it ultimately evokes sarcomere contraction [modified by 12].

Skeletal muscle channelopathies can result from mutations on any of the proteins expressed on the sarcolemma and involved in the mechanism just described. Most of the patients affected by a skeletal muscle channelopathy shows a familial form of disease, caused by either a loss- or a gain-of-function mutation [5]. These aberrations modify ion channel activity with a central role in the control of membrane excitability [13], notably clinical evidences are mainly apparent only in the skeletal muscle, leaving cardiac and neuronal functions undamaged [9]. Ion channel dysfunctions could be responsible for opposite clinical manifestations: uncontrolled repetitive muscle fiber discharges due to a general increase of membrane excitability manifest as muscle stiffness and hypertonia, referred as myotonia, on the other hand, muscle weakness resulting in transient paralysis episodes depends on a general fiber inexcitability [5; 14].

Primary channelopathies causing an increased sarcolemma excitability are linked to non-dystrophic forms of myotonia (NMD) that could manifest at the beginning on an effort and be alleviated (myotonia) or aggravated (paramyotonia) by the prolongation of it [14]. Muscle fibers of these patients typically show prolonged burst of action potentials generated by the sarcolemma itself without a proper stimulus from the motor neuron [9]. Genetic analysis associated NMD to mutations of CLCN1 gene (coding for the voltage-gated chloride channel ClC1), SCN4A gene (encoding the α pore-forming subunit of the sodium channel Nav1.4) or both genes [10]. In NMD patients, CLCN1 loss-of-function mutations may reduce skeletal muscle resting

chloride conductance that is physiologically controlled by CIC1 channels, while SCN4A gain-of-function mutations could lead to an increased tissue excitability due to altered mechanisms as an impaired inactivation or an enhanced activation. As a general consideration, myotonic dystrophy (DM), being the most common one among myotonic disorders, needs to be mentioned. Although DM is not usually considered a channelopathy, it should be noted that mutations of the dystrophiamyotonia protein kinase (DMPK) gene in patients affected by DM type 1 (DM1) and mutations of the zinc finger protein 9 (ZNF9) gene in patients affected by DM type 2 (DM2) induce defects in the processing of some mRNAs among which the one coding for the muscle chloride channels [15].

Periodic paralysis (PP) episodes manifest when resting membrane potential is unphysiologically depolarized, this condition consequently induces voltage-gated sodium channel inactivation, leading to a general situation of tissue inexcitability [9]. Based on serum potassium concentration during paralysis episodes, PP are classified as hypokalemic periodic paralysis (HypoPP) or hyperkalemic periodic paralysis (HyperPP), depending on whether potassium blood levels tends to be low or high respectively [14]. Sarcolemmal plasma membrane could be more prone to depolarization because of sodium, potassium or calcium conductance is altered. In particular, SCN4A mutations could modify Nav1.4 activity causing an increased or even a persistent inward Na^+ current, defects of inactivation or a hyperpolarized shift of activation. Loss-of-function alterations of inward rectifier potassium channel coding genes (KCNJ2, KCNJ18

and KCNJ5 coding for Kir2.1, Kir2.6 and Kir3.4 respectively) could reduce K^+ conductance at rest promoting depolarization events [9]. Finally it has been reported that missense substitution at arginine in the S4 segment within the voltage-sensor domains of Nav1.4 or of the dihydropyridine receptor Cav1.1 (gene CACNA1S) could generate an anomalous inward cationic current making muscle cells more sensitive to the paradoxically depolarizing effect of low extracellular potassium [10]. Interestingly, mixed NMD and PP syndromes have been reported [14] with patients suffering from fluctuating episodes of myotonia or paralysis (fig. 4) [9].

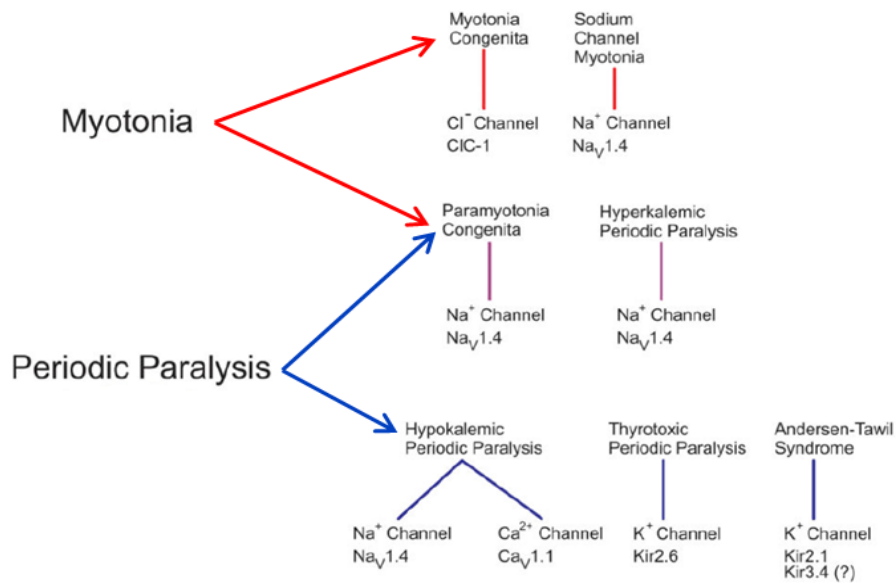


Fig. 4. Spectrum of skeletal muscle channelopathies [9]. Syndromes could be characterized by myotonic or periodic paralysis episodes or even a combination of both.

As previously reported, skeletal muscle channelopathies mainly affect muscle fiber functions because CIC1, Nav1.4 and Cav1.1 are specifically expressed in the sarcolemma. This is not true considering mutations on Kir channel encoding genes since they are expressed also in other tissues, so clinical manifestations may not be restricted to skeletal muscle. All the mutations are dominant except for CIC1 variations that are often recessive even if they could also have a dominant or a semi-dominant inheritance pattern [9].

Neuromuscular junction channelopathies.

Skeletal muscle functions could also be altered due to defects of neuromuscular junction physiological aspects [16]. Neuromuscular junction channelopathies are an heterogeneous group of disorders that includes inherited forms defined as congenital myasthenic syndromes (CMS) [17]. CMS patients might complain muscle fatigue and have block of synaptic transmission time or transmission itself [18]. The disease could be determined by mutations of proteins expressed at the level of presynaptic membrane (nerve), synaptic cleft or postsynaptic membrane (muscle end plate) in the neuromuscular junction [16]. CMS most common type is caused by mutations in the muscle nicotinic acetylcholine receptor (nAChR) [17], a ligand-gated cationic channel expressed on the sarcolemmal plasma membrane consisting of five subunits. AChRs change a little their stoichiometry during human life, indeed γ subunits are only expressed in the fetus, being substituted by ϵ subunits in adult receptor composition $(\alpha_1)_2\beta_1\delta\epsilon$. Each

subunit is characterized by a large extracellular N-domain that binds ACh molecules and by four transmembrane domains (M1-4) with M2 domains defining the pore region and the selectivity filter. The receptors is fully open after the binding of two ACh molecules and it closes when ligand dissociates. Otherwise, desensitization could happen whether ligand is not removed [19]. Mutations in any of the genes coding for adult subunits have been described (CHRNA1, CHRNB1, CHRND and CHRNE coding for α_1 , β_1 , δ and ϵ subunits respectively) and the diseases associated with them are divided in three groups, distinguishing between primary AChR deficiency, slow or fast channel syndromes. All variants are inherited with a recessive pattern except for the ones responsible for slow channel syndromes, that are dominant [17].

Neurological channelopathies.

In this paragraph “neurological channelopathies” are intended as the channelopathies affecting neurons. Neurological channelopathies could have an autoimmune or a genetic cause [20].

In the first case, autoantibodies against ligand-gated or voltage-gated channels are product by the organism itself. It seems that autoantibodies are directly pathogenic because they act reducing the expression or altering the function of receptors or ion channels located in the plasma membrane of neurons or glial cells [20]. Notably, this feature differentiates autoimmune neurological channelopathies from paraneoplastic neurological diseases, in which antibodies link

intracellular antigens, so they should not be directly pathogenic. Symptoms could be various based on which area of the nervous system is involved but they can manifest in patients of every ages [21]. Immunotherapies are useful [20] even if responses could be slow and some side effects could sometimes arise. In the future, a more specific therapy against B cells or plasma cells producing the autoantibodies should avoid these problems [21]. Up to now, autoantibodies against several targets have been identified such as voltage-gated calcium channels VGCC (in Lambert Eaton myasthenic syndrome and in cerebellar ataxia associated with VGCC antibodies), voltage-gated potassium channels VGKC (in acquired neuromyotonia, in Morvan's Syndrome, in limbic encephalitis and in forms of epilepsy and hyperekplexia), $\alpha 3$ ganglionic AChR (in autoimmune autonomic neuropathies), glutamate receptors (encephalitis associated with NMDA receptor or with AMPA receptor antibodies), gamma-aminobutyric acid (GABA) receptors (epilepsy associated with antibodies to GABA receptor) and aquaporin-4 (in neuromyelitis optica) [20].

Considering genetic neurological channelopathies, they typically cause episodic attacks among whose intervals neurological functions are usually normal as nervous system development is in general unaffected [22]. Moreover some pathologies may appear following an age-dependency with symptoms manifesting in specific phase of life, such as only childhood or only adulthood with onset from puberty [18]. In some patients, deficits could sometimes be resolved with time [17] while in some others they remain unfixed [22]. These disorders

are difficult to classify because of *locus heterogeneity*, meaning that various mutations on different genes determine similar phenotypes and because of *allelic heterogeneity*, which consists in distinct mutations of the same gene causing variable phenotypes [19]. Most of the neurological channelopathies currently known are inherited in an autosomal dominant fashion but heterogeneity is complicated by partial penetrance, interaction with other genes and environmental factors [22]. Ion channels in the nervous system are fundamental for the generation, the repression and the propagation of action potential, thus aberrations could severely affect tissue homeostasis but the comprehensive consequences depends on the specific neuronal circuitry involved (inhibitory or excitatory) [17]. In conclusion, mutations of ion channel genes expressed in the nervous system are extremely tricky to categorize and the most common phenotypes are epilepsy, migraine, movement disorders (cerebellar ataxia), disorders of peripheral nerve and autonomic functions (fig. 5) [22].

Epilepsies are quite widespread neurological disorders affecting around 3% of the world's population during lifetime [18]. Etiology could depend on various abnormalities, as metabolic brain disorders, abnormalities of cortical development, brain trauma or structural lesions of brain besides genetic causes [16]. Epileptic seizures arise from synchronized electrical discharge of neurons in the central nervous system (CNS) and symptoms could be different based on age of the patient, cause, brain region involved and seizure origin (focal or generalized) [18]. Disease heterogeneity makes difficult a complete understanding of the pathophysiological mechanisms at the basis of

seizures. Despite a remarkable number of genes associated to the different forms of pathology, next-generation sequencing techniques are continuously expanding the panel, improving diagnosis criteria.

Epilepsy and migraine

	Na ⁺	K ⁺	Ca ²⁺	GABA _A	Nicotinic
Epilepsy	<i>SCN1A</i>	<i>KCNQ2</i>	<i>CACNA1H</i>	<i>GABRA1</i>	<i>CHRNA2</i>
	<i>SCN1B</i>	<i>KCNQ3</i>		<i>GABRB3</i>	<i>CHNRA4</i>
	<i>SCN2A</i>	<i>KCNMA1</i>		<i>GABRG2</i>	<i>CHRN2</i>
Migraine	<i>SCN1A</i>		<i>CACNA1A</i>		

Cerebellar ataxia and excessive startle

	K ⁺	Ca ²⁺	Glycine
Ataxia	<i>KCNA1</i> <i>KCNC3</i>	<i>CACNA1A</i>	
Hyperreflexia			<i>GLRA1</i> <i>GLRB</i>

Peripheral nerve disorders

Pain Erythema	<i>SCN9A</i>
--------------------------------	--------------

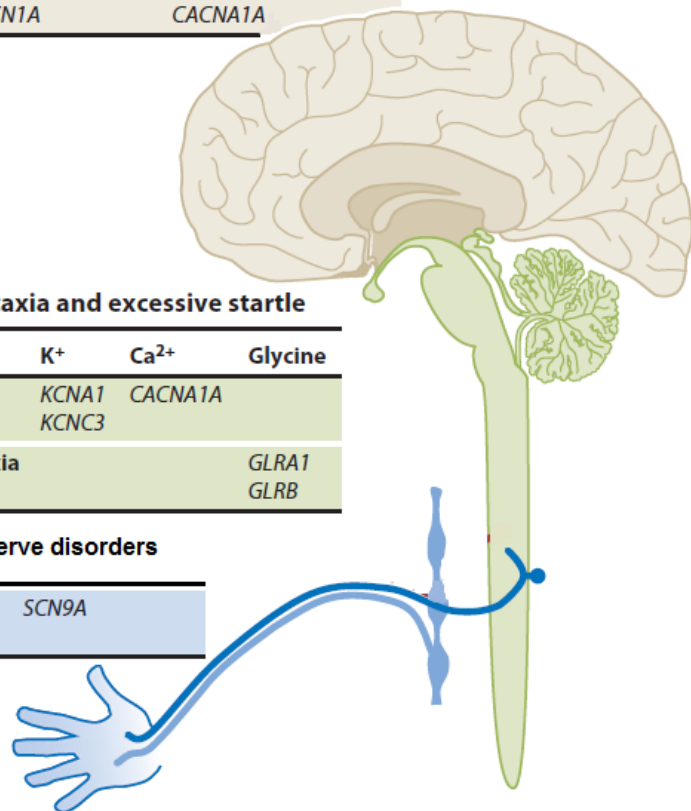


Fig. 5. Schematic representation of the main ion channel genes and manifestations involved in neurological channelopathies [modified from 22].

Up to now, mutations have been identified in genes encoding sodium, potassium and calcium channels, GABA and glutamate receptors (tab. 1) [23]. Furthermore, variants in genes that were not expected to be involved in epilepsies were also described, as single nucleotide polymorphisms were identified in the chloride channel genes CLCN1 and CLCN2 three times more frequently in epileptic patients than in controls [17].

Channel	Gene	Channel	Epilepsy syndrome(s)
Sodium	SCN1A	α subunit of $\text{Na}_v1.1$	Severe myoclonic epilepsy of infancy (SMEI) Intractable epilepsy with generalised tonic-clonic seizures (IEGTC) Migrating partial seizures of infancy (MPSI)
	SCN1B	β subunit of $\text{Na}_v1.1$	Generalised epilepsy with febrile seizures (GEFS+)
	SCN2A	$\alpha 2$ subunit of $\text{Na}_v1.2$	SMEI GEFS+ SMEI Ohtahara syndrome Benign familial neonatal infantile seizures (BFNS) West syndrome Infantile spasms GEFS+
	SCN3A SCN8A	$\alpha 3$ of $\text{Na}_v1.3$ $\alpha 8$ subunit of $\text{Na}_v1.6$	Partial epilepsy Infantile epileptic encephalopathy
	Potassium	KCNQ2	$\text{K}_v7.2$
KCNQ3 KCNA1		$\text{K}_v7.3$ Calcium-activated potassium BK (Big Potassium) channel	Benign familial neonatal convulsions Generalised epilepsy with paroxysmal movement disorder
KCNA1 KCNA2 KCND3		$\text{K}_v1.1$ $\text{K}_v1.2$ $\text{K}_v6.2$	Epilepsy with episodic ataxia Myoclonic epilepsy and ataxia Developmental delay, epilepsy and neonatal diabetes mellitus (DEND syndrome)
KCNT1		Sodium-activated potassium channel	MPSI
Calcium		CACNA1H CACNA1A	α subunit of t-type calcium channels $\text{Ca}_v2.1$ channel α subunit
	Acetylcholine receptor (AChR)	CHRNA4, CHRNA2, CHRNB2, CHRNB3	Subunits of nicotinic AChR receptor
GABA	GABRA1	α subunit of GABA receptor	Childhood absence epilepsy Idiopathic generalised epilepsy (IGE) Juvenile myoclonic epilepsy (JME) Infantile spasms, Lennox-Gastaut
	GABRB2 GABRB3	$\beta 2$ subunit of the GABA receptor $\beta 3$ subunit of GABA receptor	Infantile spasms, Lennox-Gastaut Absence epilepsy Infantile spasms, Lennox-Gastaut
	GABRD	δ subunit of GABA receptor	GEFS+ JME
	GABRG2	$\gamma 2$ subunit of GABA receptor	GEFS+ SMEI Childhood absence epilepsy IGE

Tab. 1. Epilepsy syndromes caused by inherited mutations in ion channel genes [17].

Migraine due to ion channel malfunctioning is usually linked to autosomal inherited mutations [22] and it can manifest with or without aura. Studying models of migraine with aura, results showed that pathogenesis depends on cortical spreading depression consisting of an initial rapid spike of increased neuronal activity followed by long-lasting suppression of excitability spreading across the cortex. In particular, depression wave is correlated with long-lasting depolarization and variations in ion channel concentrations [18]. Familial hemiplegic migraine (FHM) is likely the most studied type. FHM affected patients could suffer from severe aura, visual, somatosensory or dysphasic symptoms previous or during migrainous headache [17]. Based on the genetic determinant, FHM are classified in three subtypes. FHM1 patients carry gain-of-function mutations in CACNA1A gene encoding the pore-forming $\alpha 1$ subunit of the P/Q calcium channel Cav2.1. These channels are expressed at synapses both in the CNS and in the peripheral nervous system (PNS), FHM1 mutations increased current density in cerebellar neurons enhancing neurotransmitter release. Loss-of-function mutations in ATP1A2 gene have been described in FHM2 subtype, which is controversially enclosed between channelopathies. The gene encodes the $\alpha 2$ subunit of the Na^+/K^+ ATPase3 that has a role in the maintenance of transmembrane ion gradients. FHM3 is associated to heterozygous mutations in SCN1A gene coding for the neuronal voltage-gated sodium $\alpha 1$ channel subunit, Nav1.1. Pathogenesis of FHM3 patients is less understood since some patients present also seizures, suggesting

an eventual close relationship between these migraine and epilepsy [17; 18].

Cerebellar dysfunctions are present in episodic ataxia (EA, counting two subtypes EA1 and EA2) and in spinocerebellar ataxia (SCA). In EA1 patients, missense mutations were found in KCNA1 gene encoding the neuronal voltage-gated delayed rectifier potassium channel Kv1.1, which controls axon excitability both in the CNS and in the PNS, while in EA2 forms non-sense, frame shift, splice site and missense mutations were described on CACNA1A gene associated to reduced calcium current or folding and trafficking modifications. Mutations of CACNA1A gene or of voltage-gated potassium channel genes KCNC3 and KCND3 are instead described in SCA patients, in which symptoms are usually not episodic but progressive. KCNC3 gene encodes the cerebellar expressed Kv3.3 channel that is implicated in fast repolarization of neurons during high frequency repetitive firing. KCND3 gene codes for another cerebellar expressed potassium channel (Kv4.3) whose functions have not been completely defined even if mutations seem to produce trafficking alteration [17]. Hyperekplexia is a rare disorder characterized by neonatal hypertonia, hyper-reflexia, myoclonic jerks and excessive startle response to acoustic, visual or other stimuli. Mutations mostly affect genes encoding subunits of the hetero-pentameric postsynaptic glycine receptor chloride channel (GlyR). The α subunit coding for GLRA1 gene is involved in about 80% of the total familial forms of disease, mutations of the β subunit encoding gene GLRB are also described. GlyRs control the fast-response, inhibitory glycinergic

neurotransmission in the brainstem and spinal cord, hyperekplexia patients have generally increased excitability in pontomedullary reticular neurons and abnormal spinal reciprocal inhibition [17; 18]. Mutations are indeed loss-of-function inherited in an autosomal dominant or recessive fashion [19]. Hyperekplexia could also be rarely caused by mutations in presynaptic glycine transporter type 2 (SLC6A5) gene [17].

Finally, pain syndromes and neuropathies could be caused by ion channelopathies resulting in either absence of or hypersensitivity to painful stimuli [16]. Nociception is guaranteed by both ligand- and voltage-gated channels whose physiological roles could be modified in presence of mutations. Variations of genes encoding voltage-dependent sodium (Nav1.7, Nav 1.9) or potassium channels (Kv1.1, Kv7.2) and non-selective cationic channels (TRP 1, TRPV4) have been identified (tab. 2) [17]. In particular, several mutations have been found in SCN9A gene that codes for α subunit of Nav1.7 channels expressed in dorsal root ganglion neurons where they regulate excitability of pain fibers. SCN9A autosomal dominant gain-of-function mutations could lower the voltage threshold for sodium current, as it happens in primary erythromelalgia, or could determine impaired channel fast inactivation or persistent current, as it happens in paroxysmal extreme pain disorder. However, both modifications induce an increased action potential firing frequency, clinically manifesting with an enhanced sensitivity to pain. On the other hand, autosomal recessive loss-of-function mutations produce non-functional channel expression, preventing a normally reaction to

painful stimuli in the patients, for example in congenital insensitivity to pain or in hereditary sensory and autonomic neuropathy type IID [17; 18]. Some patients affected by familial neuropathies (Charcot-Marie-Tooth disease type IIC, scapuloperoneal spinal muscular atrophy and congenital distal spinal muscular atrophy) present severe motor dysfunctions. Gene TRPV4 is involved, both gain-of- and loss-of-function mutations are reported but disease mechanisms are not yet completely understood. An impaired muscle activity is also common in peripheral nerve hyperexcitability, which is usually included in EA1 phenotypes. Mutations in potassium channels gene have been associated to these disorders [17].

Peripheral nerve channelopathies				
Pain	Painful syndromes	Primary Erythromelalgia	Nav1.7	SCN9A
		Paroxysmal extreme pain disorder	Nav1.7	SCN9A
		Familial episodic pain syndrome	TRP 1	TRPA1
	Nav1.9		SCN11A	
	Insensitivity to pain	Congenital insensitivity to pain	Nav1.7	SCN9A
			Nav1.9	SCN11A
Neuropathies Motor and sensory neuropathies	HSMNIIC		TRPV4	TRPV4 channel
	Scapuloperoneal SMA			
	Congenital Distal SMA			
	HSANIID		Nav1.7	SCN9A
Peripheral Nerve Hyperexcitability	EA1		Kv1.1	KCNC1
			Kv7.2	KCNQ2

Tab. 2. Pain syndromes and neuropathies caused by mutations in ion channel genes (HSMNIIC = Charcot-Marie-Tooth disease type IIC; SMA = spinal muscular atrophy; HSANIID = hereditary sensory and autonomic neuropathy type IID; EA1 = episodic ataxia type 1) [17].

Cardiac channelopathies.

Cardiac channelopathies, also termed as inherited arrhythmias, are primary cardiac electric diseases caused by dysfunctional ion channels involved in the cardiac action potential and its conduction [24]. Disorders can be either not symptomatic or manifest as life-threatening arrhythmogenesis, syncope or sudden cardiac death. Affected patients usually have a normally structured heart and their electrocardiogram (ECG) may or may not show any changes, both features could complicate a correct diagnosis [25]. ECG is the recording of heart electrical activity obtained through the application of electrodes on the body surface. Electrical phenomena in the different parts of the heart are shown in a normal ECG as the typical P-Q-R-S-T complexes (fig. 6), however ECG shape could vary depending on where electrodes are placed, thus locations have been standardized. Autonomously depolarization of sinus node cells that starts cardiac electrical activity is seen as P wave. Therefore action potentials propagate exciting firstly the electrically-active cells in the atrio-ventricular node, then in His bundle and in Purkinje fiber finally stimulating myocardium contraction. These electrical phenomena shape QRS complex while the latter ventricular repolarization is responsible for T-wave [26].

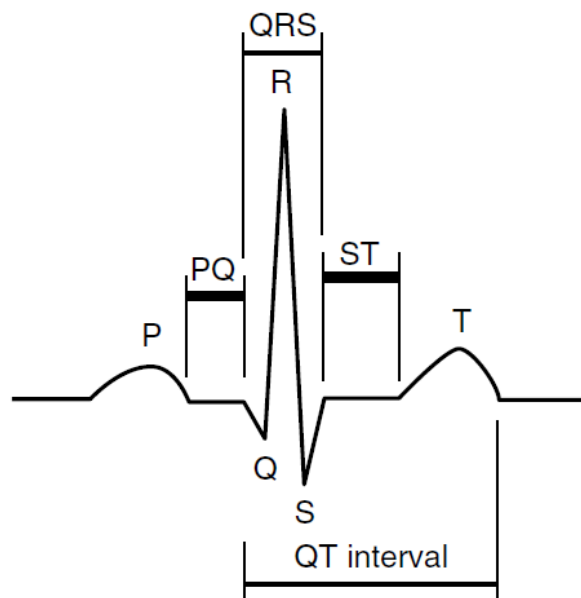


Fig. 6. P-Q-R-S-T complex of a normal heart [adapted from 26].

Cardiac ion channel abnormalities could depend both on mutations in genes encoding the proteins themselves and in genes encoding ion channel accessory proteins [27]. Although some of them are autosomal recessively transmitted, mutations involved in inherited arrhythmias are mainly autosomal dominant [24]; heterogeneity is complicated by genetic or environmental modifiers and by variable expression and incomplete phenotype observed in members of affected families [25]. Whole exome sequencing techniques are considerably improving the panel of genes involved in the pathogenesis of cardiac channelopathies [27], redefining diagnosis criteria, allowing pre-symptomatic identification of individuals at risk and ameliorating prognosis [28]. Unfortunately, despite the enormous

progresses, an important part of familial arrhythmias could not benefit of a genetic diagnosis [25]. In general, aberrant sodium, potassium or calcium currents linked to mutated ion channels expressed in the plasma membrane of cardiac cells (myocytes) could cause cardiac defective activity inducing arrhythmogenesis (fig. 7) [25]. The major cardiac channelopathies are long QT syndrome (LQTS), short QT syndrome (SQTS), Brugada syndrome (BrS), and catecholaminergic polymorphic ventricular tachycardia (CPVT) (tab. 3) [29].

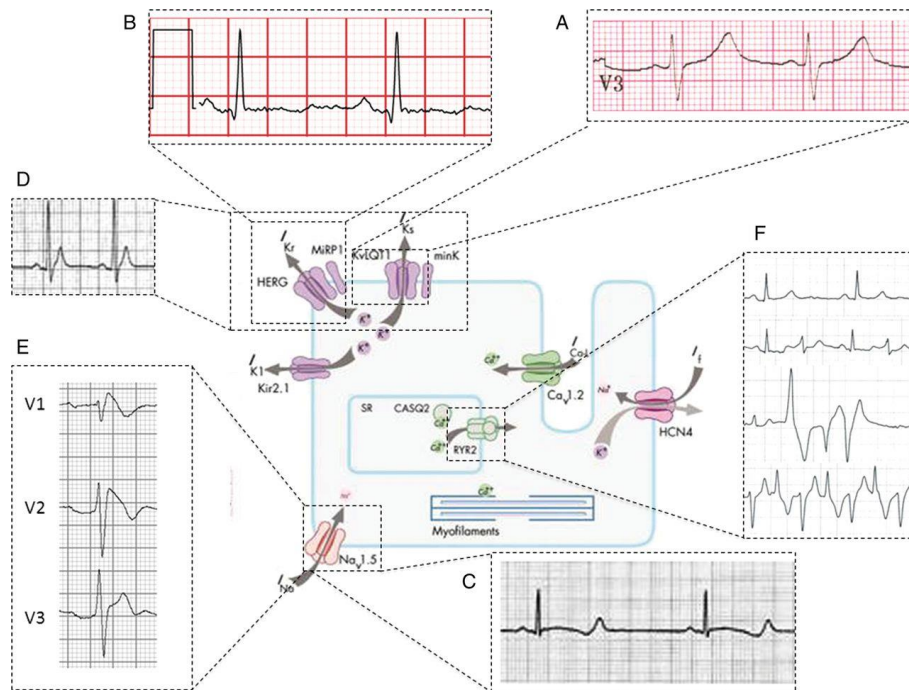


Fig. 7. Characteristic ECGs of the various cardiac channelopathies and the main cardiac ion channels involved in inherited ion channel diseases. Loss-of-function mutations in KCNQ1 and KCNH2 lead to LQTS1 (A) and LQTS2 (B), respectively. Gain-of-function mutations in KCNQ1 or KCNH2 lead to SQTS (D). Gain-of-function mutations in SCN5A lead to LQTS3 (C), loss-of-function mutations lead to BrS (E). Loss-of-function mutations in RYR2 lead to CPVT (F) [28].

Channel	Disease	Inheritance	Gene	Protein
Sodium	LQT 3	AD	<i>SCN5A</i>	Nav1.5
	LQT 10	AD	<i>SCN4B</i>	Navβ ₄
	LQT 17	AD	<i>SCN1B</i>	Navβ ₁
	BrS 1	AD	<i>SCN5A</i>	Nav1.5
	BrS 2	AD	<i>GPD1-L</i>	Glycerol-3-P-DH-1
	BrS 5	AD	<i>SCN1B</i>	Navβ ₁
	BrS 7	AD	<i>SCN3B</i>	Navβ ₃
	BrS 16	AD	<i>SCN2B</i>	Navβ ₂
	Br S 17	AD	<i>SCN10A</i>	Navβ
	BrS 19	AD	<i>PKP2</i>	Plakophilin-2
Sodium-associated	LQT 9	AD	<i>CAV3</i>	M-Caveolin
	LQT 12	AD	<i>SNTA1</i>	α-Syntrophin
	BrS 10	AD	<i>RANGRF</i>	RAN-G-release factor (MOG1)
	BrS 14	AD	<i>SLMAP</i>	Sarcolemma associated protein
Potassium	LQT 1	AD/AR	<i>KCNQ1</i>	Kv7.1 hERG/Kv11.1
	LQT 2	AD	<i>KCNQ2</i>	MinK
	LQT 5	AD/AR	<i>KCNE1</i>	MiRP1
	LQT 6	AD	<i>KCNE2</i>	Kv2.1/Kir2.1
	LQT 7	AD	<i>KCNJ5</i>	Kv3.4/Kir3.4
	LQT 13	AD	<i>KCNH2</i>	hERG/Kv11.1
	SQT 2	AD	<i>KCNQ1</i>	Kv7.1
	SQT 3	AD	<i>KCNJ2</i>	Kv2.1/Kir2.1
	BrS 6	AD	<i>KCNE3</i>	MiRP2
	BrS 8	AD	<i>KCNJ8</i>	Kv6.1/Kir6.1
	BrS 9	AD	<i>HCN4</i>	Hyperpolarization cyclic nucleotide-gated 4
	BrS 11	AD	<i>KCNE5</i>	Potassium voltage-gated channel subfamily E member1 like
	BrS 12	AD	<i>KCND3</i>	Kv4.3/Kir4.3
	CPVT 3	Sex-related	<i>KCNJ2</i>	Kv2.1/Kir2.1
	Potassium-associated	LQT 11	AD	<i>AKAP9</i>
BrS 18		AD	<i>ABCC9</i>	ATP-binding cassette transporter of IK-ATP (SUR2A)
Calcium	BrS 3/SQT 4	AD	<i>CACNA1C</i>	Cav1.2
	BrS 4/SQT 5	AD	<i>CACNB2B</i>	Voltage-dependent β-2
	BrS 13	AD	<i>CACNA2D1</i>	Voltage-dependent α ₂ /δ ₁
	BrS 15	AD	<i>TRPM4</i>	Transient receptor potential M ₄
	SQT 6	AD	<i>CACNA2D1</i>	Voltage-dependent α ₂ /δ ₁
	LQT 8	AD	<i>CACNA1C</i>	Cav1.2
	LQT 14	AD	<i>RYR2</i>	Ryanodine Receptor 2
	LQT 15	AD	<i>CALM1</i>	Calmodulin 1
	LQT 16	AD	<i>CALM2</i>	Calmodulin 2
	CPVT 1	AD	<i>RYR2</i>	Ryanodine Receptor 2
	CPVT 2	AR	<i>CASQ2</i>	Calsequestrin 2
Calcium-associated	LQT 4	AD	<i>ANK2</i>	Ank-B
	CPVT 4	AR	<i>TRDN</i>	Triadin
	CPVT 5	AD	<i>CALM1</i>	Calmodulin 1

Tab. 3. Main ion channels and associated proteins related to inherited arrhythmias (AD = autosomic dominant; AR = autosomic recessive). Some genes could be involved in the pathogenesis of different cardiac channelopathies [25].

LQTS disorders, the most common cardiac channelopathies [29], are characterized by a longer QT interval (≥ 450 ms) on ECG, depending on either increased depolarizing currents or on a delayed reduced cardiac repolarization [30]. Up to now, more than 600 genetic alterations have been reported [25] with the majority of them being inherited with an autosomal dominant pattern [29]. Despite several genetically distinct LQTS types have been described, almost 90% of the identified mutations locates in three genes: KCNQ1 (encoding the α subunit of the voltage-gated potassium channel Kv7.1), KCNH2 (encoding the α subunit of the voltage-gated potassium channel Kv11.1) and SCN5A (encoding the voltage-gated sodium channel Nav1.5) causing LQTS1, LQTS2, and LQTS3 respectively [28]. In particular, alterations in genes coding for potassium channels are loss-of-function mutations that reduce potassium repolarizing currents, while SCN5A gain-of-function mutations increase the late inward Nav1.5 current that slows cardiac repolarization. Both groups of aberrations result in a prolonged QT interval [27]. However some patients carry mutations on less common genes, as for example variants on KCNJ5 gene, encoding an inward rectifier potassium channel Kir3.4, that decreases protein membrane expression or on genes coding for β subunits isoforms of cardiac sodium channels, which cause a negative change in the sodium dependent voltage in the activation of the channel [25; 27]. Aberrant structural proteins could also be involved. Mutations on caveolin-3 (CAV3 gene) or α 1-syntrophin (SNTA1 gene) increase Nav1.5 late inward current, on kinase-anchor protein-9 (AKAP9 gene) reduce potassium delayed

currents, on L-type calcium channel (CACNA1C gene) augment the depolarizing calcium current physiologically involved in the prolongation of the plateau phase within the cardiac action potential and on calmodulin-1 and -2 (CALM1 and CALM2 gene respectively, both expressed in the left ventricle) seem to prolong repolarization by more than one mechanism [27].

SQTS is a group of rare heterogeneous disorders characterized by a shortening of the QT interval (≤ 330 ms) on the ECG and an increased risk of atrial or ventricular fibrillation predisposing to sudden cardiac death [28]. These characteristics make of SQTS the severest form among inherited arrhythmias with clinical manifestations that usually happen during rest, sleep or exertion [29]. Reduced QT interval could depend on an increased dispersion of repolarization or on a reduced activity of depolarizing currents [30]. Familial forms of these disorders have been linked to autosomal dominant gain-of-function mutations on gene encoding potassium channels (KCNQ1, KCNH2 and KCNJ2 coding for the α -subunit of the inward rectifier Kir2.1) or autosomal dominant loss-of-function mutations on gene encoding calcium channels (CACNA1C, CACNB2 and CACNA2D1) [27]. Variants on KCNQ1, KCNH2 and KCNJ2 genes are associated to SQTS type 1, 2 and 3 respectively, all of them induce increased potassium repolarizing currents that consequently shorten action potentials [25]. SQTS type 4, 5 and 6 are instead linked to mutations on genes encoding L-type calcium channel subunits that cause a reduction of depolarizing currents. These patients are characterized by a shorter QT interval and by a precordial ST elevation reminiscent of

BrS. Because BrS is the dominant phenotype, it is generally believed that they should be classified as such [27].

BrS is a rare inherited cardiac channelopathy whose affected patients may suffer syncope, ventricular fibrillation or tachycardia linked to high risk for sudden cardiac death and their ECG is generally characterized by the presence of an ST elevation in leads V1-V3 [31]. ST elevation, also referred as J wave, is a positive deflection at the end of the QRS complex [32] and two different patterns could be recognized in BrS patients based on this particular feature. The so called “coved type” could be seen in BrS type 1, in these cases, J wave is followed by an inverted negative T wave. On the other hand, in BrS type 2 and 3, also denoted as “saddle-back type”, ST segment, with or without elevation, remains at least 0.5 mm above the isoelectric baseline and then generate a positive or a biphasic T wave [27; 33]. The majority of BrS patients lacks of a genetic diagnosis, indeed pathogenic altered genes have been found with an autosomal dominant inheritance only in almost 30-35% of clinically diagnosed cases. Moreover it is believed that about 25-30% of familial BrS forms are associated with loss-of-function mutations in SCN5A gene, that codes for the sodium channel Nav1.5 responsible for phase 0 of cardiac action potential. Other aberrations were found in genes encoding sodium channel regulating proteins, as SCN1B, SCN2B and SCN3B (encoding Nav1.5 β subunits), SCN10A and GPD1-L (encoding Nav1.8 and glycerol-3-phosphate dehydrogenase 1-like respectively), both with a modulating role on Nav1.5 membrane expression and function, or RAN guanine nucleotide release factor

and sarcolemmal membrane-associated protein encoding genes (RANGRF and SLMAP respectively) that physiologically control Nav1.5 trafficking. Potassium channels could sometimes be altered. Gain-of-function mutations in several genes were described: KCNKE3, KCNE5, KCNJ8, KCND3 and HCN4 coding for acid-sensitive potassium channel protein TASK-1, potassium channel subunit β MiRP4, potassium inwardly rectifying channel Kir6.1, voltage-gated potassium channel Kv4.3 and hyperpolarization-activated cyclic nucleotide-gated potassium channel 4 respectively. Genes encoding potassium channels modulating proteins could also be involved: aberrant MiRP2 proteins (KCNE3 gene) were linked to altered modulation of transient outward current I_{to} in the human heart. Finally, calcium homeostasis could be involved in the pathogenesis of BrS. This group includes variations on L-type calcium channel subunits, previously discussed concerning SQTs disorders, and on TRPM4 gene encoding transient receptor potential melastatin protein 4, that is a calcium-activated nonselective cation channel with a role in conduction block [34]. Etiology of BrS is not yet completely understood and three different theories are currently available: the depolarization theory, the repolarization theory and the neural crest theory. The first one is related to sodium channel mutations that cause slow conduction and predispose to electrical reentry. The second theory is consistent with calcium or potassium current alterations that exaggerate phase 1 notch in the epicardium, shorten action potentials and favor transmural dispersion of repolarization leading to phase 2 reentry. The last theory suggests that an abnormal expression of

cardiac neural crest cells in the right ventricular outflow cause an abnormal connexin expression (Cx43) promoting arrhythmias. Anyway, no theory seems to be exhaustive, so discussion about pathophysiology of the disease is still open [27; 35].

CPVT is a rare cardiac channelopathy in which adrenaline-driven bi-directional and polymorphic ventricular arrhythmias lead to sudden cardiac death [25]. ECG at rest is usually regular and heart is prevalently structurally and functionally normal, ventricular arrhythmias tend to manifest with physical exercise or emotional stress events. Symptoms often appear in childhood or adolescence [29]. Impaired calcium and potassium currents were observed in familial CPVT forms. Concerning calcium homeostasis, aberrant proteins cause an increased calcium outflow from sarcoplasmic reticulum during the plateau of action potential, consequently altering sarcolemmal membrane potential towards late depolarization [25]. Almost 60% of cases (CPVT1 type) present both autosomal dominant and recessive mutations on gene encoding ryanodine receptor/ Ca^{2+} release channel RyR2, which is located on the sarcoplasmic reticulum and whose role is crucial for cardiac muscle contraction [27]. Other CPVT types are associated to alterations on calcium homeostasis impairments, patients could carry mutations on CASQ2 gene, coding for calsequestrin, the major Ca^{2+} binding protein in the sarcoplasmic reticulum, CALM-1 gene or TRDN gene, encoding triadin, an integral membrane protein involved in anchoring calsequestrin to the junctional sarcoplasmic reticulum and allowing its functional coupling

with RyR2 [25]. Finally, potassium balance could also be altered, in particular, mutations on KCNJ2 gene could cause CPVT type 3 [29].

Channelopathies of non-excitables tissues.

Ion channel activities are fundamental not only in excitable but also in non-excitables tissues where they physiologically control endocrine secretions, transepithelial transport of salt and water, intracellular signaling and functions of intracellular organelles [36]. Thus, channelopathies are not a prerogative of skeletal muscle, brain and heart but they could also condition respiratory, endocrine and renal systems and the gastro-intestinal tract.

Respiratory system is composed by two types of airways: the conducting and the respiratory ones. Both of them are covered by an aqueous film defined as airway surface liquid or alveolar lining fluid whose function is to favor the convective movement of fluid up the airways for the bacterial mucociliary clearance and to prevent alveoli from collapsing [37]. Ion channels strictly regulate epithelium-based hydroelectrolytic secretions and intracellular Ca^{2+} levels that are involved in the activation of resident and circulating lung cells [38]. Despite it could be classified as a systemic disease, the most studied channelopathy of the respiratory system is probably cystic fibrosis (CF), whose patients may suffer from severe and chronic pulmonary infections, ultimately leading to irreversible airway damage and respiratory failure. The disease is caused by mutations on cystic fibrosis transmembrane conductance regulator (CFTR) gene encoding

chloride channels that contribute to the control of the volume of liquid on epithelial surface through chloride secretion and sodium absorption inhibition [2]. Up to now, more than 2000 CFTR variants have been described. Mutations are inherited following an autosomal recessive pattern and could be sub classified based on their functional consequences (tab. 4) [39].

CF type	I	II	III	IV	V	VI
CFTR defects	No functional CFTR protein	CFTR trafficking defect	Defective channel regulation	Decreased channel conductance	Reduced synthesis of CFTR	Decreased CFTR stability
Type of mutations	Nonsense, frameshift or canonical splice	Missense, aminoacid deletion	Missense, aminoacid change	Missense, aminoacid change	Splicing defect, missense	Missense, aminoacid change

Tab. 4. CFTR mutations could be divided in six classes based on their functional consequences [39].

Ion channel deficits are also studied in asthma, an inflammatory disorder of the conducting airways linked to bronchial hyper-responsiveness. Several ion channels are expressed by the different cells implicated in the disease which are epithelial, airway smooth muscle (ASM) and immune cells. Recently, sensory channels of nerves that innervate lungs are gaining interest because of their control on central aspects of airways physiology (gland secretions, epithelial transport, vessel dilation and ASM contraction) [38]. All lung cells are activated by an increase of intracellular calcium concentration, thus an

altered cytoplasmic calcium homeostasis seems to biochemically trigger asthma. Studies described several mutations in genes encoding proteins which could be involved in the pathogenesis of the disease because of their roles in calcium homeostasis, as gene coding for TRP cationic channels, ORMDL3 (encoding for a calcium regulating protein located on the endoplasmic reticulum) and AT2A2 (encoding sarco/endoplasmic reticulum Ca^{2+} -ATPase 2). Furthermore, some respiratory symptoms could appear when a channelopathy, mainly affecting another system, becomes severe, as it could happens for example considering life-threatening respiratory insufficiency in hypokalemic periodic paralysis, in congenital myasthenic syndrome or in long QT syndrome [2].

A huge number of channelopathies of the endocrine systems have been identified, since endocrine cells physiologically exploit ion channel electrical activity to coordinate their functions. Considering pancreatic β cells, aberrant inwardly-rectifier adenosine triphosphate-sensitive potassium (K_{ATP}) channels could cause various disorders of insulin secretion. In neonatal diabetes mellitus, gain-of-function mutations in genes encoding for K_{ATP} channel subunits SUR1 and Kir6.2 (gene ABCC8 and KCNJ11 respectively) maintain the channel in its open state leading to an increased channel activity that consequently reduces insulin secretion. The same genes could also carry loss-of-function mutations that conversely decrease channel activity and increase insulin secretion, a condition that could be observed in hyperinsulinemic hypoglycemia [2]. Another endocrine channelopathy is primary aldosteronism, one of the most common

causes of secondary hypertension, characterized by a massive overproduction of the mineralocorticoid hormone aldosterone by adrenal glands. In some familial forms of the disease, mutations on genes encoding ion channels have been found, such as on KCNJ5 (coding for inwardly-rectifying potassium channel Kir3.4), ATP1A1 (coding for $\alpha 1$ subunit of Na^+/K^+ ATPase), ATP2B3 (encoding plasma membrane calcium transporter ATPase 3), CACNA1D (coding for the $\alpha 1$ subunit of L-type voltage calcium channel Cav1.3), CACNA1H (encoding $\alpha 1$ subunit of the T-type voltage calcium channel Cav3.2) [40]. Among these variations, gain-of-function mutations on KCNJ5 gene are particularly interesting as they have been linked both to inherited and acquired forms of primary aldosteronism. Mutations are expected to cause a loss of selectivity of potassium conductance shifting to an increase of sodium conductance, cytoplasmic membrane consequently tends to depolarize and aldosterone is secreted [2]. Endocrine channelopathies could sometimes induce bone disease, as it happens in osteopetrosis, a rare genetic disease characterized by an impairment of the activity of osteoclasts, that are responsible for bone remodeling through the dissolution of bone mineral and the degradation of organic matrix. Familial forms of osteopetrosis could be either autosomal dominant (ADO) or autosomal recessive (ARO). Almost 70% of ADO type II patients carry an heterozygous dominant negative mutation on CLCN7 gene, encoding voltage-gated chloride channel 7 (ClC-7) that provides chloride conductance necessary for extracellular acidification during bone reabsorption. CLCN7 loss-of-function mutations were identified also in ARO patients, in addition to

mutations on genes associated to CIC-7 protein, such as OSTM1 coding for CIC-7 auxiliary β subunit and to genes coding for other ion channels, such as TCIRG1 encoding the $\alpha 3$ subunit of the proton pump V-ATPase [41].

Thinking about functions of the kidney, it is easy to imagine that renal channelopathies are an extensive and heterogeneous group of diseases, whose functional consequences depend on where affected channel is expressed along the nephron (fig. 8).

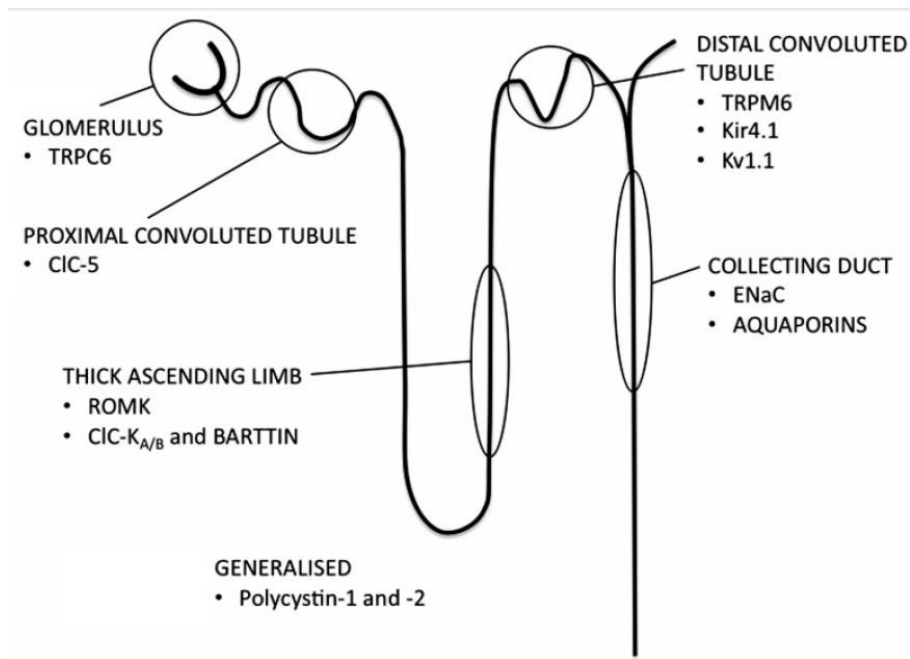


Fig. 8. Renal channelopathies could impair several functions according on their expression along the nephron [36].

Several renal channelopathies are well characterized. Among them, one of the most common pathology is autosomal dominant polycystic kidney disease (ADPKD), a generalized renal disorder characterized by progressive renal cyst formation and caused by mutations in PDK1 or PDK2 gene, encoding polycystin 1 or 2 and responsible for about 85% and 15% of ADPK forms respectively. PDK1 encodes polycystin 1, a protein located in the plasma membrane that interact with other associated proteins, among which there is polycystin 2 (also known as TRPP2), a non-selective cationic calcium permeable channel that is located not only in the cytoplasmic membrane but also in organelles membrane. Although etiology of the disease is still unclear, it has been demonstrated that gain-of-function PDK2 mutations lead to a major calcium influx due to increased channel activity. Different cationic channels of the TRP family are expressed throughout the nephron. TRPC6 is a calcium-permeable cation channel expressed in podocytes (glomerular epithelial cells) with a role in the regulation of intracellular calcium signaling. TRPC6 gain-of-function mutations have been associated to autosomal dominant form of focal and segmental glomerulosclerosis. In particular, aberrant channels are characterized by an increased activity leading to enhanced calcium influx due to either imbalanced gating property or major plasma membrane expression. TRPM6 gene instead codes for TRPM6 cationic channel expressed in the distal convoluted tubule that is permeable both to magnesium and calcium, TRPM6 alterations are indeed described in familial forms of hypomagnesemia with secondary hypocalcemia (HSH). Loss-of-function mutations,

generally resulting in absence of protein expression, are inherited by the patients following an autosomal recessive fashion. Deficits on ion transporters expressed in the thick ascending limb result in some forms of Bartter syndrome, a disease in which symptoms as metabolic alkalosis, hypokalemia, hyperreninemia and hyperaldosteronemia could appear with different levels of severity. Loss-of-function mutations in gene *KCNJ1*, encoding inwardly rectifying potassium channel, Kir1.1 (also known as renal outer-medullary K⁺ channel ROMK) are described in Bartter syndrome type 2 patients. Functional consequences could vary, leading to the production of a non-functional truncated protein, to an imbalanced protein trafficking or to the expression of a protein with altered regulatory regions. Bartter syndrome type 3 and type 4 are related to modifications in gene *CLCNKB* and *BSND*, encoding the chloride channel ClC-Kb and its β subunit barttin respectively. Furthermore barttin could assemble with another kidney chloride channel, ClC-Ka, both heteromeric complexes are involved in renal salt reabsorption. Moreover impaired chloride homeostasis is also a feature of Dent disease, in which imbalance depends on alterations on *CLCN5* gene, which codes for the voltage-gated chloride channel ClC-5 and is mainly expressed in the proximal convoluted tubule. In general, these mutations produce a truncated protein with no remaining activity. Considering distal tubule disorders, they include not only TRPM6-dependent HSH but also dysfunctions of Kir4.1 and Kv1.1 potassium channels. *KCNJ10* encodes the ATP-sensitive inward rectifier potassium channel Kir4.1 that has a role in the regulation of voltage membrane and in magnesium transport, thus

KCNJ10 mutations could cause hypomagnesaemia because of aberrant proteins could lack of function or be characterized by a reduced plasma membrane expression, an uncorrect folding, an altered pH sensitivity or a non-physiological pore gating. Hypomagnesaemia could also depend on KCNA1 autosomal dominant mutations resulting in non-functional voltage-gated potassium Kv1.1 channel, that contribute to TRPM6 activity aimed to magnesium reabsorption. Finally, mutations in genes encoding ion channels expressed in the collecting duct could also cause renal channelopathies. Epithelial sodium channels (EnaC), heteromultimeric channels composed of three subunits (α , β , and γ encoded by SCNN1A, SCNN1B and SCNN1G gene respectively), are expressed in the apical membrane of epithelial cells mainly in the kidney, but also in colon and lung, where they play a central role in sodium reabsorption. Autosomal dominant mutations in the β and γ subunits of ENaC result in a general increase of channel activity due to an enhanced expression or to an increased open probability. Whether gain-of-function mutations induce overactivity (Liddle syndrome), loss-of-function mutations cause underactivity (autosomal recessive pseudohypoaldosteronism type 1). Autosomal recessive mutations are described in any of the three subunits of ENaC. Inherited or acquired nephrogenic diabetes insipidus (NDI) appears when kidney is no more able to concentrate the urine in response to antidiuretic hormone. Mutations in AQP2 gene, coding for the water channel aquaporin 2 AQP2, were associated to both autosomal dominant and recessive forms of familial NDI while the more prevalent acquired NDI forms could result from drugs or

chronic kidney diseases. Both types of NDI could induce a reduced AQP2 expression, a defective AQP2 trafficking to the apical plasma membrane or a general AQP2 defective function [2; 36].

Channelopathies is an emerging trend also in the field of gastrointestinal (GI) dysfunctions [42], indeed ion channels are expressed by epithelial and smooth muscle cells and by sensory neurons of GI tract and play central roles in the control of gastric acid production and secretion in the stomach, of fluid absorption and secretion in the gut, in the regulation of GI motility and in the coding of sensory signals, such as pain [43]. In particular, ion channel dysfunctions could be involved in functional gastro-intestinal disorders (FGID), an heterogenic group of multisystem diseases characterized by a general visceral hypersensitivity and an impaired GI motility. Considering GI epithelia, a missense variant has been described on GUCY2C gene, encoding guanylate cyclase 2C protein in a familial form of severe secretory diarrhea. The gain-of-function mutation induces a significantly increase in cGMP production that consequently activates CFTR channel, leading to a situation of hypersecretion. Voltage-gated sodium Nav1.5 channels are expressed in GI smooth muscle cells, mutations in SCN5A gene have been associated to inflammatory bowel syndrome. Furthermore, a mutation on TCAP gene, coding for Nav1.5 associated protein telethonin, was found in a patient affected by GI pseudobstruction. Finally, aberrant voltage-gated sodium channels Nav1.7, Nav1.8 and Nav1.9 (SCN9A, SCN10A and SCN11A gene respectively), generally associated to pain sensation diseases, are also critical for visceral sensation in GI tract [42].

Scope of the thesis.

Chapter 2.

A mutation in SCN4A gene, encoding voltage-dependent sodium channel Nav1.4, was found for the first time in a patient affected by myotonic dystrophy type 2 (DM2). Aim of the work was the functional characterization of mutant Nav1.4 compared to wild-type channel through patch clamp experiments. Results seemed to suggest that mutation acts as a modulator factor worsening DM2 phenotype.

Chapter 3.

The work is aimed to evaluate a mutation in KCNJ2 gene, coding for inwardly-rectifying Kir2.1 potassium channel, identified in a family affected by autism. Whole-cell patch clamp and confocal microscopy imaging experiments provide evidence for a gain-of-function of the mutant protein associated to an altered protein distribution.

Chapter 4.

Genetic studies on a cohort of patients affected by Brugada Syndrome showed a significant increase of CNV deletions in gene GSTM3, encoding a glutathione-S-transferase. Whole-cell patch clamp experiments were performed to unravel the reason why GSTM3 reduced expression could promote arrhythmogenic events when oxidative stress was induced.

Chapter 5.

A variants of KCNT1 gene, encoding Slack (a sodium-activated potassium channel) was recently linked to a Non-Familial BrS patient lacking of SCN5A variants. Patch clamp experiments were performed comparing wild-type and mutant channels in increasing sodium

intracellular concentrations. We also investigated whether the position of the mutation in the amino acid sequence could influence the response of the channel toward cytoplasmic stimuli, whose the channel is known to be sensitive. Our data indicated that the mutation seemed to be responsible for altered biophysical channel characteristics that could be linked to BrS pathological condition.

References.

- [1] Imbrici P. et al., Therapeutic approaches to genetic ion channelopathies and perspectives in drug discovery. *Front Pharmacol.* 2016 May 10;7:121.
- [2] Kim J.B., Channelopathies. *Korean J Pediatr.* 2014 Jan;57(1):1-18.
- [3] Ptáček L.J., Episodic disorders: channelopathies and beyond; *Annu Rev Physiol.* 2015;77:475-9.
- [4] Kullmann D.M. et al., Neurological channelopathies: new insights into disease mechanisms and ion channel function; *J Physiol.* 2010 Jun 1;588(Pt 11):1823-7.
- [5] Jurkat-Rott K. et al., Sodium channelopathies of skeletal muscle result from gain or loss of function; *Pflugers Arch.* 2010 Jul;460(2):239-48.
- [6] Curran J. et al., Alternative paradigms for ion channelopathies: disorders of ion channel membrane trafficking and posttranslational modification; *Annu Rev Physiol.* 2015;77:505-24.
- [7] Lehmann-Horn F. et al., Membrane defects in paramyotonia congenita with and without myotonia in a warm environment. *Muscle Nerve.* 1981 Sep-Oct;4(5):396-406.

- [8] Hoffman E.P., Voltage-gated ion channelopathies: inherited disorders caused by abnormal sodium, chloride, and calcium regulation in skeletal muscle. *Annu Rev Med.* 1995; 46:431–441.
- [9] Cannon S.C., Channelopathies of skeletal muscle excitability; *Compr Physiol.* 2015 Apr;5(2):761-90.
- [10] Burge J.A. et al., Novel insights into the pathomechanisms of skeletal muscle channelopathies. *Curr Neurol Neurosci Rep.* 2012 Feb;12(1):62-9.
- [11] Pirkmajer S. et al., Na,K-ATPase regulation in skeletal muscle. *Am J Physiol Endocrinol Metab.* 2016 Jul 1;311(1):E1-E31.
- [12] Nelson B.R. et al., Skeletal muscle-specific T-tubule protein STAC3 mediates voltage-induced Ca²⁺ release and contractility. *Proc Natl Acad Sci U S A.* 2013 Jul 16;110(29):11881-6.
- [13] Suetterlin K. et al., Muscle channelopathies: recent advances in genetics, pathophysiology and therapy. *Curr Opin Neurol.* 2014 Oct;27(5):583-90.
- [14] Loussouarn G. et al., Physiological and Pathophysiological Insights of Nav1.4 and Nav1.5 Comparison. *Front Pharmacol.* 2016 Jan 14;6:314.
- [15] Day J.W. et al., RNA pathogenesis of the myotonic dystrophies. *Neuromuscul Disord.* 2005 Jan;15(1):5-16.
- [16] Ryan D.P. et al., Episodic Neurological Channelopathies. *Neuron.* 2010 Oct 21;68(2):282-92.

- [17] Spillane J. et al., Genetic neurological channelopathies: molecular genetics and clinical phenotypes. *J Neurol Neurosurg Psychiatry*. 2016 Jan;87(1):37-48.
- [18] Jurkat-Rott K. et al., Hereditary Channelopathies in Neurology. *Adv Exp Med Biol*. 2010;686:305-34.
- [19] Kullmann D.M. et al., Neurological disorders caused by inherited ion-channel mutations. *Lancet Neurol*. 2002 Jul;1(3):157-66.
- [20] Kleopa K.A., Autoimmune Channelopathies of the Nervous System. *Curr Neuroparmacol*. 2011 Sep;9(3):458-67.
- [21] Vincent A. Developments in autoimmune channelopathies. *Autoimmun Rev*. 2013 Apr;12(6):678-81.
- [22] Kullmann D.M. Neurological channelopathies. *Annu Rev Neurosci*. 2010;33:151-72.
- [23] Lascano A.M. et al., Seizures and Epilepsies due to Channelopathies and Neurotransmitter Receptor Dysfunction: A Parallel between Genetic and Immune Aspects. *Mol Syndromol*. 2016 Sep;7(4):197-209.
- [24] Chockalingam P. et al, Channelopathies - Emerging Trends in The Management of Inherited Arrhythmias. *Indian Pacing Electrophysiol J*. 2015 Apr 1;15(1):43-54.
- [25] Campuzano O. et al., Genetics of channelopathies associated with sudden cardiac death. *Glob Cardiol Sci Pract*. 2015 Oct 13;2015(3):39.
- [26] Sansone M. et al., Electrocardiogram Pattern Recognition and Analysis Based on Artificial Neural Networks and Support Vector Machines: A Review. *J Healthc Eng*. 2013;4(4):465-504.

- [27] Spears D.A. et al., Genetics of inherited primary arrhythmia disorders *Appl Clin Genet*. 2015 Sep 18;8:215-33.
- [28] Lieve K.V. et al., Inherited ion channel diseases: a brief review. *Europace*. 2015 Oct;17 Suppl 2:ii1-6.
- [29] Behere S.P. et al., Inherited arrhythmias: The cardiac channelopathies. *Ann Pediatr Cardiol*. 2015 Sep-Dec;8(3):210-20.
- [30] Choy L. et al., Cardiac disease and arrhythmogenesis: Mechanistic insights from mouse models. *Int J Cardiol Heart Vasc*. 2016 Sep;12:1-10.
- [31] Brugada R. et al. Brugada Syndrome. *Methodist Debaquey Cardiovasc J*. 2014 Jan-Mar;10(1):25-8.
- [32] Badri M. et al., Cellular and ionic basis of J-wave syndromes. *Trends Cardiovasc Med*. 2015 Jan;25(1):12-21.
- [33] Sheikh A. S. et al., Brugada syndrome: a review of the literature. *Clin Med (Lond)*. 2014 Oct;14(5):482-9.
- [34] Sarquella-Brugada G. et al., Brugada syndrome: clinical and genetic findings. *Genet Med*. 2016 Jan;18(1):3-12.
- [35] Brugada P. Brugada syndrome: More than 20 years of scientific excitement. *J Cardiol*. 2016 Mar;67(3):215-20.
- [36] Loudon K.W. et al., The renal channelopathies. *Ann Clin Biochem*. 2014 Jul;51(Pt 4):441-58.
- [37] Saint-Criq V. et al., Role of CFTR in epithelial physiology. *Cell Mol Life Sci*. 2016 Oct 6.
- [38] Valverde M.A. et al., Ion Channels in Asthma. *J Biol Chem*. 2011 Sep 23;286(38):32877-82.

- [39] Elborn J.S. Cystic fibrosis. *Lancet*. 2016 Nov 19;388(10059):2519-2531.
- [40] Dutta R.K. et al., Genetics of primary hyperaldosteronism. *Endocr Relat Cancer*. 2016 Oct;23(10):R437-54.
- [41] Coudert A. E. et al., Osteopetrosis and Its Relevance for the Discovery of New Functions Associated with the Skeleton. *Int J Endocrinol*. 2015;2015:372156. doi: 10.1155/2015/372156.
- [42] Beyder A. et al., Ion channelopathies in functional GI disorders. *Am J Physiol Gastrointest Liver Physiol*. 2016 Oct 1;311(4):G581-G586.
- [43] Fuentes I.M. et al., Ion channels, ion channel receptors, and visceral hypersensitivity in irritable bowel syndrome. *Neurogastroenterol Motil*. 2016 Nov;28(11):1613-1618.

Chapter 2:

SCN4A mutation as modifying factor of Myotonic Dystrophy Type 2 phenotype.

E. Bugiardini ^{a,1}, I. Rivolta ^{b,1}, A. Binda ^b, A. Soriano Caminero ^c, F. Cirillo ^d, A. Cinti ^e, R. Giovannoni ^e, A. Botta ^f, R. Cardani ^g, M.P. Wicklund ^c, G. Meola ^{a,g,*}.

^a Department of Biomedical Sciences for Health, IRCCS Policlinico San Donato, University of Milan, Italy.

^b Department of Health Science, University of Milan Bicocca, Italy.

^c Department of Neurology, Penn State Hershey Medical Center, Hershey, PA, USA.

^d Laboratory of Stem Cells for Tissue Engineering, IRCCS Policlinico San Donato, Italy.

^e Department of Translational Surgeon and Medicine, University of Milan Bicocca, Italy.

^f Department of Biomedicine and Prevention, Tor Vergata University of Rome, Italy.

^g Laboratory of Muscle Histopathology and Molecular Biology, IRCCS Policlinico San Donato, Italy.

* Corresponding author.

¹ These authors contributed equally to the manuscript.

Neuromuscular Disorders (2015), Apr;25(4):301-7.

doi:10.1016/j.nmd.2015.01.006

Abstract

In myotonic dystrophy type 2 (DM2), an association has been reported between early and severe myotonia and recessive chloride channel (*CLCN1*) mutations. No DM2 cases have been described with sodium channel gene (*SCN4A*) mutations. The aim is to describe a DM2 patient with severe and early onset myotonia and co-occurrence of a novel missense mutation in *SCN4A*. A 26-year-old patient complaining of hand cramps and difficulty relaxing her hands after activity was evaluated at our department. Neurophysiology and genetic analysis for DM1, DM2, *CLCN1* and *SCN4A* mutations were performed. Genetic testing was positive for DM2 (2650 CCTG repeat) and for a variant c.215C>T (p.Pro72Leu) in the *SCN4A* gene. The variation affects the cytoplasmic N terminus domain of Nav1.4, where mutations have never been reported. The biophysical properties of the mutant Nav1.4 channels were evaluated by whole-cell voltage-clamp analysis of heterologously expressed mutant channel in tsA201 cells. Electrophysiological studies of the P72L variant showed a hyperpolarizing shift (−5 mV) of the voltage dependence of activation that may increase cell excitability. This case suggests that *SCN4A* mutations may enhance the myotonic phenotype of DM2 patients and should be screened for atypical cases with severe myotonia.

Keywords: Myotonic dystrophy type 2; Myotonia; SCN4A; N-terminus

1. Introduction

Myotonic dystrophy type 2 (DM2, PROMM, OMIM #602668) is an adult onset muscular dystrophy caused by a CCTG repeat expansion in *CNBP* gene on chromosome 3q21 [1]. The expanded RNA transcripts modify the activity of specific RNA binding proteins involved in regulating alternative splicing. The resulting missplicing of several genes is thought to account for the multisystem nature of the disease including cardiac, cerebral and endocrine involvement, along with proximal weakness and myotonia [2]. Missplicing of the skeletal muscle chloride channel, *CLC-1*, leads to a transcript coding for a non-functional channel. Consequent reduced resting chloride conductance increases the electrical excitability of the muscle and causes myotonia [3].

Myotonia in DM2 is usually mild and sometimes may be difficult to elicit even with electromyographic evaluation [4,5]. Recent studies have found an association between DM2 patients with prominent myotonia and heterozygous recessive *CLCN1* mutations on chromosome 7q35 [6,7]. Mutations of *CLCN1* which encodes the skeletal muscle voltage-gated chloride channel (*CLC-1*) are responsible for myotonia congenita (recessive Becker disease, OMIM # 255700; dominant Thomsen disease, OMIM # 160800). Mutations are “loss of function” causing reduced sarcolemmal chloride conductance and enhanced excitability [8]. The additive effects of *CLCN1* missplicing caused by DM2 expansion and *CLCN1* mutation may cause an atypical DM2 phenotype characterized by severe and

early myotonia [7].

Another gene implicated in myotonic disorders is *SCN4A* on chromosome 17q23.3 (Myotonia, Potassium-aggravated, OMIM # 608390). *SCN4A* codes for Nav1.4, the voltage gated sodium channel (VGSC) expressed in skeletal muscle [9]. *SCN4A* mutations usually produce a “gain of function” effect causing impaired inactivation or enhanced activation of the Nav1.4 channel resulting in muscle excitability [8]. To date, a possible additive influence of *SCN4A* mutation to the DM2 phenotype has never been evaluated.

In our study we investigated a DM2 patient with severe and early onset myotonia without mutation in *CLCN1* gene. We identified a novel missense mutation c.215C>T (p.Pro72Leu) in *SCN4A* gene that represents the first mutation ever reported affecting the cytoplasmic N terminus domain of Nav1.4. To investigate the biophysical alteration of P72L substitution we performed whole-cell voltage clamping in a heterologous expression system showing the Nav1.4 mutant gain of function effect.

2. Materials and methods

2.1. Patient

The patient, a Caucasian 26-year-old woman, was evaluated in the Department of Neurology at the Penn State Hershey Medical Center. The patient gave written informed consent for genetic analysis in agreement with Helsinki convention. Clinical information on other family members was obtained during the interview.

2.2. Molecular genetic analysis

Genetic analysis of *DMPK*, *CNBP*, *CLCN1* and *SCN4A* genes was performed by Athena Diagnostics, Inc. (Marlborough, MA) using the Complete Myotonia evaluation kit, which has been developed for the molecular diagnosis of myotonic dystrophy type 1 (DM1), myotonic dystrophy type 2 (DM2), myotonia congenita and sodium channel myotonia.

DM1 and DM2 repeat expansion mutations on *DMPK* gene (Chr19q13.3) and *CNBP* gene (Chr3q21.3) were evaluated utilizing polymerase chain reaction (PCR) amplification of genomic DNA followed by high resolution electrophoresis to determine the number and the size range of CTG and CCTG repeats.

DNA sequence analysis of *CLCN1* and *SCN4A* gene was performed by PCR amplification of highly purified genomic DNA, followed by automated bi-directional DNA sequencing of the entire coding region of *SCN4A* (24 exons, NM_000334) and *CLCN1* (23 exons, NM_000083). Sequencing also included the highly conserved flanking intronic sequence of the exon–intron splice junctions for all coding exons and 10 bases of intronic DNA surrounding each exon. Additional information is available by contacting Athena Diagnostic, Inc. *SCN4A* exon 1 has also been analyzed by direct sequencing in 100 control individuals.

2.3. Functional analysis of WT and p. P72L Nav1.4 channels

The c.215C>T mutation was engineered into Wild-Type (WT) *SCN4A* complementary DNA (cDNA), received from Maria Essers

Department of Clinical Research Ion Channels and Channelopathies University of Bern in the pRc/CMV2 plasmid by site directed mutagenesis using the QuikChange II site-directed mutagenesis kit (Stratagene). The construct was sequenced to confirm the correct introduction of mutation and ensure the validity of sequence. Beta 1 subunit (a kind gift from Prof. Hugues Abriel, University of Bern, Switzerland) was subcloned in a pIRES vector engineered with EGFP. WT and P72L SCN4A mutant channels were transiently expressed in tsA201 cells using Fugene. An equal amount (0.5 g) of alpha and beta 1 subunits were transfected. To mimic the heterozygous condition, 0.25 g of each alpha subunit were transfected. The expression of the channels was studied 48 h after transfection.

Membrane currents were measured using whole-cell patch clamp with Axopatch Multiclamp 700B amplifier (Axon Instruments, Foster City, CA), as previously described [10]. Recordings were made at room temperature. Internal solution contained (mmol/L) 50 aspartic acid, 60 CsCl, 5 disodiumATP, 11 EGTA, 10 HEPES, 1 CaCl₂, 1 MgCl₂, pH 7.4 adjusted with CsOH. Extracellular solution contained (mmol/L) 130 NaCl, 2 CaCl₂, 5 CsCl, 1.2 MgCl₂, 10 HEPES, 5 glucose, pH 7.4 adjusted with CsOH. In the experiments designed to measure the voltage dependence of activation, external sodium was reduced to 65 mM using n-methylglucamine as Na⁺ substitute. Holding potential was -80 mV.

2.4. Statistical analysis

Pooled data are presented as mean \pm SD; n denotes the number of

cells. To minimize the effect of culture-to-culture variability, cells were prepared expressing each construct and data from at least three separate transfections were pooled for each comparison. An ANOVA was performed for multiple comparison, followed by a modified t test with Fisher correction (ORIGIN 10). Values of $p < 0.05$ were considered significant, in figures indicated with *.

3. Results

3.1. Patient

A 26-year-old female patient complained of hand cramps and difficulty relaxing her hands from the age of 20. She reported pain in her shoulders and soreness of forearms following exercise. There were no clear triggers and specifically neither cold nor diet exacerbated her symptoms. She had no episodic weakness. She tried mexiletine that improved her stiffness slightly but stopped it due to gastrointestinal side effects. Over the past 2 years, she had noted weakness in her hands. In terms of family history, her 54-year-old mother had cataracts removed and complained of hand cramping. Neurological examination of the patient showed grip and thenar percussion myotonia with warm up phenomenon and mild distal weakness. Needle EMG examination revealed abundant, overlapping, myotonic discharges in most of the muscles examined and myopathic motor units predominantly in her distal muscles. Short and prolonged exercise testing was normal.

3.2. Molecular genetic analysis

No expansion to suggest DM1 was found in *DMPK* (Chr19q13.3), while a pathogenic 2650 CCTG repeat diagnostic of DM2 was found

in intron 1 of *CNBP* (Chr3q21.3).

Analysis of the coding sequence and intron/exon junctions of *CLCN1* was normal.

Sequencing of *SCN4A* revealed a missense variant of unknown clinical significance c.215C>T causing a proline to leucine amino acid substitution (p.P72L) in the cytoplasmic N-terminus domain (Fig. 1).

The c.215C>T genetic variation was not found in 200 chromosomes from 100 control individuals, thus excluding the possibility of a single nucleotide polymorphism (SNP) with a frequency of more than 1%. Additionally it has not been reported in the Human Genome Mutation database (HGMD; <http://www.hgmd.cf.ac.uk>) and the NCBI's single nucleotide polymorphism (SNP; <http://www.ncbi.nlm.nih.gov/SNP>) online database. The causative likelihood of this variant was also evaluated using bioinformatics program PolyPhen-2 (Polymorphism Phenotyping-2; <http://genetics.bwh.harvard.edu/pph2>). This *in silico* analysis provided a PSIC score of "1" (sensitivity: 0.00; specificity: 1.00), which indicates that the mutation is "probably" damaging.

3.3. Functional analysis of WT and p.P72L *Nav1.4* channels

A detailed functional characterization of the *SCN4A* WT and mutant was performed in transiently transfected tsA201 cells in the presence of the beta1 subunit. The level of the expression was highly variable, as the standard deviation showed, but no differences were found in the current density measured in high sodium (84.8 ± 33.6 pA/pF, n = 19; 124.5 ± 43.6 pA/pF, n = 15; 95.5 ± 48.1 pA/pF, n = 17 for WT, WT/P72L and P72L, respectively). Fig. 2A represents typical families

of current traces recorded in low sodium from WT, or WT/P72L or P72L channel. We did not find any mutation induced sustained current measured 25 ms after a step to -10 mV, being the I_{sus} $2.3 \pm 1.5\%$ of the peak current for WT, $2.1 \pm 1\%$ for WT/P72L and $1.7 \pm 0.5\%$ for P72L. To characterize the kinetics of the fast inactivation process, a biexponential function was used to fit the decay of the peak current traces elicited by a 25 ms depolarizing pulse from -80 to -10 mV. While the fast time constant of inactivation of the mutated channels was indistinguishable from the one of WT (0.7 ± 0.1 ms, $n = 11$; 0.6 ± 0.03 ms; $n = 15$; 0.6 ± 0.08 ms; $n = 10$ for WT, WT/P72L and P72L, respectively); the slow one was significantly faster (2.1 ± 0.8 ms; 0.7 ± 0.1 ms; 0.8 ± 0.1 ms for WT, WT/P72L and P72L, respectively). The mutation did not affect the voltage dependence of inactivation (V_h -55.71 ± 0.6 mV, $n = 20$; V_h -54.26 ± 0.7 mV, $n = 19$; V_h -54.23 ± 1 mV, $n = 19$ for WT, WT/P72L and P72L, respectively), but in contrast caused a small hyperpolarized shift of the V_h of the voltage dependence of activation (V_h -27.37 ± 2.7 mV, $n = 12$; V_h -31.41 ± 1.8 mV, $n = 7$; $p = 0.005$ and V_h -32.60 ± 1.5 mV, $n = 7$, $p = 7.64 \cdot 10^{-4}$, for WT, WT/P72L and P72L, respectively), as shown in Fig. 2B. It is well known that a shift in the voltage dependence of activation affects the overlap between the activation and inactivation curve and the overlap-resulting non inactivating current, so called window current, can be measured by a ramp pulse protocol. As expected, we observed a consistent mutation-induced shift in the voltage dependence peak of the window current (-31.7 ± 0.4 mV for WT, $n =$

9; -36.7 ± 0.6 for WT/P72L, $n = 11$ and -36.5 ± 0.4 mV for P72L, $n = 9$) (Fig. 2C) with no change in the window current amplitude (0.1 ± 0.07 pA/pF; 0.08 ± 0.05 pA/pF; 0.09 ± 0.05 pA/pF for WT, WT/P72L and P72L, respectively).

Moreover, the mutation slowed the time course of recovery from fast inactivation (Fig. 3A). The time necessary to recover the 80% of the current was 2.5 ± 0.1 ms for WT, $n = 20$; 4.8 ± 0.1 ms for WT/P72L, $n = 24$ and 7.1 ± 0.2 ms for P72L, $n = 23$, $p < 0.001$. Despite the fact that in the protocol we used to study of the recovery from fast inactivation, the duration of the conditioning pulse was 100 ms, we are aware from the literature [11] that a slower recovery from inactivation can be associated with an enhanced slow inactivation process; thus we tested if this was the case of the mutation presented here. Contrariwise, we found that the slow inactivation developed more quickly for the WT channel compared to the mutant ($t_{1/2}$ being 14 ± 2 s, $n = 6$; 32 ± 8 s, $n = 6$ and 37 ± 8 s, $n = 5$ for WT, WT/P72L and P72L, respectively with $p < 0.05$) and the difference became permanently significant within 10 seconds of depolarization (Fig. 3B). Moreover, we tested the voltage dependence of the steady state slow inactivation (Fig. 3C) measured using a 5 second pre-pulse, followed by a 20 ms at holding potential to allow, again, the recovery from fast inactivation and a test pulse and found that the mutation induced a depolarized shift of about 4 mV ($V_h -23.2 \pm 3.1$ mV, $n = 9$; $V_h -27.9 \pm 1$ mV ($p < 0.01$), $n = 7$; $V_h -28.7 \pm 1.7$ mV ($p < 0.01$), $n = 7$ for WT, WT/P72L and P72L, respectively). The time course of the recovery from the slow inactivation did not

appear to be altered by the mutation (Fig. 3D).

Finally, considering that the mutated channels required a prolonged time to recover from the fast inactivation, we addressed the frequency-dependent modulation of the *SCN4A* activity by pacing the cells at 20 or at 70 Hz. While the pacing at 20 Hz did not alter the peak amplitude neither of the WT channel, nor of the mutants; when the cells were paced at 70 Hz, we found a reduction of the peak current by 20% in the WT and by 24% and 28% ($p < 0.05$) in WT/P72L and P72L channel protein (Fig. 4).

4. Discussion

In this study we report the first case of a patient positive for DM2 (2650 CCTG repeat) with a concomitant mutation in *SCN4A*. This novel missense mutation P72L is remarkable because it represents the first mutation described in the cytoplasmic N terminus of Nav1.4.

This 26-year-old woman affected by DM2 presented an atypical phenotype characterized by early and severe myotonia. *CLCN1* recessive mutations have been reported to enhance the myotonic phenotype in DM2 [6,7]. However, no mutation on the *CLCN1* gene was found in our patient while screening of *SCN4A* revealed a novel mutation c.215C>T (p.Pro72Leu) localized in the cytoplasmic N-terminus. Most mutations of Nav1.4 channel have been found in the third and fourth homologous domain [12], whereas no mutations have been reported in the cytoplasmic N-terminus. The cytoplasmic N-terminus domain is composed of 128 amino acid residues, and it is highly conserved among all the species. Missense mutations in this

domain have been described in other VGSC as in SCN1A gene (Nav1.1) [13], in SCN8A gene (Nav1.6) [14] and in SCN5A gene (Nav1.5) [15]. In SCN5A the N-cytoplasmic mutations lead to a various effect on biophysical proprieties of the channel resulting in cardiac disease as long QT syndrome or Brugada syndrome [15].

In our case a functional alteration caused by the P72L mutation was confirmed by patch clamp whole-cell recording on tsA201 cells expressing heterologous mutant channels. More specifically the most prominent effects caused by P72L mutation were a hyperpolarized shift of the voltage dependence of activation, a slower recovery of fast inactivation, a slower kinetic of entry in the slow inactivation, and a destabilized steady state of the slow inactivation.

The shift of the voltage dependence of activation increases excitability of the cell decreasing the threshold for action potential and has been reported in previous *SCN4A* mutations causing hyperkalemic periodic paralysis or sodium channel myotonia [16,17]. Since slow inactivation may have a role in determining the presence of a myotonic or a paralytic phenotype [11,18], we investigated the development, the steady state and the recovery of slow inactivation caused by P72L substitution. Our data suggested that the mutation induced a slower entry in the slow inactivation state and that the availability curve is slightly shifted in the depolarizing direction. However compared to other mutations causing disruption of slow inactivation and paralytic episodes [19,20], the difference is minimal. Indeed for both P72L and WT channels slow inactivation is nearly complete at 0 mV.

Furthermore the mutation presented here induced a slowing in the recovery from inactivation that could compensate the “too high” availability of the channels due to the slow entry in the slow inactivated state. All these factors together, in our opinion, are in agreement with the absence of episodic weakness in our patient supporting a pure myotonic phenotype.

Although the data reported above show increased excitability we presently do not know if a lone P72L mutation of the *SCN4A* gene can cause myotonia in an otherwise healthy individual because lone mutations in the N-terminal domain of Nav1.4 have never been reported. Bearing in mind that other unknown factors may contribute to the atypical phenotype of our patient, we suggest that the mutation described may act as a modulating factor increasing the severity of myotonia.

The functional effect caused by the P72L mutation may be interpreted considering that while proline is usually solvent-exposed, despite its aliphatic chain, and it is commonly found in turns, leucine is a highly hydrophobic residue and it is usually buried within the core of the structure of a folded protein. P72 is the central residue of a triplet of proline and belongs to the region formed by the segment comprised by aminoacids 56 and 78 that is potentially disordered and unstructured (www.elm.eu.org) [21]. It has recently been recognized that many functionally important protein segments lie in regions intrinsically disordered. These short peptides can contain functional sites important for protein function that may be altered by amino acid substitution as

in our case. Indeed we do not know exactly what this domain does, but our data clearly demonstrate it is involved with channel gating.

5. Conclusions

We describe the first case in the literature of associated DM2 and *SCN4A* mutations. The clinical practical consequence is relevant. Indeed we confirm that the presence of severe and early myotonia in DM2 should prompt investigation for other factors. If *CLCN1* screening is negative this case supports for screening *SCN4A* gene. Further screening of *SCN4A* in DM2 cases with atypical myotonic phenotype is likely to reveal other cases in the future.

Authors' contribution

E. Bugiardini: drafting and revising the manuscript; study concept; interpretation of data. I. Rivolta: drafting and revising the manuscript; acquisition of data (electrophysiology), analysis of data, statistical analysis. A. Binda: acquisition and analysis of electrophysiological data. A. Soriano Caminero: acquisition and analysis of clinical data. F. Cirillo: acquisition and analysis of data. A. Cinti: acquisition and analysis of data, construct preparation. R. Giovannoni: revising the manuscript. A. Botta: DNA analysis and interpretation of the molecular data; revising the manuscript. R. Cardani: study concept; revising the manuscript. M.P. Wicklund: study concept; acquisition of clinical data; revising the manuscript. G.Meola: study concept; revising the manuscript.

Acknowledgment

The authors thank Dr. R. Mannikko and Dr. K. Suetterlin, University College London (UCL) Institute of Neurology, for critically reviewing the manuscript.

This study was supported by FMM-Fondazione Malattie Miotoniche.

Fig. 1

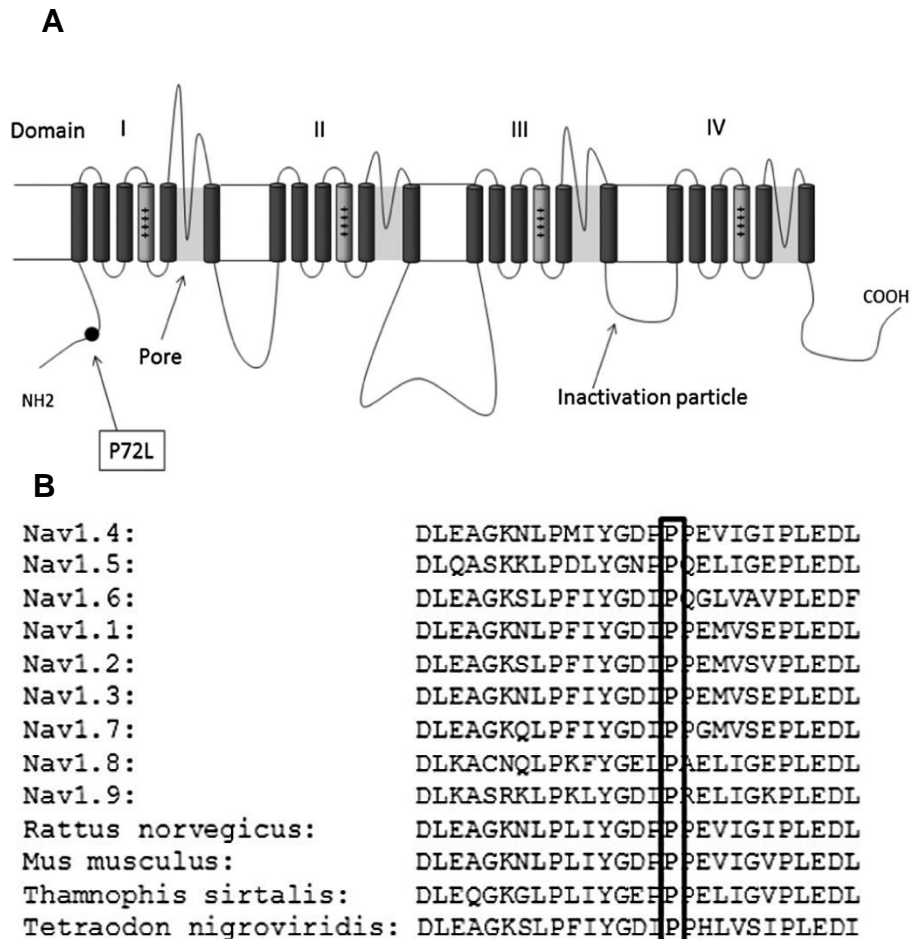


Fig. 1. Mutation p. P72L in *SCN4A* gene. (A) Schematic representation of the skeletal muscle sodium channel (Nav1.4) structure. P72L is located in the cytoplasmic N-terminus domain where mutations have never been described. (B) Proline 72 is well conserved amino acid among orthologs of the voltage-gated sodium channel and among several species.

Fig. 2

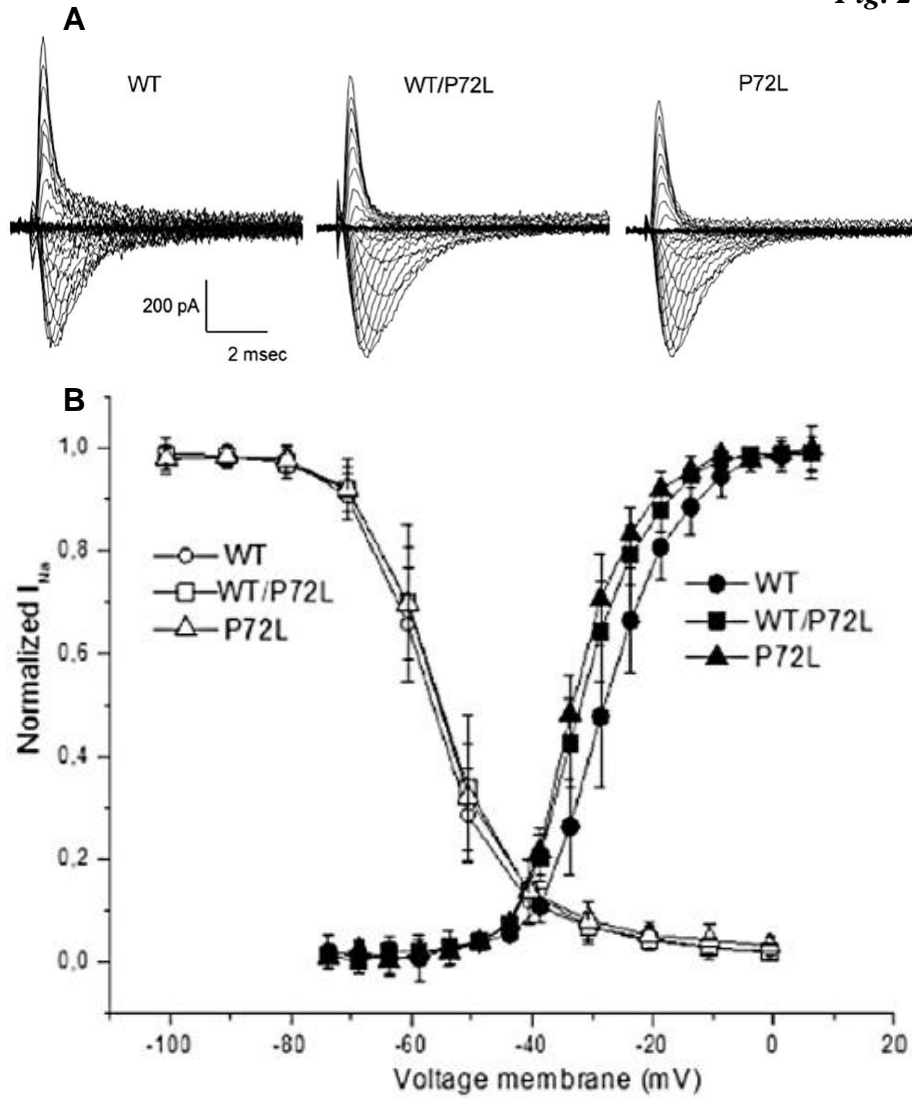


Fig. 2. Biophysical characterization of wild-type and P72L mutant Nav1.4. (A) Typical families of current traces recorded in response to a series of voltage pulses from -75 mV to $+10$ mV, in 5-mV increment, for wild-type (WT), WT/P72L, and for P72L channels.

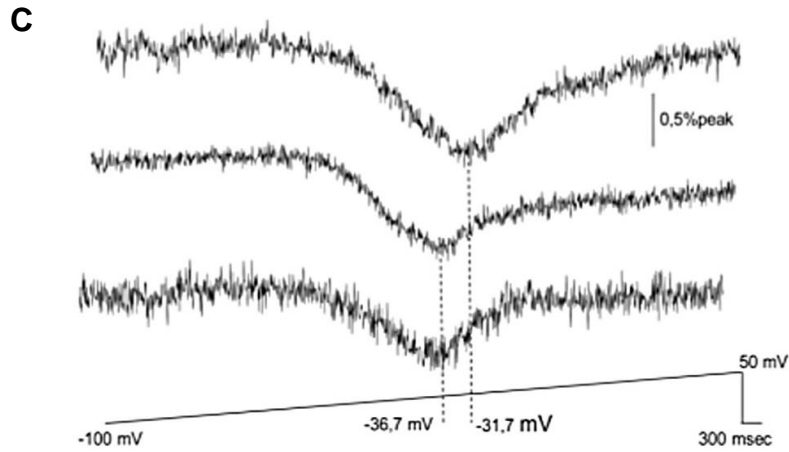


Fig. 2. Biophysical characterization of wild-type and P72L mutant Nav1.4. (B) Steady state activation (filled symbols) and inactivation (empty symbols) relationships. Activation properties were determined from I/V relationship by normalizing peak I_{Na} to driving force and maximal I_{Na} , and plotting normalized conductance vs membrane voltage. Steady state activation data were fitted with a Boltzmann function. The voltage-dependence for inactivation was measured by applying a series of conditioning pulses (500 ms) from -110 mV to $+20$ mV in 10 mV increments before assaying current availability at a test voltage of -10 mV for 25 ms. Test voltage currents were normalized to the current measured after the -120 mV pulse and plotted versus conditioning pulse voltage. (C) Averaged sodium sensitive current was measured in response to a voltage ramp protocol (-100 to $+50$ mV in 300 ms) for WT (upper trace, $n = 9$), WT/P72L (middle trace, $n = 9$) and P72L (lower trace, $n = 9$) channels. The dotted lines evidence the voltage at which the window current showed its maximal value.

Fig. 3

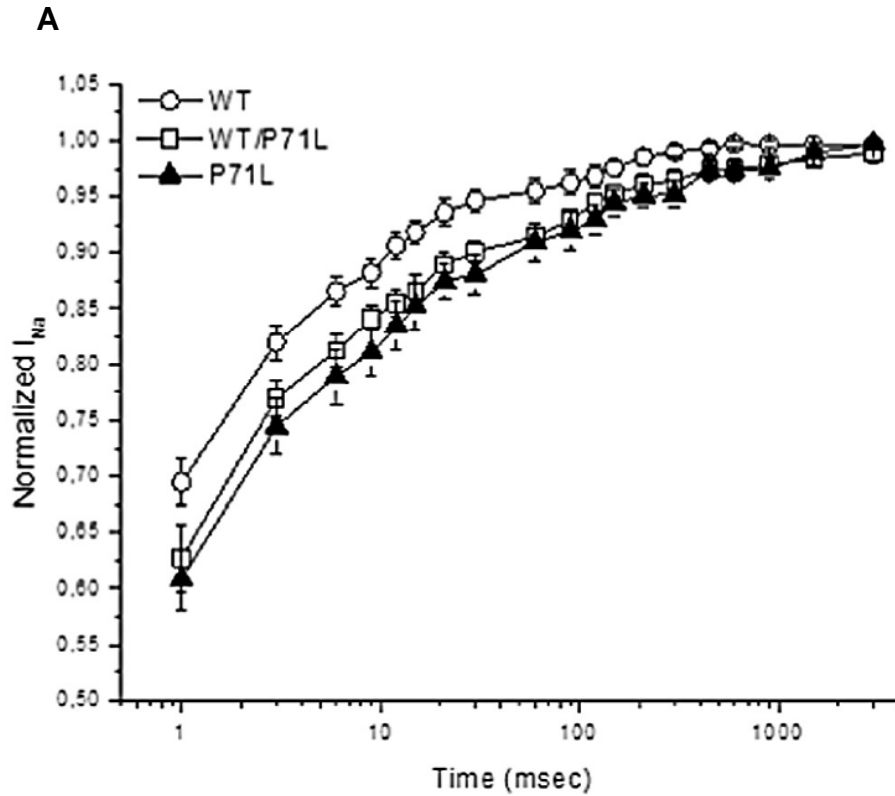


Fig. 3. Evaluation of the recovery from fast inactivation and properties of slow inactivation. (A) Time course of recovery from fast inactivation induced by a conditioning pulse (100 ms, -10 mV) followed by a test pulse at -10 mV after a variable-duration (1–3000 ms) return to -100 mV. Plot shows amplitude of peak current, normalized to fully recovered current, as function of time after imposition of the conditioning pulse for WT (open circles, $n = 20$), WT/P72L (open square, $n = 24$) and for P72L (filled triangles, $n = 23$).

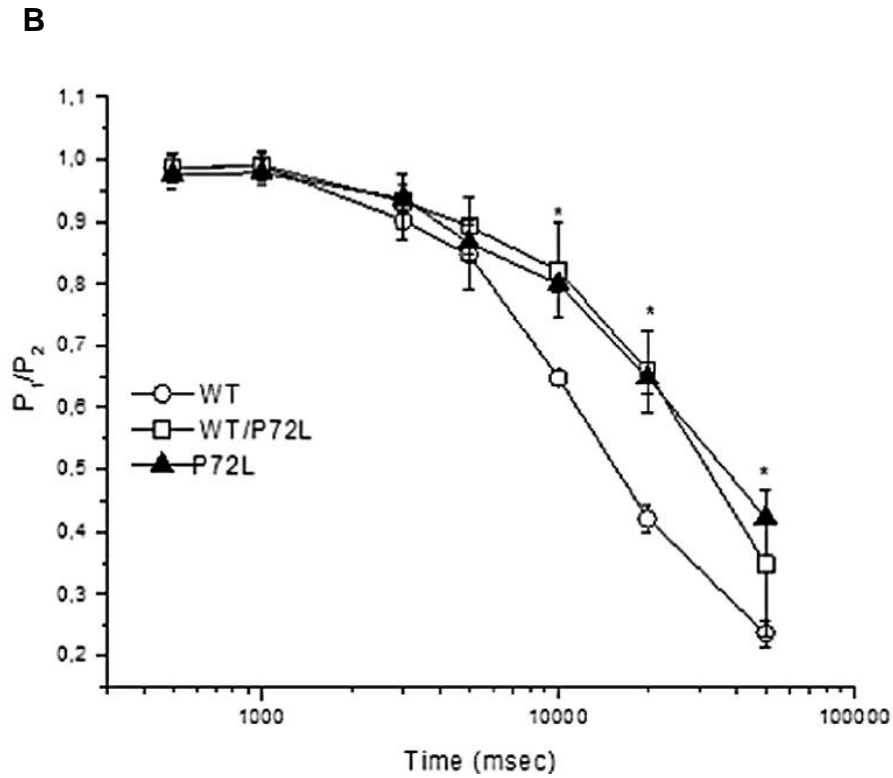


Fig. 3. Evaluation of the recovery from fast inactivation and properties of slow inactivation. (B) Time dependence of the onset of slow inactivation was measured using a two pulse protocol. Voltage was stepped from the holding potential of -100 mV to -10 mV for various times (P1, 500 to 50 000 ms), stepped back to -100 mV for 20 ms to let the channels recover from fast inactivation and then to -10 mV (P2, 10 ms) to record sodium current. The resulting P2/P1 ratio was plotted against the P1 duration.

Fig. 3

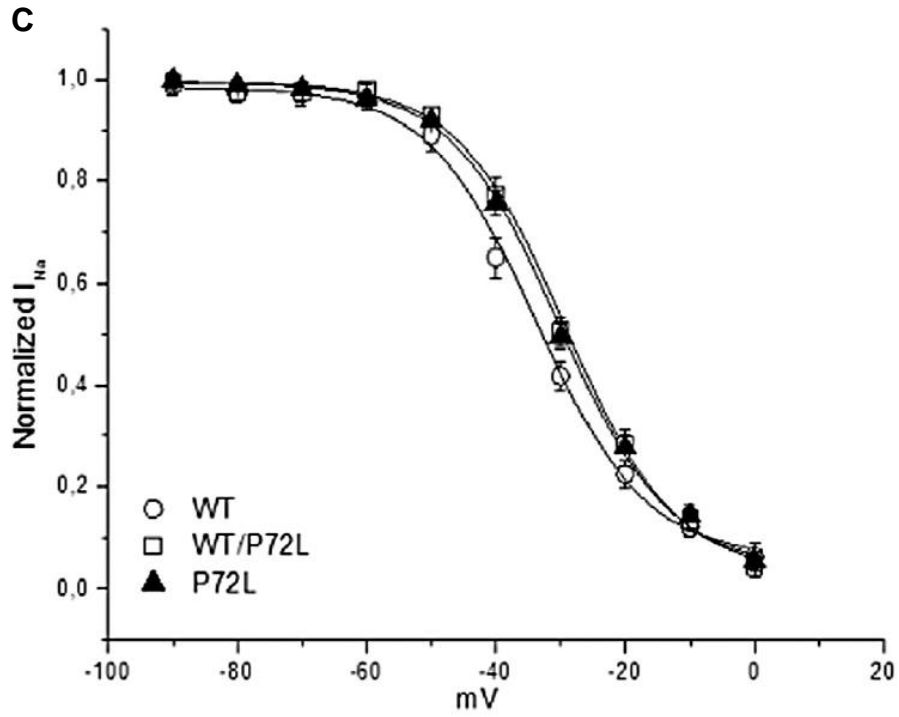


Fig. 3. Evaluation of the recovery from fast inactivation and properties of slow inactivation. (C) Steady-state slow inactivation determined by a series of 5 s prepulses from -130 to $+10$ mV. A brief return (20 ms) to -100 mV let the channels recover from fast before the test pulse to -10 mV (WT, $n = 9$; WT/P72L, $n = 7$; P72L, $n = 7$).

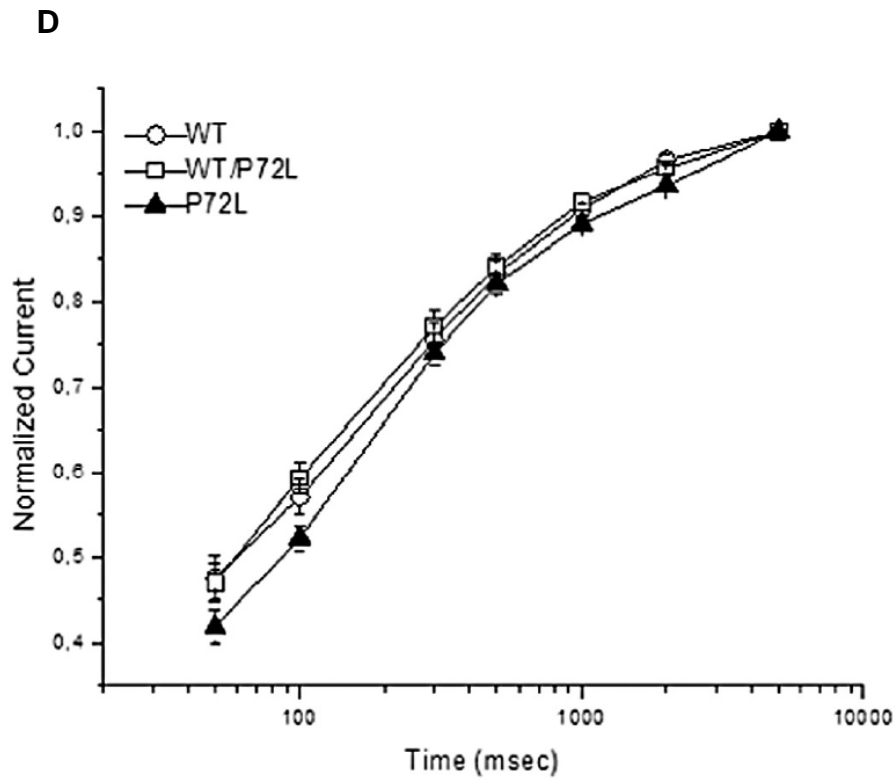
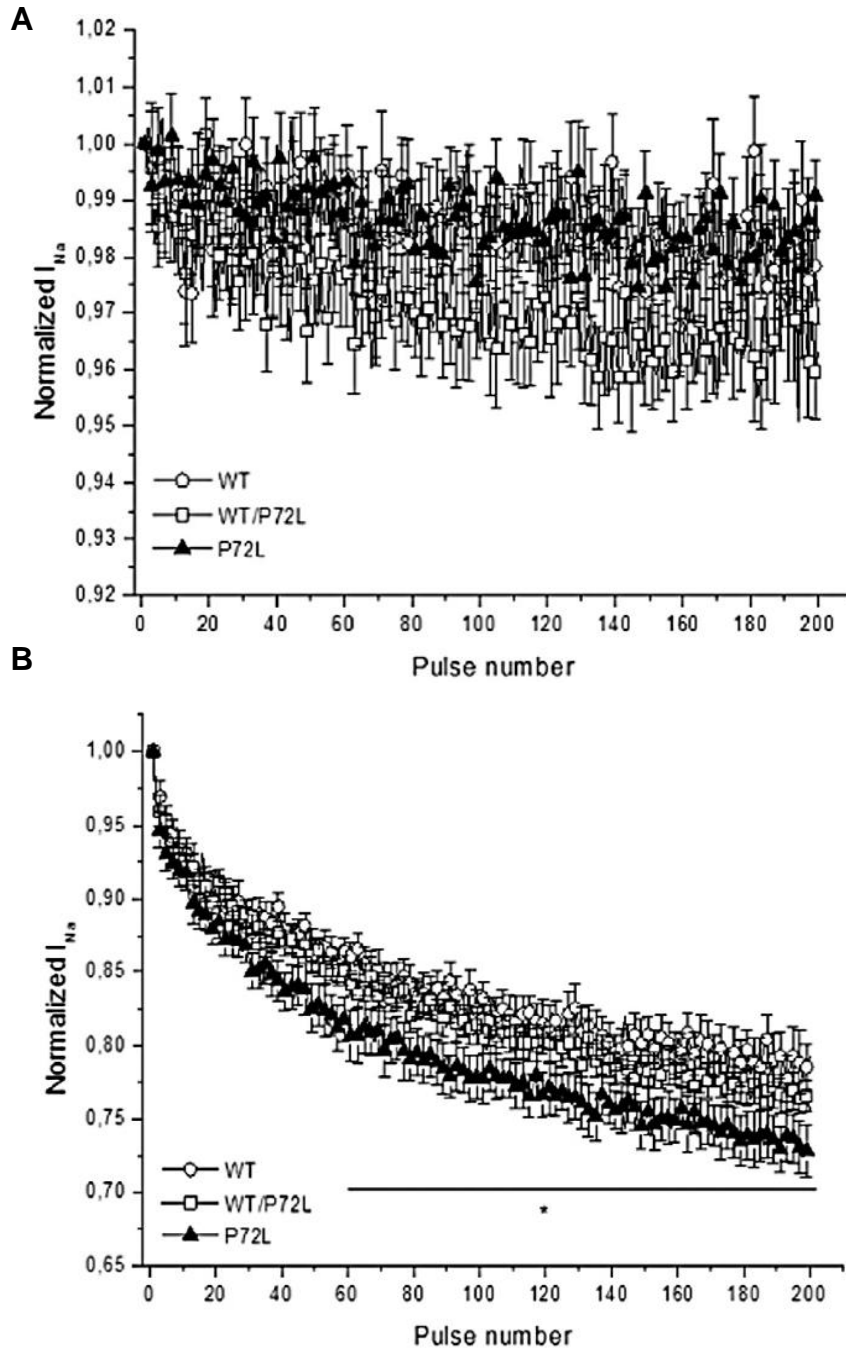


Fig. 3. Evaluation of the recovery from fast inactivation and properties of slow inactivation. (D) Recovery from slow inactivation was determined by a 5 s depolarization pulse to -10 mV followed by a variable-duration return (50–5000 ms) to -100 mV and a test pulse to -10 mV for 10 ms to record sodium current. The data were normalized to the currents recorded with a short control pulse to -10 mV before each episode (WT, $n = 9$; WT/P72L, $n = 12$; P72L, $n = 10$).

Fig. 4



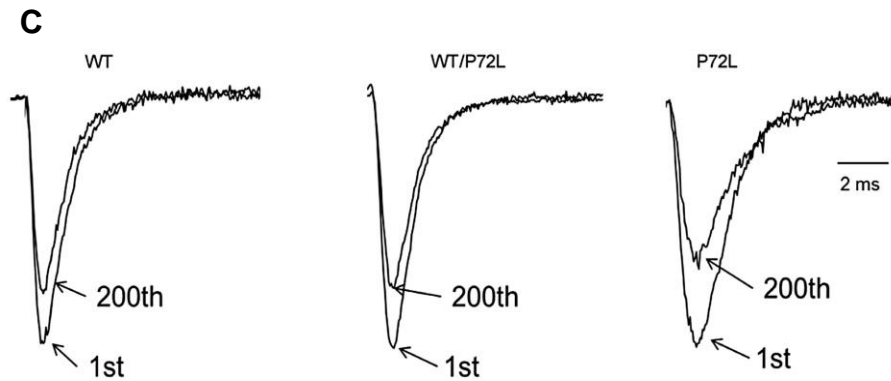


Fig. 4. Response of the WT, WT/P72L and P72L channels to pulse train stimulation. (A and B). Peak currents were recorded applying a use-dependent protocol pulsing at -10 mV, at 20 Hz and 70 Hz respectively and normalizing each peak amplitude to the 1st step amplitude. For WT (open circle) $n = 14$; for WT/P72L (open squares) $n = 18$ and for P72L (filled triangles) $n = 20$. (C) Typical first and last (200th) steps evoked by a 70 Hz use-dependent protocol.

References

- [1] Liquori C.L. et al., Myotonic dystrophy type 2 caused by a CCTG expansion in intron 1 of ZNF9. *Science* 2001;293:864–7.
- [2] Day JW et al., RNA pathogenesis of the myotonic dystrophies. *Neuromuscul.Disord* 2005;15:5–16.
- [3] Mankodi A. et al.. Expanded CUG repeats trigger aberrant splicing of ClC-1 chloride channel pre-mRNA and hyperexcitability of skeletal muscle in myotonic dystrophy. *Mol Cell* 2002;10:35–44.
- [4] Meola G. et al., Myotonic dystrophy type 2 and related myotonic disorders. *J Neurol* 2004;251:1173–82.
- [5] Milone M. et al., Myotonic dystrophy type 2 with focal asymmetric muscle weakness and no electrical myotonia. *Muscle Nerve* 2009;39:383–5.
- [6] Suominen T. et al., High frequency of co-segregating CLCN1 mutations among myotonic dystrophy type 2 patients from Finland and Germany. *J Neurol* 2008;255:1731–6.
- [7] Cardani R. et al., Co-segregation of DM2 with a recessive CLCN1 mutation in juvenile onset of myotonic dystrophy type 2. *J Neurol* 2012;259:2090–9.
- [8] Matthews E. et al., The non-dystrophic myotonias: molecular pathogenesis, diagnosis and treatment. *Brain* 2010;133:9–22.
- [9] Catterall W.A. et al., International Union of Pharmacology. XLVII. Nomenclature and structure-function relationships of voltage-gated sodium channels. *Pharmacol Rev* 2005;57:397–409.
- [10] Rivolta I. et al., A novel SCN5A mutation associated with long

QT-3: altered inactivation kinetics and channel dysfunction. *Physiol Genomics* 2002;10:191–7.

[11] Takahashi M.P. et al., Enhanced slow inactivation by V445M: a sodium channel mutation associated with myotonia. *Biophys J* 1999;76:861–8.

[12] Vicart S, . et al., Human skeletal muscle sodium channelopathies. *Neurol Sci* 2005;26:194–202.

[13] Harkin L.A. et al., The spectrum of SCN1A-related infantile epileptic encephalopathies. *Brain* 2007;130:843–52.

[14] Sharkey L.M. et al., The ataxia3 mutation in the N-terminal cytoplasmic domain of sodium channel Na(v)1.6 disrupts intracellular trafficking. *J Neurosci* 2009;29:2733–41.

[15] Gutter C. et al., Characterization of N-terminally mutated cardiac Na(+) channels associated with long QT syndrome 3 and Brugada syndrome. *Front Physiol* 2013;4:153.

[16] Cummins T.R. et al., Functional consequences of a Na⁺ channel mutation causing hyperkalemic periodic paralysis. *Neuron* 1993;10:667–78.

[17] Petitprez S. et al., A novel dominant mutation of the Nav1.4 alpha-subunit domain I leading to sodium channel myotonia. *Neurology* 2008;71:1669–75.

[18] Cannon S.C., Pathomechanisms in channelopathies of skeletal muscle and brain. *Annu Rev Neurosci* 2006;29:387–415.

[19] Bendahhou S. et al., Activation and inactivation of the voltage-gated sodium channel: role of segment S5 revealed by a novel

hyperkalaemic periodic paralysis mutation. *J Neurosci* 1999;19:4762–71.

[20] Bendahhou S. et al., Impairment of slow inactivation as a common mechanism for periodic paralysis in DIIS4-S5. *Neurology* 2002;58:1266–72.

[21] Wright P.E. et al., Intrinsically unstructured proteins: re-assessing the protein structure-function paradigm. *J Mol Biol* 1999;293:321–31.

Chapter 3:

Functional characterization of a novel KCNJ2 mutation identified in an Autistic proband.

I. Rivolta ¹⁺, A. Binda ¹⁺, C. Villa ¹, E. Chisci ¹, M. Beghi ², C. M. Cornaggia ¹, R. Giovannoni¹, Romina Combi¹ *

¹ School of Medicine and Surgery, University of Milano-Bicocca, Monza, Italy

² Azienda Ospedaliera "Guido Salvini", Garbagnate Milanese, Italy

* Corresponding author

⁺ These authors contributed equally to this work

Submitted to PLOS One (2016)

Abstract

Inwardly rectifying potassium channels have been historically associated to several cardiovascular disorders. In particular, loss-of-function mutation in the Kir2.1 channel has been reported in cases affected by Andersen-Tawil syndrome while gain-of-function mutations in the same channel cause the short QT3 syndrome. Recently, a missense mutation in Kir2.1 as well as mutations in the Kir4.1 were suggested to be involved in autism spectrum disorders suggesting a role of potassium channels in these diseases and introducing the idea of the existence of K⁺ channel autism spectrum disorders. Here, we report the identification in an Italian affected family of a novel missense mutation (p.Phe58Ser) in the *KCNJ2* gene detected in heterozygosity in a proband affected by autism and borderline for short QT syndrome type 3. The mutation is located in the N-terminal region of the gene coding for the Kir2.1 channel and in particular in a very conserved domain. *In vitro* assays demonstrated that this mutation results in a gain of function of the protein and an altered protein distribution suggesting in particular an increase of the channel export to the plasma membrane.

Keywords: Autism spectrum disorder; KCNJ2; potassium channel; mutation; patch clamp

1. Introduction

Inwardly-rectifying (Kir) potassium channels are widely expressed in several excitable and non excitable tissues playing a key role in the maintenance of the resting membrane potential and consequently in the regulation of cell excitability. Approximately 15 Kir clones were identified and grouped in 7 different families based on sequence similarity and functional properties: Kir1.x – Kir7.x. Kir2.x family includes five isoforms sharing the biophysical characteristics of strong inward rectification that is due to a highly voltage-dependent block of the channel pore by intracellular polyamines and Mg^{2+} [1-2]. In particular, Kir2.1 (IRK1/*KCNJ2*) is the major isoform underlying the inward-rectifier current IK1 in the human ventricular muscle [3]. High levels of this isoform were also reported in the brain (mainly hippocampus, caudate, putamen and nucleus accumbens) [4] and skeletal muscle.

Mutations in *KCNJ2* leading to loss-of-function of Kir2.1 have been linked with Andersen-Tawil syndrome, a cardiovascular disease characterized by QT prolongation, predisposition to cardiac tachyarrhythmias [5] as well as skeletal abnormalities, mood disorders and seizures [6]. On the other hand, Kir2.1 gain-of-function mutations cause the type-3 variant of the short QT syndrome which results in QT shortening and increased risk of sudden cardiac death [7]. Recently, a role of Kir channels was reported in autism spectrum disorders (ASDs) due to the identification of two mutations (p.Arg18Gln and p.Val84Met) in the *hKCNJ10* gene coding for the Kir4.1 subunit as well as one mutation in the *KCNJ2* gene (p.Lys346Thr) coding the

Kir2.1 subunit. All of these mutations resulted in a gain-of-function of the relevant Kir channel [6]. ASDs are heterogeneous disorders characterized by a neurodevelopment impairment with complex aetiology: several environmental risk factors have been reported and a strong genetic basis is accepted with an estimated heritability upwards of 90%. Nonetheless, autism specific genetic aetiology remains largely unknown.

Here, we report the identification of a novel missense mutation (*KCNJ2*- p.Phe58Ser) located in the coding region of the *KCNJ2* gene in a ASD patient showing a borderline shortening of the QT interval at the electrocardiogram (ECG). The mutation was detected in heterozygosity in the proband of a family where both ASDs and cardiovascular diseases segregate. *In vitro* assays demonstrated that this mutation results in a gain-of-function of the Kir2.1 channel and suggested an impairment in its trafficking in the cell.

2. Materials and methods

2.1. Genetic analysis

The sample is composed by an Italian family showing three cases of ASDs and several cases of different cardiovascular diseases (Fig 1A). Informed written consent was obtained from all participants in the study in accordance with the study protocols approved by the University of Milano-Bicocca ethical committee. For each participant venous blood was collected in BD Vacutainer® Blood Collection Tubes containing 5.4mg K₂EDTA (spray-dried) and genomic DNA was extracted using the Wizard genomic DNA purification kit

(Promega, Madison, WI, USA).

Comprehensive mutational analyses of *KCNJ2* and *KCNJ10* were performed using polymerase chain reactions (PCRs) and DNA sequencing. PCRs were performed under standard conditions directly on genomic DNA using the GoTaq Master Mix (Promega). Flanking primers (Sigma-Aldrich, St. Louis, Mo, USA) designed with the Oligo 6.0 software were used to amplify *KCNJ2* and *KCNJ10* translated sequences. Primer sequences are available on request. Sequencing reactions were performed on both strands using the BigDye Terminator Cycle Sequencing kit v1.1 and an automated ABI-3130 DNA sequencer (Applied Biosystems, Foster City, CA). ChromasPro v1.34 (Technelysium Ltd.) software was used for mutation detection. Sequences were compared with the RefSeq sequences NM_000891 (*KCNJ2*) and NM_002241.4 (*KCNJ10*).

2.2. Plasmids and mutagenesis

A pCMS-EGFP vector containing the wild-type *KCNJ2* cDNA was kindly provided by Prof. Minoru Horie (Shiga University of Medical Science, Japan) [9]. The c.173T>C (p.Phe58Ser) mutation was introduced by site-directed mutagenesis using the Quick Change II XL kit (Stratagene, La Jolla, CA, USA). The cDNA was completely resequenced after mutagenesis. Wild-type and mutant cDNA was also sub-cloned into a pcDNA3.1-NT-GFP-TOPO vector (Invitrogen) for sub-cellular localization studies. Plasmids were purified using QIAGEN Plasmid Maxiprep kit (QIAGEN, Hilden, Germany) following the suggested protocol. All constructs were verified by sequence analysis.

2.3. Transfection and cell culture

Two cell lines were used for heterologous expression: tsA201 and CHO cells. The former are mainly used for biochemical studies because copious amounts of protein can be generated; however, these cells had been avoided for electrophysiological measurements because of their endogenous voltage-gated K^+ currents [10, 11] and for this purpose CHO cells were preferred. Cell lines were cultured in a controlled environment (5% CO_2 , $37^\circ C$); tsA201 cells were maintained in Dulbecco's Modified Eagle Medium (DMEM; Sigma) while CHO cells were maintained in Ham's F12 (Sigma-Aldrich). Both the media were added with fetal bovine serum (10%), L-Glutamine (2 mM), penicillin G (100 U/mL) and streptomycin sulfate (100 $\mu g/mL$). Cells were transiently transfected with 1 μg of plasmid containing wild-type or mutant *KCNJ2* using FuGene reagent (Promega) according to the manufacturer protocol.

2.4. Electrophysiology recordings and analysis

I_{K1} current was recorded 48 hours after transfection with pCMS-EGFP-hKCNJ2-WT or pCMS EGFP-hKCNJ2-p.Phe58Ser. CHO cells medium was replaced with an extracellular solution containing (in mM): NaCl 135, KCl 4.8, $CaCl_2$ 1.8, $MgCl_2$ 1, HEPES 5, glucose 10 (pH 7.4 with NaOH). Pipettes were filled with an intracellular solution containing (in mM): KAsp 132, KCl 15, $MgCl_2$ 1, HEPES 5 (pH 7.3 with KOH). $BaCl_2$ 1 mM was added to the bath solution to selectively block the inward rectifying current. Whole-cell patch clamp recordings were performed at room temperature using pipettes pulled to a resistance of 2-5 $M\Omega$ (Model P-97 Sutter Instruments). Currents

acquisition was made with a Multiclamp 700B (Axon Instruments) amplifier, data were digitized with a Digidata 1440A (Axon Instruments) and pClamp 10.3 software (Molecular Devices) was used for the analysis. I_{K1} data were plotted as barium-sensitive currents and presented as mean \pm SEM. The rectification index was calculated as the ratio of the outward current at -60 mV divided by the absolute value of the inward current at -100 mV multiplied by 100 [12].

2.4 Immunocytochemistry and imaging

tsA201 cells were plated in 35 mm glass-bottom dishes and transiently transfected with the pcDNA3.1-NT-GFP-TOPO-hKCNJ2-WT or pcDNA3.1-NT-GFP-TOPO-hKCNJ2-p.Phe58Ser coding for a wild-type or mutant Kir2.1 channel fused with the GFP protein at the N-terminus. 48 hours after transfection cells were fixed in methanol for 6 minutes at -20°C , washed three times with high salt buffer (10 min each). Anti-Kir2.1 (mouse monoclonal, 1:100; Abcam) and anti-ZO1 (rabbit polyclonal, 1:50; Invitrogen) were incubated overnight in GDB at 4°C . After three high salt buffer, cells were incubated with Alexa conjugated secondary antibodies (goat anti-mouse Alexa Fluor488, goat anti-rabbit Alexa Fluor 568; Invitrogen) diluted in GDB, at room temperature for 1 hour. $1\mu\text{M}$ of 4',6-diamidino-2-phenylindole (DAPI) in PBS was used to stain cell nuclei(5 min). Confocal laser scanning microscopy was used to study the ion channel cellular distribution. Images were acquired by an LSM710 inverted confocal microscope equipped with a Plan-Neofluar 63×1.4 oil objective (Carl Zeiss, Oberkochen, Germany). Images were acquired at $\lambda_{\text{em}}=610$ nm to detect ZO-1 on the plasma membrane, $\lambda_{\text{em}}=488$ nm to detect the ion

channel, and $\lambda_{em}=460$ nm to detect the nuclei.

2.5. Statistical analysis

Data are presented as mean \pm SEM. Two-tailed Students *t* test was used to compare means; $p<0.05$ was considered statistically significant and indicated with * .

3. Results

3.1. Phenotypes

The proband (individual III-1, Fig 1A) is now a 23 years old man with an ASD diagnosed during the attendance of asylum when he showed a language delay (he started to speak at the age of about three years) as well as a gestural automatism in the form of "flicker" (with the arms makes the gesture of flying repeatedly). Moreover, he was hyperactive and had severe relationship problems. Currently he finished an art school and worked as a storekeeper in a hypermarket. He's still followed by psychiatrists and educators in an educational and job placement project for people with disabilities. For a long time he lived basically isolated and with few interpersonal relationships. The ECG examination (not shown) performed on the 171 proband after the identification of the here reported mutation showed a borderline shortening of the QT interval (QTc of 320 ms and Qrs of 120 ms). The father (individual II-1, Fig 1A) is a healthy man of 54 years with only rare episodes of childhood asthma reported in his history; his schooling is up to high school without any reported evident problems concerning performance or relationship with other guys. He is currently employed in a large company and has a life of relationship

substantially normal. No detailed psychological tests were available for this subject.

Both paternal grandfather (individual I-1, Fig 1A) and grandmother (individual I-2, Fig 1A), 82 and 80 years old respectively, are alive; the grandfather was always in good health (it's only reported the presence of gout in recent years); the grandmother, from the age of 45-50 years reported episodes of angina pectoris. Her brother (individual I-3, Fig 1A) died for a sudden cardiac arrest while sleeping at around 50 years old without any previous warning while her sister (individual I-4, Fig 1A) was operated to heart last year and has a nephew (individual III-3, Fig 1A) (son of the son) with an important and diagnosed autism spectrum disorder with severe disorganization of development. No detailed psychological tests were available for these individuals.

The brother (individual II-2, Fig 1A) of proband's father, born in 1966, takes Cardioaspirin for not well defined heart problems. The daughter (individual III-2, Fig 1A) of this brother, who is now 7 years old, has been under scrutiny for an autism spectrum disorder: she has a language delay, gestural automatism in the form of "flicker" (the same automatism of the proband) and she has little relationships and communication skills.

The mother (individual II-5, Fig 1A) of the proband is a 51 years old woman with a history of idiopathic generalized epilepsy with age-related onset, generalized tonic-clonic seizure and photosensitivity; the epilepsy onset was reported at age 11 while at present she has rare attacks. The average schooling is superior and she is currently enrolled

in a public company. Her father (individual I-6, Fig 1A) died at the age of 94 years old and her mother (individual I-7, Fig 1A) at 66 years old for cancer, not having presented particular diseases in life.

3.2. Mutational screening

Sequencing of the coding region, intron-exon boundaries of *KCNJ2* revealed that the proband is a heterozygote for a missense mutation (Fig 1B). Nucleotide numbering from here onward is according to cDNA position (RefSeq accession number NM_000891 starting from the first nucleotide of the ATG start codon).

The mutation consists of a T>C transition at cDNA position 173 (c.173T>C), which leads to a non conservative Phe to Ser change at position 58 (p.Phe58Ser) in the N-terminal cytoplasmic domain of Kir2.1 (Fig 1C). This mutation was detected in the heterozygous state also in the proband's father (II-1) who inherited the mutated allele from his mother (I-2), while it was absent in the epileptic mother (II-5)(Fig 1A). Unfortunately, parents of the other affected members of the family were not collaborative thus a cosegregation study between the mutation and ASDs was not feasible.

The mutation was not previously reported in literature nor present in SNP databases. The aminoacid change in Kir2.1 was predicted to be damaging (PolyPhen2, Mutation Taster) and affected a highly evolutionary conserved aminoacid (Fig 1D). No mutations were detected in the coding region of *KCNJ10*.

3.3. Cellular electrophysiology

Whole cell IK1 currents were acquired through a steps protocol of the duration of 400 ms with a holding current of -60 mV and steps

amplitude from -120 mV to $+10$ mV. In Fig. 2 are shown barium-sensitive current traces from a CHO cell expressing wild-type or mutant KCNJ2 (panel A left and right, respectively). As a general comment, the transfection with the mutated plasmid yielded a great heterogeneity in terms of amplitude of the current recorded: an abundant group of cells (36%) showed too large current and they had to be discarded since not suitable for the voltage control; this situation occurred more rarely with the WT (25% of the cells patched). In line with this observation, the cells transfected with Kir2.1-p.Phe58Ser channels exhibited a significant higher current density compared to ones transfected the wild-type: in particular, at -55 mV, when the outer current is at its maximum, the current density was 26.1 ± 12.9 pA/pF in cell expressing the mutant and 3.8 ± 1.2 pA/pF in those expressing the wild-type cDNA ($p < 0.001$). Moreover, the rectification profile of the channel was also affected: the rectification index, in fact, was $20 \pm 2.1\%$ for the mutant and $8.9 \pm 2.0\%$ for the wild-type channel ($p < 0.001$).

3.4. Immunocytochemistry and imaging

In order to investigate whether the increase in whole-cell Kir2.1 current density is attributable to a higher abundance of channels on the surface membrane, confocal imaging was performed on tsA201 cells transiently transfected with pcDNA3.1-NT-GFP-TOPO-hKCNJ2-WT or pcDNA3.1-NT-GFP TOPO-hKCNJ2-p.Phe58Ser vector. Analogous vectors were previously produced and successfully used to analyze the effect on the channel trafficking of several mutations detected in patients affected by arrhythmia showing that the introduction of the

GFP at the N-terminus of the *KCNJ2* cDNA did not affect its expression [13]. We used zonula occludens 1 (ZO-1), a protein associated to tight junction and expressed by tsA201 cells, as membrane marker to standardize the ion channel quantification.

Acquired images revealed for both wild-type and mutant channels a clear membrane localization, but also an intracellular labeling (Fig 3), most likely due to the presence of the protein in the endoplasmic reticulum and in the Golgi apparatus. Nevertheless the presence of the mutation in the channel appeared to cause a higher expression at the plasma membrane as suggested by the fluorescence quantification: 0.77 ± 0.21 a.u. for WT 0.88 ± 0.25 a.u. for p.Phe58Ser (n=351 and 342 images, respectively, from three different experiments, $p < 0,001$) (Fig 3).

4. Discussion

In this article we report a novel mutation (p.Phe58Ser) within the *KCNJ2* gene in an Italian proband of a family where both ASDs and cardiovascular disease segregate. The mutation was found in heterozygosis in the proband showing autism and a borderline short QT syndrome type 3 (SQT3) as well as in the father and paternal grandmother who shows in her family additional two ASDs cases as well as a brother died by sudden cardiac arrest. Unfortunately the DNA of these relatives was not available. The mutation causes the change of a highly conserved hydrophobic Phenylalanine (Phe) to a hydrophilic Serine (Ser) located in the N-terminal region of the protein. This is the second mutation in *KCNJ2* detected in a patient

showing autism and SQT3 syndrome: the previously reported mutation (p.Lys346Thr) was detected in monozygotic twins and functional studies revealed an increase of the channel's surface expression and stability at the plasma membrane, a reduction in protein degradation and altered protein compartmentalization [14]. The here reported mutation showed similar effects: in particular, the p.Phe58Ser exhibited a five-fold higher current density compared to the wild-type in the whole range of voltage tested (data not shown) and a weaker rectification at depolarized voltages. These results are in line with the observation that the residue p.Phe58 resides within a short cluster of highly conserved basic aminoacids (from aminoacid 44 to 61) in the cytoplasmic N-275 terminus which is required for Golgi exit [15]. It was demonstrated that the cell surface expression of Kir2.1 channel from the Golgi is controlled by a signal-dependent process that provides a mechanism to regulate the targeting of the channel to the sarcolemma and the transverse tubule at optimal densities for appropriate electrical signal transmission [16]. The unusual Golgi exit signal is dictated by a tertiary structure localized within the confluence of the cytoplasmic NH₂ and COOH terminal domains [16]. The signal creates an interaction site that allows properly folded Kir2.1 channels to insert into clathrin-coated vesicles at the trans-Golgi for export to the cell surface [17]. The p.Phe58Ser mutation could be a modification factor for the above described tertiary structure owing to the fact that an apolar aminoacid with a large aromatic residue is substituted by a polar one with a residue consisting in only a hydroxyl group.

Evidences accumulated over the last 20 years indicated that K⁺ channel function depends on multicomponent protein complexes that help in the assembly and delivery of the right channel subunits to the right place in the cell membrane at the right time [17]. The Kir2.1 protein can coassemble with all other members of its family [18]. In particular, a short beta strand, β A(N), of the N-terminal domain overlapping the aminoacid 58 was recognized as an important site that interacts extensively with the C- terminal domain of a neighboring subunit, indicative of its structural role in the subunit assembly by intersubunit interaction [19]. Therefore, mutations like the p.Phe58Ser which is located in the interaction site, may impair the function of both homomeric Kir2.1 and heteromeric channel formed with other Kir2.x subunits. The heteromultimerization may also contribute to the heterogeneity of phenotypes seen in patients and their relatives bearing Kir2.1 mutations. On the basis of what kind of subunits interact each other to form the heterodimeric structure we can have a modulation of channel activity. The hypothesis of a different trafficking of the mutant channel is supported by the confocal imaging showing an increased presence of the channel on the plasma-membrane. In order to obtain this set of data, we switched to a different expression vector than that used for the electrophysiological characterization of the channels. The reason being related to the possibility not to have GFP in the cytosol and, thus, to have a fluorescent image attributable only at the proteins of interest. Moreover, we chose to identify the channel not through the GFP bound at its N-terminal, since this signal was not consistent and

constant among experiments. Rather we used a regular antibody against Kir2.1 that allowed to obtain a more reliable signal. Although immunofluorescence is an ideal method for qualitatively looking at protein distribution at the level of individual cells, effort was required to ensure that it was quantifiable. To this aim, we looked for a method to standardize the fluorescent signal emitted by the antibody bound to the KCNJ2 channel. Several trials using DiI C12(3) were unsuccessful because this lipophilic fluorescent dye labels the cells membrane and yield a very good staining of in vivo cells. For in vitro acquisition, though, the staining was not homogeneous within the same coverslip, for this reason we decided to rely on the fluorescent labeling of a constitutive membrane protein such as ZO-1. Setting these conditions, we were able to quantify and normalize the fluorescence associated to the protein of our interest. Our data showed that the fluorescence associated to the p.Phe58Ser bearing channel appeared to be significantly higher as compared to the wild-type, suggesting indeed either an enhanced export or a higher stability of the protein at the plasma membrane owing to the presence of the mutation. It is clear that the increment observed with the imaging technique is not as high as the one obtained with patch clamp. The latter is a more specific and precise method of measurement. Simultaneous confocal imaging and patch clamp recordings would be the best to use in this case. Nevertheless, the confocal analysis, with 15% of increment in the fluorescence associated to the mutant channel goes in the same direction with the result obtained with the electrophysiological data. In conclusion, the identification of an increased current density at a

physiological range of voltages in the presence of mutations is consistent with the autistic phenotype which is normally associated to an altered neuronal excitability: a Kir2.1 overexpression in the plasma-membrane has been shown to affect activity by lowering the resting membrane potential and therefore the cell excitability [20].

Although a functional effect of the *KCNJ2*-327 p.Phe58Ser mutation was demonstrated by our results, a direct role of the mutation in ASDs and/or cardiovascular disorders pathogenesis has still to be proved. This could be done only by the identification of new families with the mutation cosegregating with these diseases because, unfortunately, affected relatives of the proband were not compliant and did not participate to the study and an incomplete penetrance could not be excluded owing to the detection of the variant in the father and grandmother which are not reported as affected by evident intellectual or social impairments (although it's worthwhile to note that they never underwent to detailed psychological examination tests). Moreover, additional functional studies are needed to verify the here reported results in non-heterologous systems such as neurocytes, astrocytes or cardiomyocytes. Finally, the development and study of specific transgenic mouse models could give an indication on the phenotype specifically associated to the mutation. However, this is the second variant detected in the *KCNJ2* gene in ASDs patients showing shortening of the QT interval and causing altered cell distribution of the relevant channel and this recurrence suggests that individuals with such an altered channel density in the plasma membrane could be more prone to develop these diseases.

In conclusion, the present paper strengthens the importance of a mutation screening of the whole *KCNJ2* gene in patients affected by ASDs.

Acknowledgment

We are in debt to prof Mauro Pessia for his role of consultant in the work and we thank collaborative family members for their participation in the study.

Fig. 1

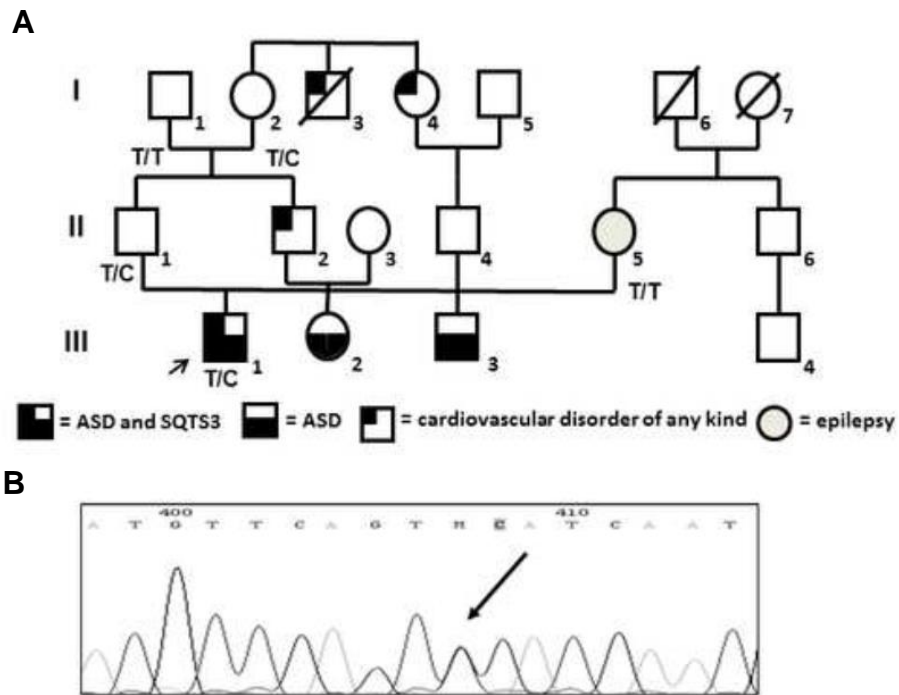


Fig. 1. Familial genetic history, electropherogram of the proband and schematic representation of the ion channel. A: Pedigree of the family in which the mutation has been identified showing the segregation of the c.173 T>C (p.Phe58Ser) mutation in collaborative relatives, the arrow indicates the proband. B: Electropherogram from the proband heterozygous for the transition c.173 T>C (RefSeq NM_000891) that corresponds to the missense mutation p.Phe58Ser.

Fig. 1

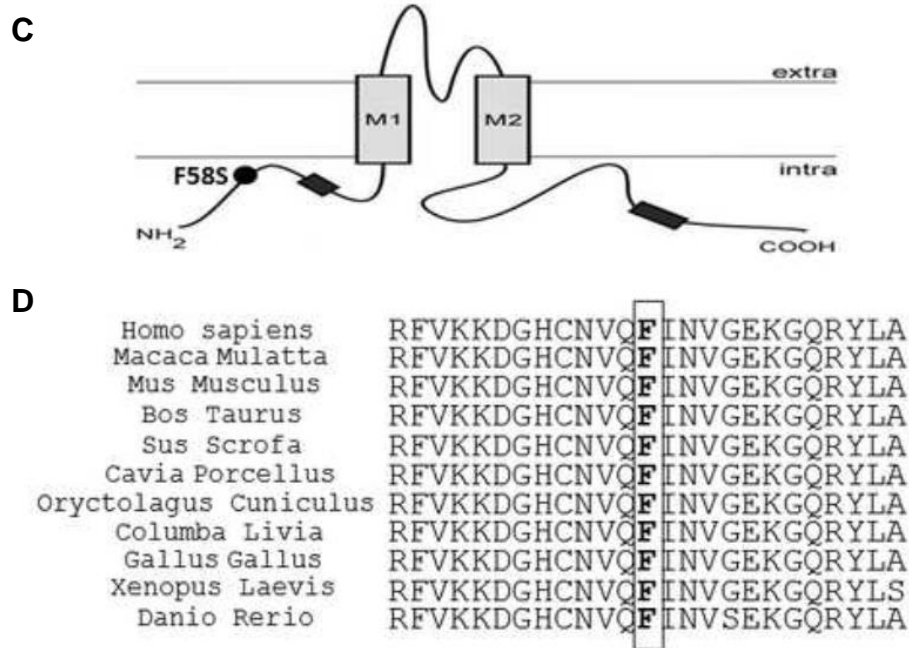


Fig. 1. Familial genetic history, electropherogram of the proband and schematic representation of the ion channel. C: Diagram of the Kir2.1 channel molecular complex. Intra and Extra are intracellular and extracellular. p. Phe58Ser (indicated by an arrow) is located in a short beta strand, $\beta A(N)$, involved in the heteromeric interactions and overlapping the N-terminal part of the Golgi export signal. Export signals for Golgi (at the N-terminus) and endoplasmic reticulum (at the C-terminus) are represented by boxes. D: Amino acid multiple alignment of Kir2.1 sequence displaying evolutionary conservation of Phenylalanine (F) residue across species (modified from [8]). The mutant F at position 58 is boxed.

Fig. 2

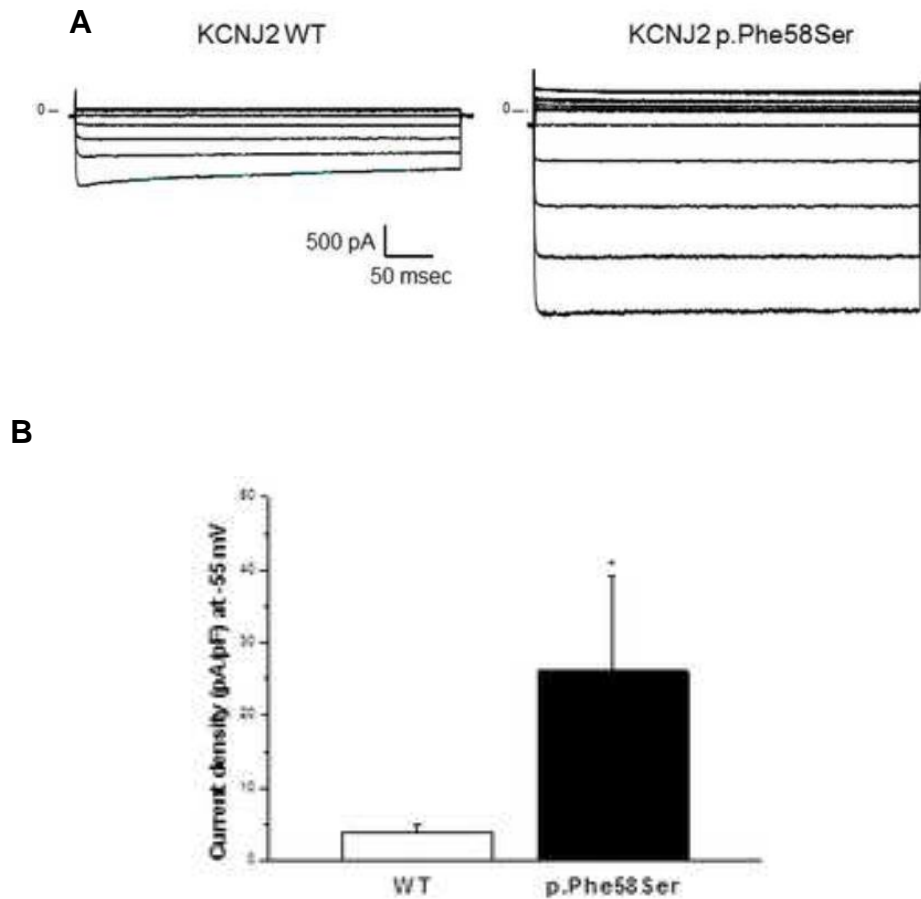


Fig. 2. Functional characterization of wild-type (WT) and mutant *KCNJ2*. A: typical families of I_{K1} barium-sensitive current traces recorded in whole-cell from CHO cells transfected with wild-type (left) and p.Phe58Ser-mutated (right) channels. B: Averaged current density measured at -55 mV (n=26 for WT and 19 for the mutant).

Fig. 2

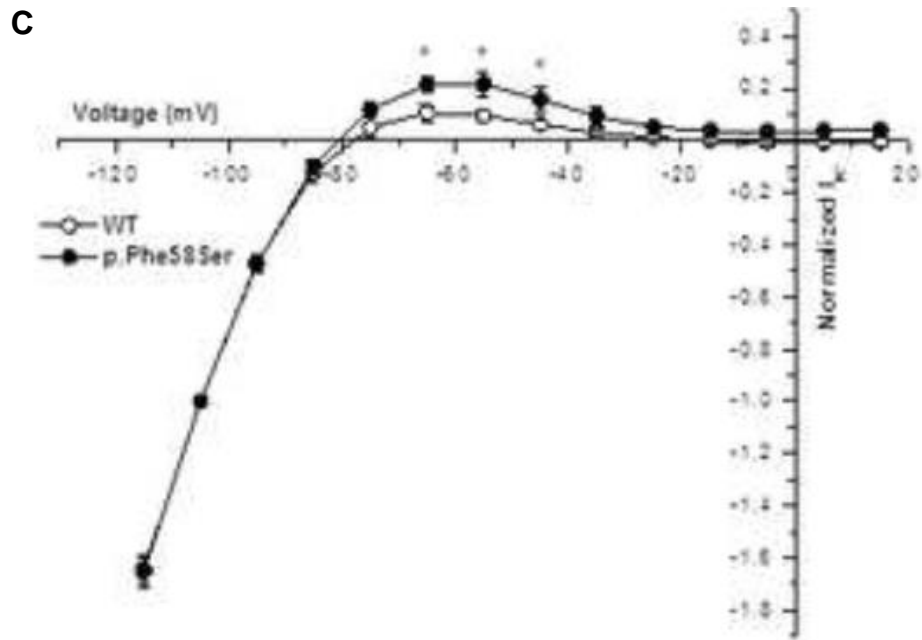


Fig. 2. Functional characterization of wild-type (WT) and mutant *KCNJ2*. C: Current-Voltage relation of normalized current (to -115 mV), showing also the difference in the rectification properties of the channel.

Fig. 3

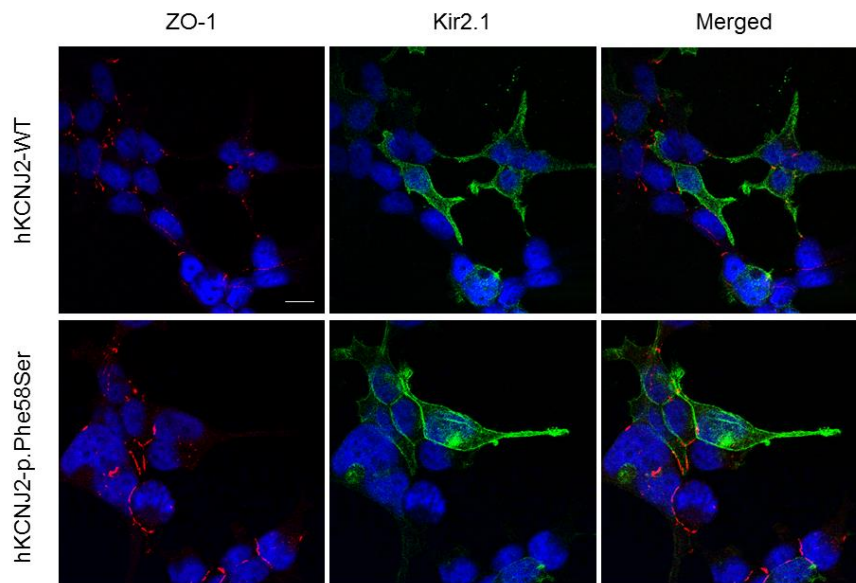


Fig. 3 . Immunofluorescence staining of tsA201 cells expressing either WT (upper panel) or p.Phe58Ser (lower panels) *KCNJ2*. Images in the left column represent ZO-1 labeled in red, in the central column Kir2.1 is stained in green and the right column represent the merged images. Nuclei were stained in blue. The scale bar is 10 μ m. The images presented are typical from three sets of experiments.

References

- [1] Lopatin A.N. et al., Potassium channel block by cytoplasmic polyamines as the mechanism of intrinsic rectification. *Nature*. 1994;372: 366-369.
- [2] Fakler B. et al., Strong voltage dependent inward rectification of inward rectifier K⁺ channels is caused by intracellular spermine. *Cell*. 1995;80: 149-154.
- [3] Melnyk P. et al., Differential distribution of Kir2.1 and Kir2.3 subunits in canine atrium and ventricle. *Am J Physiol Heart Circ Physiol*. 2002;283: H1123-1133.
- [4] Karschin C. et al., IRK (1-3) and GIRK (1-4) inwardly rectifying K⁺ channel mRNAs are differently expressed in the adult rat brain. *J Neurosci*. 1996;16: 3559-3570.
- [5] Donaldson M.R. et al., Andersen-Tawil syndrome: a model of clinical variability, pleiotropy, and genetic heterogeneity. *Ann Med*. 2004; 36: 92-97.
- [6] Guglielmi L. et al., Update on the implication of potassium channels in autism: K⁺ channel autism spectrum disorder. *Front Cell Neurosci*. 2015; 9: 34.
- [7] Priori S.G. et al., A novel form of short QT syndrome (SQT3) is caused by a mutation in the *kcnj2* gene. *Circ Res*. 2005;96: 800-807.
- [8] Hofherr A. et al., Selective Golgi export of Kir2.1 controls the stoichiometry of functional Kir2.x channel heteromers. *J Cell Sci*. 2005;118: 1935-1943.
- [9] Haruna Y. et al., Genotype-Phenotype Correlations of KCNJ2 Mutations in Japanese Patients With Andersen-Tawil Syndrome. *Hum*

Mutat. 2007;28: 208.

[10] Chandrasekhar K.D. et al., KCNE1 subunits require co assembly with K⁺ channels for efficient trafficking and cell surface expression. *J Biol Chem.* 2006;281: 40015-377 40023.

[11] Bandaranayake A.D. et al., Recent advances in mammalian protein production. *FEBS Lett.* 2014;588: 253-260.

[12] Kalscheur M.M. et al., KCNJ2 mutation causes an adrenergic-dependent rectification abnormality with calcium sensitivity and ventricular arrhythmia. *Heart Rhythm.* 2014;11: 885-894.

[13] Eckhardt L.L. et al., KCNJ2 mutations in arrhythmia patients referred for LQT testing: a mutation T305A with novel effect on rectification properties. *Heart Rhythm.* 2007;4: 323-329.

[14] Ambrosini E. et al., Genetically induced dysfunctions of Kir2.1 channels: implications for short QT3 syndrome and autism-epilepsy phenotype. *Hum Mol Genet.* 2014;23: 4875-4886.

[15] Houtman M.J.C. et al., Insights in Kir2.1 channel structure and function by an evolutionary approach; cloning and functional characterization of the first reptilian inward rectifier channel Kir2.1, derived from the California kingsnake (*Lampropeltis getula californiae*). *Biochem Biophys Res Commun.* 2014;452: 992-997.

[16] Ma D. et al., Golgi export of the kir2.1 channel is driven by a trafficking signal located within its tertiary structure. *Cell.* 2011;145: 1102-1115.

[17] Willis B.C. et al., Protein assemblies of sodium and inward rectifier potassium channels control cardiac excitability and arrhythmogenesis. *Am J Physiol Heart Circ Physiol.* 2015;308:

H1463-1473.

[18] Preisig-Muller R. et al., Heteromerization of Kir2.x potassium channels contributes to the phenotype of Andersen's syndrome. *Proc Natl Acad Sci USA*. 2002;99: 7774-7779.

[19] Pegan S. et al., Cytoplasmic domain structures of Kir2.1 and Kir3.1 show sites for modulating gating and rectification. *Nature Neurosci*. 2005;8: 279-287.

[20] De Marco García N.V. et al., Neuronal activity is required for the development of specific cortical interneurone subtypes. *Nature*. 2011;472: 351-355.

Chapter 4:

A Novel Copy Number Variant of GSTM3 in Patients with Brugada Syndrome

J.-M. J. Juang¹, I. Rivolta⁸, T.-P. Lu^{3,4}, S.-J. Lee⁵, L.-C. Lai², Y.-Y. Su²,
Y.-B. Liu¹, L.-Y. Lin¹, W.-J. Chen¹, A. Binda⁸, C.-C. Yu¹, Y.-C. Hsiao¹
, F.-T. Chiang¹, C.-T. Tsai¹, S.-F. S. Yeh⁶, L.-P. Lai¹, J.-J. Hwang¹, E.
Y. Chuang⁷, J.-L. Lin¹

¹ Division of cardiovascular center and Department of Internal Medicine, National Taiwan University Hospital and National Taiwan University College of Medicine, Taipei, Taiwan

² Graduate Institute of Physiology, National Taiwan University, Taipei, Taiwan

³ Institute of Epidemiology and Preventive Medicine, National Taiwan University, Taipei, Taiwan

⁴ Department of Public Health, National Taiwan University, Taipei, Taiwan

⁵ Department of Life Science, National Taiwan University, Taipei, Taiwan

⁶ Department of Environmental and Occupational Medicine, National Taiwan University Hospital and National Taiwan University College of Medicine, Taipei, Taiwan

⁷ Graduate Institute of Biomedical Electronics and Bioinformatics, National Taiwan University, Taipei, Taiwan

⁸ School of Medicine and Surgery, University of Milano-Bicocca, Monza, Italy

Manuscript in preparation

Abstract

Introduction

Brugada syndrome (BrS) is a life-threatening arrhythmic disease in young adults with structurally normal hearts. Although 13 BrS-causal genes have been identified in the past 20 years, in approximately 60–70% of patients with BrS the genetic cause of the disease remains unclear. The potential candidate copy number variants (CNVs) for BrS were never investigated before.

Methods

We enrolled 37 BrS patients without mutations in the 13 BrS-causal genes and randomly selected 16 BrS patients for CNV studies using Illumina Omni1-Quad microarrays. The results were validated in the remaining 21 BrS patients and 213 healthy controls using multiplex polymerase chain reaction (PCR). An *in vitro* model of HEK cells stably expressing cardiac sodium channel Nav1.5 was used to study the pathogenic mechanisms of disease.

Results

We found that copy number of *GSTM3* was significantly lower in BrS patients compared to that in the healthy controls (0.88 vs. 2.0, $p = 1.81 \times 10^{-9}$). A large-scale investigation of the CNV region of *GSTM3* in 4 world-renowned CNV databases and 6 microarray datasets showed that the *GSTM3* deletion occurred infrequently in individuals without BrS in the Asian population (37.5% vs. <1%, $p < 0.001$). Furthermore, data obtained with patch clamp technique showed that in an environment characterized by oxidative stress, *GSTM3* downregulation could lead to a significant decrease in the availability

of the cardiac sodium current.

Conclusions

In conclusion, we identified for the first time a novel CNV of *GSTM3* in BrS patients and suggested that CNV could be one of the possible genetic variants causing BrS. Moreover we demonstrated that, in a presence of an oxidative agent, a *GSTM3* reduced expression promoted a reduction in the cardiac sodium current that could eventually explain proarrhythmogenic events.

Keywords: Brugada Syndrome; copy number variations; *GSTM3*; *SCN5A*

1. Introduction

Brugada syndrome (BrS) is an inherited arrhythmia disease with a distinctive electrocardiogram (ECG) pattern that unfortunately could lead to sudden cardiac death (SCD) in the absence of identifiable structural heart defects. The prevalence of BrS is estimated to be 1–5 per 10,000 people in Europe [1]. Epidemiologic studies have shown that Southeast Asia has the highest prevalence of BrS worldwide. Compared to Western countries, the prevalence of BrS is higher in Southeast Asia (12 per 10,000) [2; 3]. The average age at the time of initial diagnosis of BrS or SCD is 40 ± 22 years, and it is more prevalent in men [4].

Although some BrS-associated genes were successfully identified through linkage analyses in familial BrS patients, more than 70% of BrS patients have no family history of SCD or BrS [5]. *SCN5A*, which was firstly identified in 1998, is the most common BrS-causal gene and is known to be responsible for around 20–25% of BrS in

Caucasian populations. The frequency of these mutations associated with BrS is even lower in the Chinese Han population (7.5–8%) [6]. After two decades, mutations in the 12 newly identified *CACNA1C*, *CACNB2b*, *CACNA2D1*, *GPD1L*, *HCN4*, *SCN1B*, *SCN3B*, *KCND3*, *KCNE3*, *KCNE5*, *KCNJ8* and *MOG1* genes account for 12–13% of BrS cases [3; 7]. However, disease-causal genes remain unknown in approximately 60–70% of patients with BrS.

Current molecular diagnosis methods can resolve less than 30-40% of BrS cases. The reasons for this include phenotyping errors, inadequate sensitivity of screening methods such as denaturing high-performance liquid chromatography and direct sequencing, mutations in non-coding regions, and mutations in unknown genes. In addition, another possibility of negative molecular screening may be the presence of copy number variations (CNVs) in genes affecting the onset of BrS, which cannot be detected using capillary sequencing. Thus, examining CNVs of BrS patients may improve the results of molecular screening [8; 9].

DNA copy number has played an important role in several biological studies, including cardiovascular diseases [10; 11]. For instance, the pathogenic process of Alagille syndrome was associated with the deletion of 20p11.2-p12 [12]. DNA CNVs can dysregulate a critical protein product through the corresponding dosage-sensitive gene. Such quantitative changes may lead to a polygenic cardiovascular disease in the concurrent presence of additional genetic or environmental factors [10]. Although traditional screening of gene mutations helps the identification of causative variants, this approach

may result in “miss the forest for the trees” because of the neglect of an important confounding factor, CNV [10]. Therefore, a better strategy is to investigate the genetic basis of a disease by concurrently studying associated gene mutations and CNVs.

To evaluate whether CNVs are important in BrS, we conducted an exploratory study in BrS patients without mutations in published BrS-causal genes. We identified that the frequency of CNV deletions in *GSTM3* was significantly higher in BrS patients than that in healthy controls. *GSTM3* encodes a glutathione S-transferase, that is important for cellular anti-oxidant activity by catalyzing the conjugation of reduced glutathione with oxidative intermediates. Conjugated molecules are less toxic and can be easily removed from the cell [13]. Cardiac oxidative stress caused by reactive oxygen species (ROS) could induce alteration in membrane currents, as, for example, it reduces both sodium current and sodium channel availability [14]. We thus investigated whether ROS effects might be more dramatic when *GSTM3* protein expression is imbalanced as in BrS patients with CNV deletions in *GSTM3*.

2. Materials and methods

2.1. Study subjects and genetic screening for the 13 published BrS-causal genes

This study was approved by the local ethical committee of the National Taiwan University Hospital (200911009R) and all study subjects gave informed consent before participating in the study.

BrS was definitively diagnosed when a coved-type ST-segment elevation (type I) pattern was observed in more than 1 right precordial

lead (V1–V3) in the presence or absence of a sodium channel blocking agent (procainamide or flecainide), and in conjunction with at least 1 of the following criteria: SCD, documented ventricular fibrillation, polymorphic ventricular tachycardia, syncope, or nocturnal agonal respirations [15-18]. BrS was definitively diagnosed by two independent cardiologists according to established criteria [17].

Genetic screening of 13 published BrS-causal genes (*SCN5A*, *CACNA1C*, *CACNB2b*, *CACNA2D1*, *GPD1L*, *HCN4*, *SCN1B*, *SCN3B*, *KCND3*, *KCNE3*, *KCNE5*, *KCNJ8*, *MOG1*), was performed with PCR. We consecutively recruited a cohort of unrelated 51 non-familial symptomatic BrS patients from medical centers or hospitals in Taiwan from 2000 (COBRA_ChiP registry). Fourteen BrS patients with any mutations or CNV in the 13 published BrS-causal genes [7] were excluded from further CNV analyses. Since some studies reported that *SCN5A* SNPs may have a functional impact on BrS [19; 20], we also excluded BrS patients with SNPs in *SCN5A* for further studies.

2.2. *Illumina Omni1-Quad microarray experiments*

We randomly selected 16 BrS patients without any mutations in the 13 published BrS-causal genes and 16 unrelated age- and gender-matched healthy controls to investigate CNVs using Illumina Omni1-Quad BeadChip microarrays (Illumina, San Diego, CA). Microarray experimental procedures followed the standard protocols provided by the manufacturer. The microarray data have been submitted to the Gene Expression Omnibus with the accession number: GSE46348.

To evaluate whole-genome CNV regions (CNVRs), raw intensity data from 1.14 million SNPs and CNV probes were imported into Partek Genomics Suite software (Partek Inc., St Louis, MO) to perform CNV analysis [21]. CNVRs in sex chromosomes were excluded. Lastly, Ingenuity Pathway Analysis (IPA, Ingenuity Systems, Inc., Redwood City, CA) was performed to characterize the biological functions of genes located in CNVRs.

2.3. External validation of identified CNVR using multiplex PCR

Copy number of identified CNVR was evaluated using multiplex PCR in the original 16 and additional 21 unrelated BrS patients (validation set) and 213 unrelated healthy controls concurrently. PCR products were quantified using the Gel-Pro Analyzer 4.0 (Media Cybernetics, Rockville, MD). Band intensities of identified CNVR was normalized to the internal control and copy number was determined by multiplying the relative quantities by two.

2.4. Investigation of identified CNVR in different populations

To examine the copy number changes in identified CNVR in different populations, we investigated 4 CNV databases [22-25] and 6 microarray datasets [21; 26-31]. To reduce potential bias resulting from tissue specificity, only microarrays from the peripheral blood were included, which resulted in 1,126 samples. The criterion for identifying CNVRs were the same as those described above.

2.5. Cell cultures and GSTM3 silencing

HEK cells stably expressing SCN5A gene (encoding HEK Nav1.5 channel) were a kind gift from Prof. Hugues Abriel (University of Bern, Switzerland). Cells were cultured in a controlled environment

(5% CO₂, 37°C) and maintained in Dulbecco's Modified Eagle Medium (DMEM; Euroclone, Italy) supplemented with FBS (10%), L-Glutamine (2 mM), Pen/Strep (100 U/mL, 100 µg/mL), zeocin (200 µg/mL). HEK Nav1.5 cells were transfected with GSTM3 Silencer Select Pre-designed siRNA (20 nM; Ambion, Thermo Fisher Scientific, Italy) or with Silencer Select Negative Control #1 Pre-designed siRNA, a negative control siRNA composed by randomized amino acids of GSTM3 siRNA such as the molecule could not target any mRNAs (20 nM; Ambion, Thermo Fisher Scientific, Italy). The transfection was carried out using jetPRIME reagent (PolyPlus transfection Illkirch, France) according to the manufacturer's instructions.

2.6. Western blot

Cells were lysate 24 hours after transfection and cytoplasmic proteins were immediately extracted using NE PER[®] Nuclear and Cytoplasmic Extraction Reagents (Thermo Fisher Scientific, Italy). Protein concentrations were detected using Bradford assay reagent (Pierce Coomassie Plus Protein Assay; Thermo Fisher Scientific, Italy) following manufacturer's instructions. 25 µg of cytoplasmic proteins were separated on homemade gels (12% acrilammide) in a proper running buffer and then transferred on nitrocellulose membranes (GE Healthcare, Euroclone, Italy). Membranes were blocked with 5% non-fat dry milk in 1×TBS containing 0.1% Tween 20 (TTBS 0.1%) for 90 minutes at room temperature, washed three times in TTBS 0.1% and then incubated overnight at 4 °C with anti- α -tubulin (1:500 in TTBS 0.1% plus milk 5%, rabbit monoclonal; Cell Signaling, Danvers, MA,

USA) and anti-human glutathione S-transferase mu 3 (1:1000 in TTBS 0.1% plus milk 5%, rabbit polyclonal; Cusabio Biotech Co, College Park, MD, USA). After three TTBS 0.1% washing, membranes were incubated for 90 minutes with a proper IgG HRP conjugated antibody (donkey anti-rabbit, 1:5000 in TTBS 0.1% plus milk 1%; Santa Cruz Biotechnology) and then washed again three times in TTBS 0.1%. Proteins were detected using an enhanced chemiluminescence (ECL) detection kit (SuperSignal West Pico Chemiluminescent Substrate; Thermo Fisher Scientific, Italy) in the ImageQuant LAS 4000 instrument (GE Healthcare Life Sciences, Italy). Images were analyzed and blots were quantified with ImageJ software.

2.7. Cytotoxicity assays

Both MTT (3-(4,5-dimethylthiazol-2-yl)-2,5-diphenyltetrazolium bromide MTT Formazan powder, Sigma-Aldrich, Italy) and Lactate Dehydrogenase (LDH Cytotoxicity Detection Kit^{PLUS}, Sigma-Aldrich, Italy) assays were performed 24 hours after transfection following manufacturer's instructions. Cells were incubated either with medium or 30 or 60 minutes medium plus 15 mM tert-Butyl hydroperoxide (tBHP, Sigma-Aldrich, Italy). Absorbance emissions were measured with the multi-label spectrophotometer 98 VICTOR3 (Perkin Elmer, MA, USA) at 570 nm and at 490 nm respectively.

2.8. Electrophysiology recordings

Whole-cell patch clamp experiments were performed 24 hours after transfection. Cells medium was replaced with an extracellular solution containing (in mM) 110 N-methyl-D-glucamine, 20 NaCl, 5 CsCl, 2

CaCl₂, 1.2 MgCl₂, 10 HEPES, 5 glucose while pipettes were filled with an intracellular solution containing (in mM) 60 KAsp, 60 CsCl, 11 EGTA, 1 CaCl₂, 1 MgCl₂, 5 Na₂ATP, 10 HEPES. To induce a condition of oxidative stress, cells were incubated for 30 minutes at room temperature with an extracellular solution containing (in mM) 95 N-methyl-D-glucamine, 20 NaCl, 5 CsCl, 2 CaCl₂, 1.2 MgCl₂, 10 HEPES, 5 glucose, 15 mM tert-Butyl hydroperoxide and recordings were obtained within 60 minutes from the beginning of the treatment. Patch clamp recordings were performed at room temperature using pipettes pulled to a resistance of 2-5 MΩ (P-97 Sutter Instruments, CA, USA). Data were acquired with a Multiclamp 700B amplifier (Axon Instruments, Molecular Device, CA, USA), Digidata 1440A (Axon Instruments, Molecular Device, CA, USA) and pClamp 10.3 software (Molecular Devices, CA, USA). Sodium currents were evoked by a protocol of voltage steps ranging from -80 mV to +80 mV in 10 mV increments with a duration of 30 ms (holding potential -100 mV). Steady State Inactivation was studied applying a two steps protocol consisting of a first pulse ranging from -140 to +10 mV (duration 100 ms, increment +10 mV) followed by a pulse of +10 mV (duration 20 ms, holding -100 mV). Steady State Activation and Inactivation data were fitted with a Boltzmann function $y = 1/(1 + \exp((V-V_{1/2})/k))$ where y is the relative current, V is the membrane potential, V_{1/2} is the half-maximal voltage while k is the slope factor; Origin software (OriginLab Corporation, Northampton, Massachusetts, USA) was used.

2.9. Statistical analyses

All continuous data were expressed as mean \pm standard error. Student's *t*-test was used to compare continuous variables among different groups. Categorical variables and CNV proportions were analyzed using chi-square or Fisher's exact tests. $p < 0.05$ was considered statistically significant and indicated with *.

3. Results

3.1. Clinical characteristics of the BrS patients without mutations in 13 published BrS-causal genes

The average age at diagnosis of the 37 BrS patients without 13 published BrS-causal genes (33 men, 4 women) was 43 ± 15 years (Table 1). Eighteen patients (49%) had been resuscitated from SCD and 16 (43%) had presented with syncope or seizure. A comparison of clinical profiles from BrS patients with and without 13 published BrS-causal genes is shown in Table 1. There were no significant differences in age at diagnosis, gender, percentage of SCD or family history of SCD between the 2 groups.

3.2. Frequent CNVRs in the BrS patients without mutations in 13 published BrS-causal genes.

Most CNVRs were deletions across different chromosomes, and the proportion of deletion was much higher than that of amplification (89.2% vs. 10.8%). A total of 502 aberrant regions were observed, including 447 deletions and 55 amplifications. Importantly, no CNVs were detected in 13 published BrS-causal genes. The Refseq database revealed 91 deleted and 11 amplified genes in total. Among the 102

CNV genes, IPA was used to characterize the biological functions and signaling pathways. The results revealed five significantly enriched canonical pathways ($p < 10^{-5}$). Notably, although the 5 pathways had different cellular functions, they were primarily identified on the basis of the same genes, particularly the glutathione S-transferase (GST) mu family. Unexpectedly, all 5 genes in the GST mu family, including *GSTM1-5*, showed high frequencies of deletions, suggesting they make up a gene cluster deleted in BrS. Among the deletion located on chr1:109,996,713–110,083,552, *GSTM3* displayed the most consistent and lowest copy number (0.88). Therefore, *GSTM3* was selected for further investigations.

3.3. Clinical profiles of the BrS patients with and without the CNV in GSTM3

Twenty-eight of the 37 BrS patients without mutations in 13 published BrS-causal genes had a heterozygous deletion of *GSTM3*. Comparisons of clinical characteristics between BrS patients with or without this deletion are shown in Table 2. There were no significant differences in age at diagnosis, gender, or family history of SCD between the two groups. However, a significantly higher percentage of BrS patients with this CNV of *GSTM3* experienced SCD and received an implantable cardioverter defibrillator (ICD) implantation than those without ($p = 0.04$ and 0.01 , respectively). In contrast, BrS patients without this CNV of *GSTM3* presented with significantly higher frequency of syncope ($p=0.02$) than those with this CNV of *GSTM3*.

3.4. Validation of the CNV of GSTM3 in BrS patients and healthy controls using multiplex PCR

To design PCR primers for CNVs of *GSTM3*, the segment with the lowest copy number was targeted. In addition, a commonly used reference gene in CNV analysis, *RPPH1* [32], and one selected region with an invariable copy number were examined as internal controls. No significant difference in copy number for *RPPH1* and the selected region was observed (data not shown). In contrast, *GSTM3* copy numbers was significantly lower in BrS patients than that in healthy controls ($p = 1.81 \times 10^{-9}$). *GSTM3* showed deletions in approximately 75.7% of BrS patients, but in only 17 % of healthy controls ($p = 5.18 \times 10^{-12}$). These results indicate the CNVR of *GSTM3* is a heterozygous deletion with significantly low copy number and high frequency in BrS patients without mutations in the 13 published BrS-causal genes.

3.5. Validation of the CNV of GSTM3 by comparing large databases and microarray datasets

After multiplex PCR validations, we conducted a large-scale investigation using 4 world-renowned online CNV databases [22-25] and 6 microarray datasets. No corresponding deletion for *GSTM3* was reported in the 4 databases, including 101,923 samples in the DGV [23], which is the largest CNV database worldwide. Next, the same CNV analysis procedures were performed to explore the status of the two CNVRs in the 6 microarray datasets containing 1,126 samples. The percentage of deletions in *GSTM3* in BrS patients was significantly higher than that in healthy controls ($p < 0.001$; data not shown). To examine ethnic differences, we compared the percentage

of deletions in BrS patients with that in other Asian populations without BrS. The deletion frequencies of *GSTM3* in BrS patients was also significantly higher (37.5% vs. <1%, $p < 0.001$). These results suggested that the deletion in *GSTM3* could be associated with BrS patients without mutations in the 13 published BrS-causal genes.

3.6. Establishment and validation of a cellular model

In order to evaluate whether altered *GSTM3* CNV in BrS patients had consequences on cardiac sodium current, we firstly established an *in vitro* model of HEK cells stably expressing SCN5A gene (HEK Nav1.5) in which we could induce *GSTM3* protein expression downregulation by transfecting the cells with siRNA molecules properly designed in order to target *GSTM3*. 24 hours after the transfection, cells were lysate and western blot experiments on protein extracts were subsequently performed, confirming that siRNA transfection could reduce *GSTM3* expression on average of almost 50% compared to control cells. Moreover, when HEK Nav1.5 cells were transfected with a negative control siRNA for *GSTM3* (NEG CTRL siRNA), the expression of the protein studied was globally unchanged, confirming that only siRNA transfection was able to modify *GSTM3* expression (fig. 1). Control, siRNA and negative control siRNA transfected cells were incubated with 15 mM tBHP, an organic peroxide that triggers a condition of overall oxidative stress in the cells, and *in vitro* toxicity tests were performed. MTT assay showed that mitochondrial activity was not altered neither by the transfection nor by tBHP exposure, thus metabolic activity in the three conditions of cells tested was overall not compromised after the

incubation with the drug for 30 or even 60 minutes (fig. 2A). LDH assay was also performed. Data suggested that, despite the transfection caused a slight cytotoxicity in general ($4.35\pm 2.63\%$ in siRNA transfected cells, $3.92\pm 2.20\%$ in NEG CTRL siRNA transfected cells), the effect of tBHP application was indistinguishable in control and transfected cells after 30 min. ($8.77\pm 3.50\%$ CTRL, $8.83\pm 3.08\%$ siRNA, $10.71\pm 3.61\%$ in NEG CTRL siRNA) or 60 min. of incubation ($9.00\pm 1.76\%$ CTRL, $10.44\pm 5.61\%$ siRNA transfected cells, $11.52\pm 4.77\%$ in NEG CTRL siRNA transfected cells) (fig. 2B). These results were in line with the fact that, being tBHP an oxidative agent that among its effects induces membrane lipidic peroxidation, the administration of the drug partially damaged the plasma membrane. However, data suggested that tBHP-induced cytotoxicity was not significant.

3.7. Evaluation of *GSTM3* downregulation on cardiac sodium current

Whole-cell patch clamp experiments were performed to study the effect of oxidative stress, mimicked by the application of 15 mM of tBHP, on sodium Nav1.5 current in control, siRNA and NEG CTRL siRNA transfected cells. Current density at -10 mV was measured and results showed that this parameter was not affected by the siRNA transfections (-145.91 ± 24.35 pA/pF n=44 control, -164.43 ± 32.00 pA/pF n=20 siRNA, -146.97 ± 21.96 pA/pF n=23 NEG CTRL siRNA, fig. 3). As expected from the literature, a condition of oxidative stress triggered a decrease in the peak of I_{Na} [33], indeed sodium current density at -10 mV was significantly reduced almost of 60% both in control and in cells transfected with the negative control

(CTRL+tBHP: -55.37 ± 16.12 pA/pF $n=13$; CTRL vs CTRL+tBHP $p < 0.001$; NEG CTRL siRNA+tBHP: -64.45 ± 21.96 pA/pF $n=18$; NEG CTRL vs NEG CTRL+tBHP $p < 0.001$, fig.3). Interestingly, when GSTM3 protein expression was decreased, tBHP-induced current density reduction was about 75% less compared to unstressed cells (-41.41 ± 8.50 pA/pF $n=23$; siRNA vs siRNA+tBHP $p < 0.001$) (fig. 3). In accordance with previous studies [14; 34], no significant differences were marked in the steady state activation after drug application ($V_{1/2}$ CTRL: -24.35 ± 1.24 mV $n=13$, -21.67 ± 2.22 mV $n=6$; NEG CTRL: -24.19 ± 2.82 mV $n=6$, -19.30 ± 2.87 mV $n=6$; siRNA: -20.81 ± 4.73 mV $n=4$, -22.83 ± 5.32 mV $n=8$ without and with tBHP administration respectively; data not shown) but tBHP exposure induced a significant hyperpolarized shift of the inactivation curves (fig.4). When HEK Nav1.5 cells were treated with tBHP, $V_{1/2}$ significantly shifted of about -8 mV in the negative direction from a value of -64.00 ± 2.22 mV ($n=28$) to a value of -72.53 ± 0.97 mV ($n=6$) ($p < 0.005$). A similar shift was also observed in cells transfected with the negative control siRNA ($V_{1/2}$ -67.05 ± 1.82 mV $n=10$ and -75.87 ± 2.82 mV $n=15$ in absence and in presence of tBHP respectively; $p < 0.001$). When GSTM3 expression was downregulated, no difference in the availability curve was found ($V_{1/2}$ -64.48 ± 1.65 mV $n=19$) compared both to untransfected cells and to negative control siRNA transfected cells. But, after the induction of oxidative stress, $V_{1/2}$ showed a more negative shift (about -18 mV) compared to previous results ($V_{1/2}$ -82.85 ± 2.67 mV $n=7$; $p < 0.001$ CTRL tBHP vs siRNA tBHP). These data are in line with the hypothesis that a reduction in the expression of GSTM3 could induce

a larger effect of the oxidative stress on Nav1.5 current amplitude.

4. Discussion

Brugada syndrome is an inheritable life-threatening cardiac arrhythmia defined in 1992 with an highest prevalence in southeast Asia. After two decades, disease-causing genes in 65–70% of BrS patients still remain unclear. To our knowledge, this is the first study investigating CNVs in BrS patients. The results demonstrated that a CNV involving the deletion of GSTM3 accounted for 75.7% of BrS cases who were not detected any mutations in the 13 published BrS-causal genes (28 of 37 BrS patients, 95% confidence interval [CI]: 0.62–0.90). In addition, this deletion of GSTM3 was rarely detected in Asian populations, suggesting that it was highly associated with BrS and could be a possible genetic variant for BrS patients without mutations or CNVs in the 13 published BrS-causal genes. The deletion of GSTM3 was a heterozygous deletion containing the eighth exon and the transcription terminal loci and may have resulted in haploinsufficiency, that is one copy of a gene was deactivated due to deletions and the other functional copy of the gene could not produce a sufficient amount of the corresponding protein, whose expression has been reported in the ventricle of human heart [35]. Since the CNV contains a transcription stop codon, this deletion may result in failed transcription termination, leading to nonsense-mediated degradation of GSTM3 mRNA [36]. Furthermore, it is interesting that all 5 genes in the GST mu family showed high proportions of copy number losses. Based on the close physical locations of the 5 GSTM genes

located on chromosome 1, these genes may be deleted as a gene cluster in BrS. In addition, functional characterization of the 102 genes with CNVs also showed that the top 5 canonical pathways with very stringent p-values were composed of GST genes.

GST genes encode glutathione S-transferases which are important enzymes involved in anti-oxidant defense protecting the cells from oxidative stress [37]. Arrhythmic conditions are associated with systemic and cardiac oxidative stress caused by ROS. In excitable cardiac cells, ROS regulates both cellular metabolism and ion homeostasis. Increasing evidence suggests that elevated cellular ROS can cause alterations of membrane currents in isolated cardiac myocytes [33] and an abnormal Ca^{2+} handling, leading to arrhythmogenesis [38]. In particular, ROS induce a reduction in the total cardiac sodium current (Nav1.5 channels) and a leftward shift in their availability curve [14; 33]. Our data obtained in a cellular model of HEK cells stably expressing Nav1.5 channels after the treatment with the direct-acting oxidative agent tBHP were in line with those previous considerations. As GSTM3 CNV deletions should induce a decrease in the production of the corresponding protein, we transfected siRNA to downregulate GSTM3 expression in the HEK Nav1.5 expressing cells and observed consequences of the induction of oxidative stress in silenced comparing to unsilenced cells. Data showed that the changes in sodium current in presence of tBHP were even more dramatic than in control cells: the sodium current peak density was smaller and the steady state inactivation curve was more hyperpolarized, which implies that less sodium channel are available

to open at a certain voltage when GSTM3 expression is impaired and oxidative stress is induced. Since BrS has a heterogeneous genetic basis that can be attributed to several ion channel-related genes whose functional consequences could be more or less severe, pathophysiological mechanisms of disease are still yet elusive and several hypotheses have been formulated but not irrefutably demonstrated [39]. Interestingly, a general reduction in the total cardiac Na^+ current could be associated to a slowdown in the conduction velocity and to prolonged refractoriness in ventricular myocardium, both providing a substrate for reentry [40], one of the proposed pathophysiological mechanism of BrS [39]. Moreover, an excessive reduction of cardiac sodium current could also support transmural dispersion of repolarization between epicardium and endocardium [34], which is another mechanism suggested to explain BrS etiology [39]. Knowing that an increase of cellular oxidative stress could generally bring to a reduction in the availability of cardiac voltage gated sodium channel population, our data suggest that oxidative stress may induce more dramatic consequences on cardiac I_{Na} when GSTM3 is less expressed, which is the condition found analyzing CNV in BrS patients. These consequences on sodium current are compatible with the pathophysiological mechanism underlying the BrS.

The value of genetic mutations as a tool to evaluate recurrent arrhythmic risk in BrS is still undetermined [3]. Most of previous studies showed that there was no difference in recurrent arrhythmic events when dividing patients according to the presence or absence of

SCN5A mutations. Considering patients lacking of mutations in SCN5A gene, oxidative stress is reported to be usually more elevated in the heart of BrS patients characterized by ventricular fibrillations compared to those who do not show such episodes [41]. In this study, the percentage of SCD in BrS patients with the GSTM3 deletion CNV (and without SCN5A mutations) was significantly higher than that in the BrS patients without the deletion, which suggested that an impairment in the mechanism of rescue from oxidative stress might lead to more severe clinical presentations of the disease. The results in this study may provide an important implication that genotyping of the CNVs of GSTM3 could provide a critical reference for risk stratification of patients with BrS. In other words, we suggested that BrS patients with the CNV of GSTM3 belong to the high-risk group of SCD. Prophylactic implantation of ICD may be warranted in this high-risk group although a prospective large-scale randomized clinical trial is necessary to prove our observation.

In summary, we provided a possible link between the CNV deletion of GSTM3 in BrS patients and oxidative stress-induced modifications on cardiac sodium current, which seem to be in accordance with the mechanisms of BrS.

5. Conclusions

In conclusion, we first identified a CNV of *GSTM3* in BrS patients and suggested that CNV could be one of the possible genetic variants in BrS patients, especially in Asian population. In addition, the novel deletions in *GSTM3* was identified in non-familial symptomatic BrS

patients without *SCN5A* variants, suggesting that CNV screening could help diagnose BrS in *SCN5A* variant-negative patients.

Acknowledgments

This research was partially supported through grants NTUH 98-N1266, NTUH 100-N1775, NTUH 101-N2010, NTUH 101-S1780, VN100-08, VN101-04, NTUH 101-S1784, NTUH 102-M2224, NTUH 102-S2099, NTUH 102-S2035, NTUH 103-S2326, UN102-019 and UN 103-018, NTU CESRP-10R70602A5 and NTU ERP-10R80600 from National Taiwan University Hospital, YongLin Biomedical Engineering Center, National Taiwan University, and NSC 101-2314-B-002-168-MY2 and NSC 101-2314-B-002-173-MY2 from National Science Council. We are sincerely grateful to many cardiologists, including Dr. Shih-Ann Chen, Dr. Tsu-Juey Wu, Dr. Shoei K. Stephen Huang, Dr. Yenn-Jiang Lin, Dr. Chun-Chieh Wang, Dr. Chi-Tai Kuo, Dr. Yu-Feng Hu, Dr. Kwo-Chang Ueng, Dr. Hsuan-Ming Tsao, Dr. Kuan-Cheng Chang, Dr. Meng-Huan Lei, Dr. An-Ning Feng, Dr. Chi-Woon Kong, Dr. Wen-Chin Ko, Dr. Jin-Long Huang, Dr. Wen-Chin Tsai, Dr. Chin-Feng Tsai, Dr. Li-Wei Lo, Dr. Huey-Ming Lo, Dr. Meng-Cheng Chiang, Dr. Chun-Chieh Wang, Dr. Chih-Ping Hsia, Dr. Jen-Fu Liu, Dr. Shuenn-Nan Chiu, Dr. Mei-Hwan Wu, Dr. Ming-Tai Lin, Dr. Shuenn-Nan Chiu, Dr. Su-Kiat Chua and many other doctors in other medical centers or hospitals for referring patients to our hospital, and to the staff of the Sixth Core Lab, Department of Medical Research, National Taiwan University Hospital and Zebrafish Core facility of National Taiwan University

for technical support. We also thank the technical/bioinformatics services provided by the National Center for Genome Medicine of the National Core Facility Program for Biotechnology, National Science Council.

Tab. 1

	BrS patients without mutations (N = 37)	BrS patients with mutations (N = 14)	P-value
Age at diagnosis (y)	43 ± 15	42 ± 12	0.33
Gender (Male)	33 (89%)	13 (93%)	1
Presentation			
Sudden cardiac death	18 (49%)	4 (29%)	0.22
Seizure	4 (11%)	2 (14%)	1
Syncope	12 (32%)	4 (29%)	1
Other	3 (8%)	4 (29%)	0.08
Circumstance			
Sleeping	4 (11%)	2 (14%)	1
Awake	33 (89%)	12 (86%)	1
Documented VF or VT	23 (62%)	7 (50%)	0.34
Family history of SCD	6 (16%)	3 (38%)	0.69
Spontaneous Type I Brugada ECG	27 (73%)	10 (70%)	1
ICD implantation	25 (68%)	7 (50%)	0.33

Tab. 1. Clinical characteristics of BrS patients with or without mutations in 13 published BrS-causal genes. BrS: Brugada syndrome; ECG: electrocardiogram; ICD: implantable cardioverter defibrillator; SCD: sudden cardiac death; SNPs: single nucleotide polymorphisms; VT: ventricular tachycardia; VF: ventricular fibrillation.

Tab. 2

	BrS patients with the CNV of GSTM3 (N = 28)	BrS patients without the CNV of GSTM3 (N = 9)	P-value
Age at diagnosis (years)	44 ± 12	41 ± 18	0.5
Gender (Male)	25 (89%)	8 (89%)	0.97
Presentations			
SCD	17 (60%)	2 (22%)	0.04*
Seizure	4 (14%)	1 (11%)	0.8
Syncope	7 (25%)	6 (67%)	0.02*
Circumstance			0.20
Sleeping	2 (7%)	2 (22%)	
Awake	26 (93%)	7 (78%)	
Documented VF or VT	16 (57%)	7 (77%)	0.26
Family history of SCD	4 (14%)	4 (44%)	0.06
Spontaneous Type I Brugada ECG	16 (76%)	11 (69%)	0.71
ICD implantation	18 (64%)	2 (22%)	0.01*

Tab. 2. Comparisons of clinical characteristics between BrS patients with or without copy number variants (CNV) of GSTM3. BrS: Brugada syndrome; ECG: electrocardiogram; ICD: implantable cardioverter defibrillator; SCD: sudden cardiac death; VT: ventricular tachycardia; VF: ventricular fibrillation. *: $p < 0.05$ by chi-square or Fisher exact test.

Fig. 1

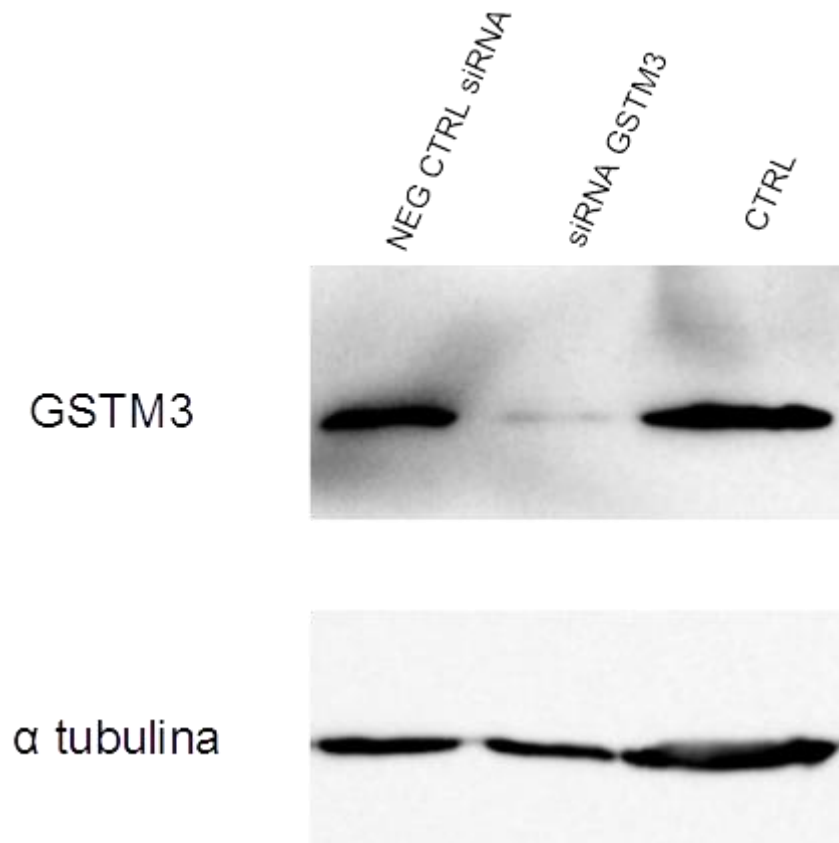


Fig. 1. Western blot results of protein extracts from CTRL: HEK cells stably expressing SCN5A gene (HEK Nav1.5), siRNA GSTM3: HEK Nav1.5 transfected with siRNA against GSTM3 , NEG CTRL siRNA GSTM3: HEK Nav1.5 transfected with GSTM3 negative control siRNA. Data were collected in 3 different experiments of transfection and at least 3 western blots have been performed for each protein extract. Despite heterogeneity of cellular lysates, data confirmed that in our cellular model GSTM3 was downregulated on average of 50%.

Fig. 2

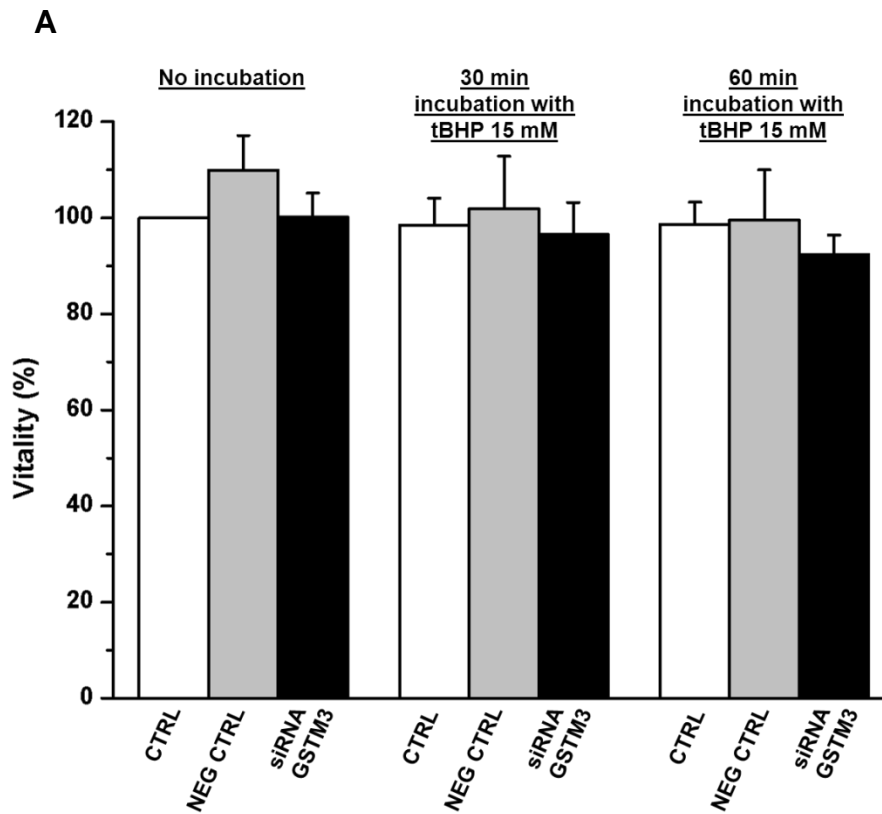


Fig. 2. Incubation with tBHP did not compromise vitality neither of non-transfected nor of transfected cells. A. MTT assay results showed that metabolic activity of the cells was not compromise on average whether oxidative stress was inducted neither after 30 nor after 60 minutes of treatment. Data were collected in 3 different experiments of transfection.

Fig. 2

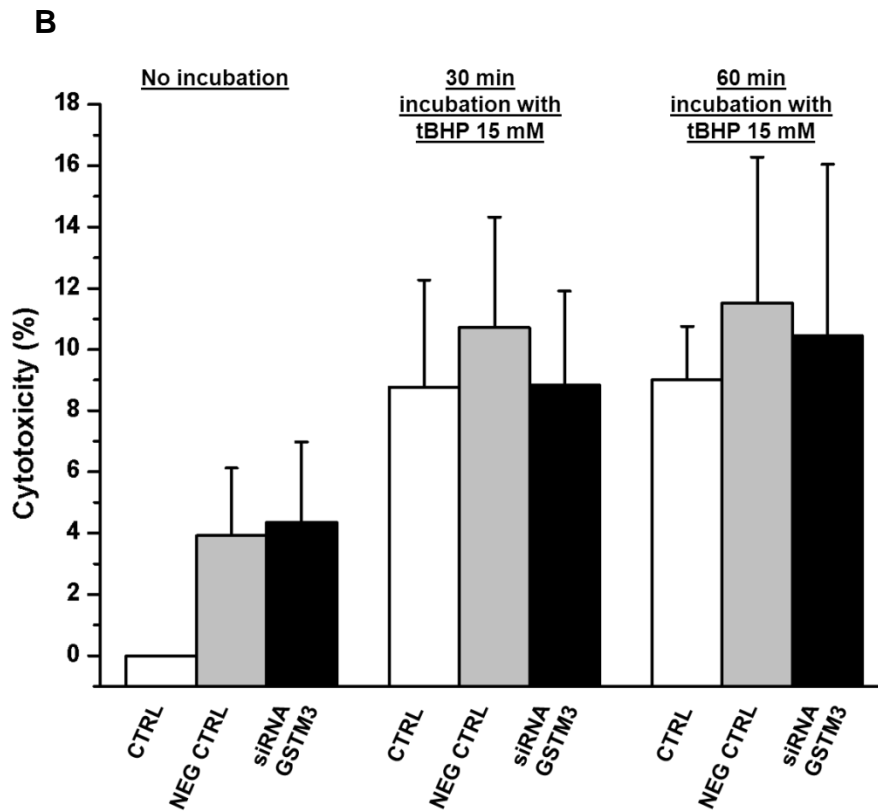


Fig. 2. Incubation with tBHP did not compromise vitality neither of non-transfected nor of transfected cells. B. LDH assay results showed that metabolic activity of the cells was slightly compromise after the transfection both of the negative control and of siRNA. However, the application of tBHP for 30 or 60 minutes induced on average 10% of cytotoxicity with no significant differences in both control and transfected cells. Data were collected in 3 different experiments of transfection.

Fig. 3

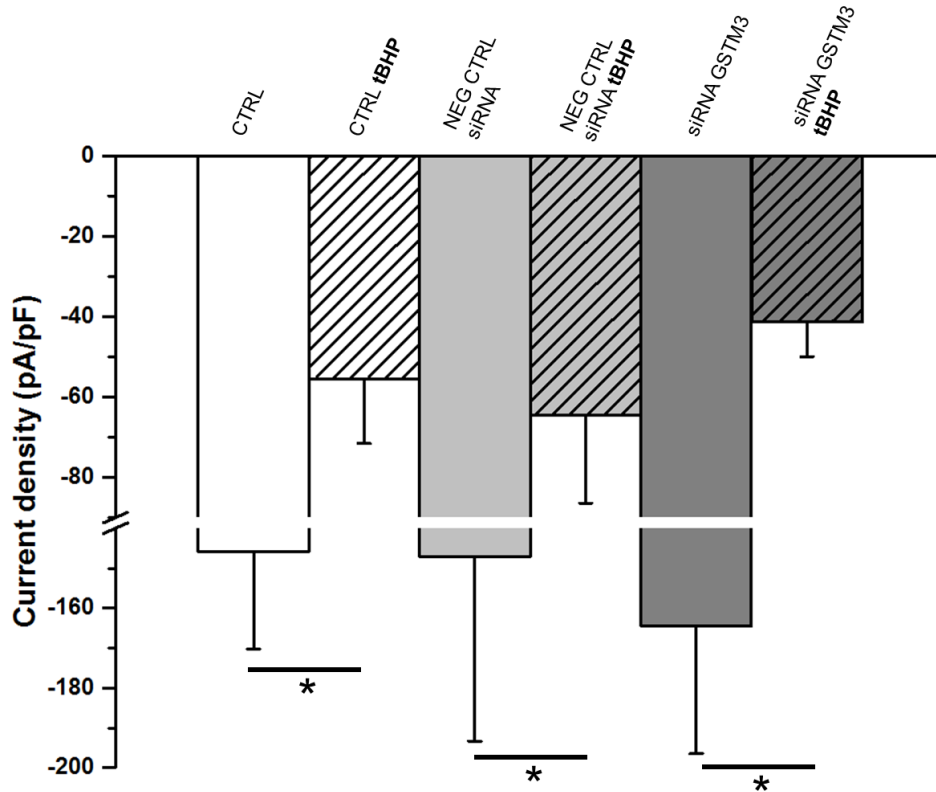


Fig. 3 Effect of the oxidative agent tBHP on the Nav1.5 current density. As expected from the literature, cells treated with tBHP, showed a reduction in the current density. When we transfected the cells with the siRNA negative control, we obtained the same result. The current density is not affected by the siRNA GSTM3 transfection, while in presence of tBHP the current density in those cells is significantly reduced to a larger extent. This result is in line with the hypothesis that a reduction in the expression of GSTM3 induce a higher oxidative stress that compromise Nav1.5 current amplitude.

Fig. 4

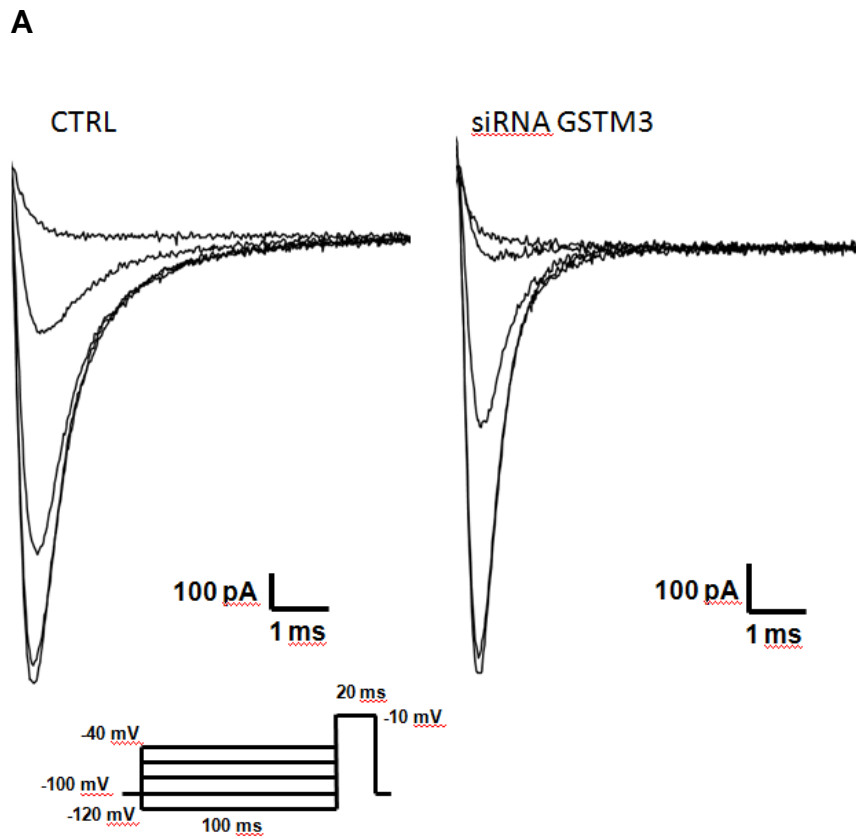


Fig. 4. Effect of the oxidative agent tBHP on the NaV1.5 availability. A. Current traces obtained applying the protocol described at the bottom of the picture showing that the oxidative stress reduced the availability of the sodium current.

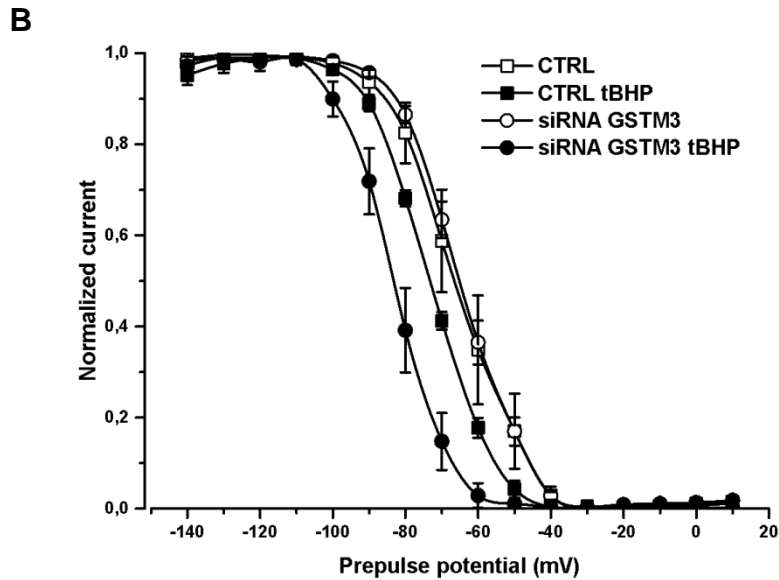


Fig. 4. Effect of the oxidative agent tBHP on the Nav1.5 steady state inactivation curve. B. A negative shift of about -8 mV was observed when control cells were treated with tBHP (open squares vs filled squares, $p < 0.001$). The same results were observed considering cells transfected with the negative control siRNA (data not reported). When GSTM3 was silenced, no difference in the availability curve was found (open circles vs open squares). The incubation of the silenced cells with tBHP, caused a negative shift of about -20 mV (open circles and squares vs filled circles, $p < 0.001$). This result clearly showed that in presence of a reduction in GSTM3 expression and an increase in oxidative stress, the availability of the sodium channels was highly decreased.

References

- [1] Berne P. et al., Brugada syndrome 2012. *Circ J.* 2012;76:1563-71.
- [2] Hermida J.S. et al., Prevalence of the brugada syndrome in an apparently healthy population. *Am J Cardiol.* 2000;86:91-4.
- [3] Mizusawa Y. et al., Brugada syndrome. *Circulation Arrhythmia and electrophysiology.* 2012;5:606-16.
- [4] Juang J.M. et al., Characteristics of Chinese patients with symptomatic Brugada syndrome in Taiwan. *Cardiology.* 2003;99:182-9.
- [5] Probst V. et al., Long-term prognosis of patients diagnosed with Brugada syndrome: Results from the FINGER Brugada Syndrome Registry. *Circulation.* 2010;121:635-43.
- [6] Juang J.-M.J. et al., Unique clinical characteristics and SCN5A mutations in patients with Brugada syndrome in Taiwan. *Journal of the Formosan Medical Association.* 2013.
- [7] Crotti L. et al., Spectrum and prevalence of mutations involving BrS1- through BrS12-susceptibility genes in a cohort of unrelated patients referred for Brugada syndrome genetic testing: implications for genetic testing. *J Am Coll Cardiol.* 2012;60:1410-8.
- [8] Barc J. et al., Screening for copy number variation in genes associated with the long QT syndrome: clinical relevance. *J Am Coll Cardiol.* 2011;57:40-7.
- [9] Redon R. et al., Global variation in copy number in the human genome. *Nature.* 2006;444:444-54.
- [10] Pollex R.L. et al., Copy number variation in the human genome and its implications for cardiovascular disease. *Circulation.*

2007;115:3130-8.

[11] Soemedi R. et al., Contribution of global rare copy-number variants to the risk of sporadic congenital heart disease. *Am J Hum Genet.* 2012;91:489-501.

[12] Li L. et al., Alagille syndrome is caused by mutations in human Jagged1, which encodes a ligand for Notch1. *Nat Genet.* 1997;16:243-51.

[13] Fletcher M.E. et al., Influence of glutathione-S-transferase (GST) inhibition on lung epithelial cell injury: role of oxidative stress and metabolism. *Am J Physiol Lung Cell Mol Physiol.* 2015 Jun 15;308(12):L1274-85.

[14] Fukuda K. et al., Oxidative Mediated Lipid Peroxidation Recapitulates Proarrhythmic Effects on Cardiac Sodium Channels. *Circ Res.* 2005 Dec 9;97(12):1262-9.

[15] Wilde A.A. et al., Proposed diagnostic criteria for the Brugada syndrome: consensus report. *Circulation.* 2002;106:2514-9.

[16] Wilde A.A. et al., Proposed diagnostic criteria for the Brugada syndrome. *European heart journal.* 2002;23:1648-54.

[17] Antzelevitch C. et al., Brugada syndrome: report of the second consensus conference: endorsed by the Heart Rhythm Society and the European Heart Rhythm Association. *Circulation.* 2005;111:659-70.

[18] Antzelevitch C. et al., Brugada syndrome: report of the second consensus conference. *Heart Rhythm.* 2005;2:429-40.

[19] Tan B.H. et al., Common human SCN5A polymorphisms have altered electrophysiology when expressed in Q1077 splice variants. *Heart Rhythm.* 2005;2:741-7.

- [20] Poelzing S. et al., SCN5A polymorphism restores trafficking of a Brugada syndrome mutation on a separate gene. *Circulation*. 2006;114:368-76.
- [21] Gunnarsson R. et al., Array-based genomic screening at diagnosis and during follow-up in chronic lymphocytic leukemia. *Haematologica*. 2011;96:1161-9.
- [22] Gamazon E.R. et al., SCAN: SNP and copy number annotation. *Bioinformatics*. 2010;26:259-62.
- [23] Iafrate A.J. et al., Detection of large-scale variation in the human genome. *Nat Genet*. 2004;36:949-51.
- [24] Shaikh T.H. et al., High-resolution mapping and analysis of copy number variations in the human genome: a data resource for clinical and research applications. *Genome Res*. 2009;19:1682-90.
- [25] Koike A. et al., Genome-wide association database developed in the Japanese Integrated Database Project. *J Hum Genet*. 2009;54:543-6.
- [26] Dickens N.J. et al., Homozygous deletion mapping in myeloma samples identifies genes and an expression signature relevant to pathogenesis and outcome. *Clin Cancer Res*. 2010;16:1856-64.
- [27] Matsuyama Y. Proteasomal non-catalytic subunit PSMD2 as a potential therapeutic target in association with various clinicopathologic features in lung adenocarcinomas. *Mol Carcinog*. 2011;50:301-9.
- [28] Kim J.C. et al., Novel chemosensitive single-nucleotide polymorphism markers to targeted regimens in metastatic colorectal cancer. *Clin Cancer Res*. 2011;17:1200-9.

- [29] Yamada K. et al., Genome-wide association study of schizophrenia in Japanese population. *PloS one*. 2011;6:e20468.
- [30] Shaw J.A. et al., Genomic analysis of circulating cell-free DNA infers breast cancer dormancy. *Genome Res*. 2012;22:220-31.
- [31] Chen P.C. et al., Use of germline polymorphisms in predicting concurrent chemoradiotherapy response in esophageal cancer. *Int J Radiat Oncol Biol Phys*. 2012;82:1996-2003.
- [32] Weaver S. et al., Taking qPCR to a higher level: Analysis of CNV reveals the power of high throughput qPCR to enhance quantitative resolution. *Methods*. 2010;50:271-6.
- [33] Bhatnagar A. et al., Oxidative Stress Alters Specific Membrane Currents in Isolated Cardiac Myocytes. *Circ Res*. 1990 Sep;67(3):535-49.
- [34] Nakjima T. et al., Selective γ -ketoaldehyde scavengers protect NaV1.5 from oxidant induced Inactivation. *J Mol Cell Cardiol*. 2010 Feb;48(2):352-9.
- [35] Uhlen M. et al., Towards a knowledge-based Human Protein Atlas. *Nat Biotechnol*. 2010;28:1248-50.
- [36] Hentze M.W. et al., A perfect message: RNA surveillance and nonsense-mediated decay. *Cell*. 1999;96:307-10.
- [37] Hayes J.D. et al., Glutathione and glutathione-dependent enzymes represent a co-ordinately regulated defence against oxidative stress. *Free radical research*. 1999;31:273-300.
- [38] Jeong E.M. Metabolic stress, reactive oxygen species, and arrhythmia. *Journal of molecular and cellular cardiology*. 2012;52:454-63.

- [39] Jellins J. et al., Brugada syndrome. *Hong Kong Med J.* 2013 Apr;19(2):159-67.
- [40] Sovari A.A. Cellular and Molecular Mechanisms of Arrhythmia by Oxidative Stress. *Cardiol Res Pract.* 2016;2016:9656078.
- [41] Tanaka M. et al., Elevated oxidative stress is associated with ventricular fibrillation episodes in patients with Brugada-type electrocardiogram without SCN5A mutation. *Cardiovasc Pathol.* 2011 Jan-Feb;20(1):e37-42.

Chapter 5:

Functional characterization of a mutation in KCNT1 gene related to non-familial Brugada Syndrome

A. Binda¹, J.-M. J. Juang², C. Cilibrasi¹, A. Bentivegna¹, I. Rivolta¹

¹ School of Medicine and Surgery, University of Milano-Bicocca, Monza, Italy

² Division of cardiovascular center and Department of Internal Medicine, National Taiwan University Hospital and National Taiwan University College of Medicine, Taipei, Taiwan

Manuscript in preparation

Abstract

KCNT1 gene encodes for Slack, a sodium-activated potassium channel, that contributes to the regulation of neuronal excitability during repetitive firing. This is the first time that a *KCNT1* mutation is linked to a Non-Familial Brugada Syndrome (BrS) in a patient lacking of *SCN5A* variants. Patch clamp experiments were performed in tsA201 cells transfected with wild-type (WT) or mutant channel. Whether no differences were noticeable between the two forms of the channel when the intracellular concentration of sodium was 10 mM, some interesting data were evident using 20 mM intracellular Na⁺ both in absence or in presence of NAD⁺, that physiologically regulates Slack channels activity with a circadian rhythm. The mutation seemed to induce a general increase of channel current density and a slowdown of the kinetics of full activation in NAD⁺ presence. Because of Slack channels are modulated by PKC, channel biophysical properties were also studied in presence of the PKC activator PMA. Data confirmed increased current density of the mutant and a slower activation kinetics in mutant respect to WT channels again in presence of NAD⁺. The mutation seemed also to promote an arrhythmogenic substrate when overexpressed in cardiomyocytes derived from human induced pluripotent stem cells and spontaneous action potentials were recorded. In conclusion, our data suggest that the studied mutation could be responsible for altered biophysical channel characteristics that might be linked to BrS pathological condition.

Keywords: Brugada Syndrome; KCNT1; Slack channels; patch clamp

1. Introduction

KCNT1 gene encodes the sodium-activated potassium channel named Slack (Sequence like a calcium-activated K⁺ channel). Slack channels are subunits of six hydrophobic transmembrane segments (S1-S6) with a pore-lining loop between S5 and S6. Though their overall structure resembles the voltage-dependent K_v potassium channel, Slack S4 segments are not characterized by the presence of positively charged residues corresponding to the K_v channels voltage sensor. Likely, this is the reason why Slack channels are poorly activated by changes in voltage membrane. The single subunit can assemble in tetramers to form the functional channel, furthermore they can also form heteromers assembling to the phylogenetically related sodium-activated potassium channel Slick [1]. Two regulators of K⁺ conductance (RCK) and many consensus sites for several kinases were found on the large cytoplasmic C-terminal domain, which counts more than 900 amino acids [2]. A NAD⁺ binding site locates within the second RCK domain [1].

Mutations in human *KCNT1* gene were identified in patients affected by diseases compromising brain functions, e.g. different types of epilepsies (autosomal dominant nocturnal frontal lobe epilepsy [3;4], early-onset epileptic encephalopathy [5-7] and malignant migrating focal seizures of infancy [4;8]) and hypomyelinating leukodystrophy [9]. Recently, a *KCNT1* mutation (R1106Q) was reported in a patient affected by Non-Familial Brugada Syndrome (BrS) [10], that is a rare cardiac channelopathy associated with ventricular fibrillation and a

high risk for sudden cardiac death [11]. Despite several genes have been associated with BrS, only 30-35% of patients are genetically diagnosed. Among them, variants on *SCN5A* gene are the most common, as they are identified in about 25-30% of patients affected by a familial form of the disease [11]. Since this is the first association of a *KCNT1* mutation and BrS, we found interesting to perform the biophysical characterization of the mutant Slack channel. As the mutation is located in the C-terminus of the protein within NAD^+ and protein kinase C (PKC) binding sites, thus we performed experiments mimicking several combinations of increased intracellular NAD^+ concentration and PKC induced phosphorylation. Finally, we studied the effect of the mutation directly on action potentials in cardiomyocytes derived from human induced pluripotent stem cells (hiPSC-CMs) in order to argue whether it could be responsible for an arrhythmogenic condition underlying BrS.

2. Materials and methods

2.1. Cell cultures and expression of recombinant channels

TsA201 cells were cultured in a controlled environment (5% CO_2 , 37°C) and maintained in Dulbecco's Modified Eagle Medium (DMEM, Euroclone, Italy) supplemented with FBS (10%), L-Glutamine (2 mM), Pen/Strep (100 U/mL, 100 $\mu\text{g}/\text{mL}$). Cells were used between 10th and 25th passage. 0.2 μg of WT or mutant R1106Q *KCNT1* gene subcloned in pAAV-IRES-hrGFP vectors were transiently expressed in tsA201 cells using jetPRIME (PolyPlus transfection, Illkirch, France) according to the manufacturer's

instructions. In order to mimic heterozygous condition, 0.1 µg of both plasmids were transiently transfected.

hiPSC-CMs (CELLular Dynamics, Madison, Wisconsin, USA) were cultured in a controlled environment (5% CO₂, 37° C) and maintained in their specific Maintenance Medium (CELLular Dynamics, Madison, Wisconsin, USA). Cells were transfected with 1 µg of plasmid expressing WT or R1106Q KCNT1 channel using Lipofectamine 2000 (Invitrogen; Thermo Fisher Scientific, Italy) according to manufacturer's instructions. Both cells systems were transfected 48 hours before patch clamp experiments were performed.

2.2. Electrophysiological recordings

Experiments in sodium basal conditions were performed replacing tsA201 cells medium with extracellular solution containing (in mM) 125 NaCl, 5 KCl, 1 CaCl₂, 1 MgCl₂, 10 HEPES, 10 4-aminopyridine and pipettes were filled with an intracellular solution containing (in mM) 10 NaCl, 130 KCl, 1 MgCl₂, 10 HEPES. Increasing sodium intracellular concentrations (from 15 up to 25 mM) were tested and extracellular solutions were adjusted to maintain cells proper osmolarity. Whole currents were evoked by a protocol of voltage steps from -80 mV to +40 mV in 20 mV increments with a length of time of 1.5 s. Holding potential was -80 mV.

hiPSC-CMs medium was replaced with extracellular solution containing (in mM) 150 NaCl, 5.4 KCl, 1.8 CaCl₂, 1 MgCl₂, 15 HEPES, 1 Na-pyruvate, 15 glucose. Pipettes were filled with an intracellular solution containing (in mM) 150 KCl, 10 HEPES, 5 NaCl, 2 CaCl₂, 5 EGTA, 5 K₂ATP. Current clamp recordings were

performed and cellular spontaneous electrical activity was recorded. Where indicated, β -nicotinamide adenine dinucleotide (NAD⁺ 1 mM; Sigma-Aldrich, Italy) was added to intracellular solution and phorbol 12-myristate 13-acetate (PMA 100 nM; Sigma-Aldrich, Italy) was added to extracellular solution; in this case cells were incubated 15 minutes before patch clamp experiments. All patch clamp recordings were performed at room temperature using pipettes pulled to a resistance of 2-5 M Ω (Model P-97 Sutter Instruments, CA, USA). Data were acquired with a Multiclamp 700B amplifier (Axon Instruments, Molecular Device, CA, USA), Digidata 1440A (Axon Instruments, Molecular Device, CA, USA) and pClamp 10.3 software (Molecular Devices, CA, USA). All the data concerning channel current density reported in the Results section refer to a depolarizing stimulus from -80 to -20 mV.

2.3. RNA extraction and end point RT-PCR

RNA was extracted from hIPSC-CMs using the RNAeasy[®] Micro kit (Qiagen, Italy) according to the manufacturer's protocol. RNA quantity and quality were then analysed using a Nanodrop[®] ND-1000 spectrophotometer (Thermo Fisher Scientific, Italy).

RNA samples were converted into first-strand cDNA using the M-MLV reverse transcriptase (Invitrogen; Thermo Fisher Scientific, Italy). cDNAs were then quantified using a Nanodrop[®] ND-1000 spectrophotometer (Thermo Fisher Scientific, Italy).

Subsequently, cDNAs were PCR-amplified using the Taq DNA polymerase (Invitrogen; Thermo Fisher Scientific, Italy) and the following primers: FW: 5' GCAAGTTCTTCCGCGAGTAC 3'; REV:

5' CCCTTCACATACTCTACCACGG 3'. Thermocycling conditions were the following: 95°C for 5 min; 30 cycles: 95°C for 30 s, 57°C for 30 s, 72°C 30 s; 72°C 7 minutes; 4°C. PCR products were resolved on 2% agarose gel and stained with 0.1% ethidium bromide. cDNA obtained smooth muscle was used as a PCR positive control, while GAPDH was used as a retrotranscription control.

2.4. Statistical analysis

Results were analyzed with Clampfit 10.3 software (Molecular Devices, CA, USA) and elaborated with Excel (Microsoft Office) and OriginPro 8 (OriginLab Corporation, Northampton, Massachusetts, USA). All data are expressed as mean±S.E. Two-tailed Students t test was used to compare means; $p < 0,05$ was considered statistically significant and indicated with * .

3. Results

3.1. WT and mutant Slack channels sodium sensitivity

Slack channels sodium sensitivity was studied in tsA201 cells transiently transfected with plasmids expressing either WT or mutant channel. Upon a depolarization stimulus, these potassium channels exhibit an outward current characterized by an initial fast followed by a slower kinetic of activation. Current recordings were firstly performed using an intracellular solution containing a basal sodium concentration (10 mM) and mutant showed no differences compared to WT channels in terms of both current density (8.32 ± 1.82 pA/pF $n=8$, 8.90 ± 2.91 pA/pF $n=10$ WT and mutant channels respectively) and the kinetics of full activation (fig. 1). When sodium intracellular

concentration $[\text{Na}^+]_i$ was progressively increased from the basal value of 10 mM up to 25 mM, as expected, current density consequently rised (fig. 2A). The increase became significant in correspondence of 20 and 25 mM $[\text{Na}^+]_i$, when mutant current densities almost doubled compared to the WT ones (20 mM $[\text{Na}^+]_i$: WT 30.89 ± 5.87 pA/pF $n=14$, R1106Q 54.62 ± 8.81 pA/pF $n=19$; $p < 0.01$; 25 mM $[\text{Na}^+]_i$: WT 30.32 ± 7.87 pA/pF $n=19$, R1106Q 61.14 ± 22.97 pA/pF $n=16$; $p < 0.05$). Heterozygous condition WT/R1106Q was evaluated when the parameter variation was maximum, thus in 20 mM $[\text{Na}^+]_i$ and data suggested a non-dominant effect of the mutation as the current density was comparable to the one of WT channel (22.19 ± 5.46 pA/pF $n=8$) (fig. 2B).

Furthermore, WT and mutant channel kinetics of full activation were overlapping at every $[\text{Na}^+]_i$ tested (data not shown).

3.2 Effects of intracellular NAD^+

It is well reported that NAD^+ molecules could directly interact with their binding site within the second RCK domain of Slack channels leading to an increase of channel open probability events, therefore enhancing the activity of the channel itself [12]. The R1106Q mutation is located in the C-terminus in the region that contains the protein NAD^+ binding domain. Thus, we wanted to evaluate whether WT and mutant channels biophysical characteristics were somehow affected by an increase of cellular NAD^+ levels, as it should physiologically happen in the organism due to circadian rhythms [13]. In presence of 1 mM NAD^+ in basal intracellular sodium, nor the current density neither the kinetics of full activation differed

significantly between WT and mutant expressing channels (fig. 3A). Interestingly, the addition of NAD^+ generally faster the kinetics of full activation (fig. 3B). At 20 mM $[\text{Na}^+]_i$, NAD^+ addition did not generate effects on the current densities since data were in line with the recordings performed without NAD^+ (20.92 ± 4.42 pA/pF $n=19$, 21.79 ± 4.55 pA/pF $n=18$, 42.28 ± 11.4 pA/pF $n=18$ respectively, $p < 0.01$ WT vs R1106Q and WT/R1106Q vs R1106Q) (fig. 4D). As far as concerned the kinetics of full activation, only the WT channels seemed to be sensitive to the presence of NAD^+ that speeded up this parameter already in basal sodium condition. In fact the time course of the activation appeared to be unaffected by the NAD^+ presence in R1106Q channels. Interestingly, heterozygous channels was intermediate between WT and homozygous one (fig. 4E).

3.3 Effects of PKC-induced channel phosphorylation in 20 mM $[\text{Na}^+]_i$
Several protein kinase C (PKC) consensus sites have been identified in the C-terminal of Slack channels where the R1106Q mutation is localized, thus we treated the cells with PMA, a well-known PKC activator, in 20 mM $[\text{Na}^+]_i$ in order to investigate whether the mutation impaired PKC modulation. Our data obtained on WT channels were in line with previous studies [14], i.e. Slack phosphorylation mediated by PKC induced a general increase of the current density (30.89 ± 5.87 pA/pF $n=14$ vs 42.28 ± 11.4 pA/pF $n=18$) (fig. 5A). Although current density was also similarly increased considering WT/R1106Q channels (22.19 ± 5.46 pA/pF $n=8$ vs 30.25 ± 9.76 pA/pF $n=16$), R1106Q channels seemed to be insensitive to PKC stimulation (54.62 ± 8.81 pA/pF $n=19$ vs 39.60 ± 13.97 pA/pF $n=13$). Once again,

the kinetics of activation showed no differences in the three conditions tested, as a general consideration, we could observe a trend towards an overall slowdown in accordance with other studies [14] (fig. 5B).

3.4 WT and mutant Slack channel overexpression in hIPSC-CMs

Having characterized the effect of the R1106Q mutation in tsA201 cells, we then switched to a more complex cellular model, closer to the native one, choosing an heterogeneous population of commercial available human cardiomyocytes derived from induced pluripotent stem cells. These cells physiologically express *KCNT1* gene (fig. 6), and, on this background, we overexpressed WT or mutant Slack coding plasmids. Action potentials recordings were categorized as atrial- or ventricular-like based on their different phenotypes (fig. 7) and their properties were evaluated (tab. 1). Slack channels overexpression did not influence action potential frequency neither in atrial-like nor in ventricular-like cells. As one might expect, an overexpression of a potassium conductance significantly shortened action potentials duration at 90% of repolarization (APD₉₀) in an similar way either in WT or in mutant transfected cardiomyocytes compared to non transfected hIPSC-CM ($p < 0.001$). Interestingly, the mutation seemed to promote one of the major arrhythmogenic mechanisms in both atrial-like and in ventricular-like cardiomyocytes; indeed the number of delayed afterdepolarization events (DADs) was significantly higher in mutant compared to non transfected and WT expressing cells ($p < 0.001$) (fig. 8).

4. Discussion

BrS is a heart disease associated with sudden cardiac death. The most common BrS-associated gene is *SCN5A*, that accounts for 25-30% of affected patients. Other genes linked to familial forms of the pathology encode for potassium or calcium channels [11]. Although *KCNT1* gene mutations are usually related to neurological disorders, recently a mutation was found in a patient affected by BrS [10]. Moreover the clinical analysis of a family affected by autosomal dominant nocturnal frontal lobe epilepsy revealed the presence of a subject affected by cardiac arrhythmia and a case of sudden death, probably linked to a cardiac anomaly [4]. Both these evidences suggest a potential central role of Slack channels in heart as well as in neurons, where physiological functions are not yet completely clearly understood. It is generally believed that these sodium-dependent potassium channels should contribute to the prolongation of the late hyperpolarization and to the genesis of afterhyperpolarization, thus sustaining reduced neuronal excitability that protects cells from repetitive firing [2].

We firstly investigated WT and mutant Slack channels in tsA cells, in a “basal” intracellular environment (sodium concentration of 10 mM), and found that the mutation did not alter neither current density nor kinetics of activation of the channel. The activity of the Slack channel is sodium-dependent, thus we characterized channel properties as intracellular sodium progressively increased up to 25 mM, finding that R1106Q mutation was associated to a progressive increased current

density that was significantly higher compared to the one obtained in the WT in presence of 20 and 25 mM intracellular sodium. We also studied heterozygous condition selecting $[Na]_i$ of 20 mM, WT/R1106Q current density was comparable with WT channels, therefore suggesting that the mutation should induce a non-dominant gain-of-function.

The mutation was located within the C-terminus near the channels NAD^+ binding site, so, considering that the essential pathway for the generation of NAD^+ in the cell is the NAMPT-dependent salvage pathway, in which NAMPT enzyme displays circadian rhythm-induced oscillations, and given that the patient we referred to had the event during the day at work [10], we proceeded exploring the possibility that the presence of NAD^+ may be relevant for the regulation of the mutant Slack channel [12]. Results showed that, the sodium-dependent current amplitude was insensitive to intracellular NAD^+ addition, but the kinetics of the full activation behavior of the R1106Q differed from the WT channel, being this last accelerated. In conclusion, the kinetics of activation of the mutant channel was insensitive to NAD^+ . All these effects seemed to be non-dominant and they appeared when sodium concentration was not basal. It is worthy to notice that, during an action potential, Slack channels should physiologically open subsequently to sodium channels, thus when intracellular sodium concentration is higher than basal. Furthermore, 20 mM $[Na]_i$ may be associated with the late phase of the fast depolarization of the action potential in the ventricular cardiomyocytes, therefore we suggested that differences of the mutant

channels might appear little by little as intracellular sodium increase. Current density and activation kinetics modifications are in line with a possible pathogenetic mechanism. Indeed, ventricular action potentials exhibit considerable morphological variation. Cardiomyocytes isolated from the epicardium have a spike-and-dome action potential with a characteristic notch sustained by a pronounced I_{to} . In contrast, endocardial myocytes have no such notch. In Brugada syndrome, a decrease in sodium or in the inward L-type calcium or an increase of the outward potassium currents (I_{to} or I_{KNa}) leads to an imbalance between the positive inward and outward currents, generating a net outward shift at the end of phase 1 of the action potential. Whichever the mechanism, regional excess of outward current may result in a phenotype transition leading eventually to a loss-of-dome action potential. Since the density of I_{to} is greater in epicardium than in endocardium, epicardial cells are more vulnerable to such perturbation. Thus, arrhythmogenesis will occur through the formation of a heterogeneous substrate, in which some regions exhibit action potential of much shorter duration than others. This event occurs heterogeneously on the ventricular wall and leads to a transmural voltage gradient, which produces the characteristic ST-segment elevation in the ECG of BrS patients [14].

It is known that PKC, an ubiquitously expressed kinase, which is reported to be present also in the heart [15], could phosphorylate the channel in several C-terminal domains. The post-translational modification induces an increase in Slack current density [16]. Several previous studies of *KCNT1* mutants channels already described

increased current densities compared to WT channel [17;18] and suggested that the mutations could introduce a phosphorylation-like state of the channel [8], thus we stimulated the cells with PMA, PKC activator (in an intracellular background of 20 mM $[Na]_i$), to test whether the C-terminal R1106Q mutation would impair the PKC-phosphorylation modulation. As expected, PMA incubation increased WT and heterozygous current densities and slow the kinetics of activation, but such modifications were not observed when considering the mutant channel. At least 11 different isozymes of the serine/threonine PKC have been identified [19]. Although the different PKC isozymes have been reported to have a unique optimal substrate, there are some features which are common to substrate sequence motifs of all PKC isozymes, such as the presence of basic amino acids at the position -2 and -3 and of an hydrophobic one in position +1 amino-terminal to the phosphorylated residue [19;20]. As in the amino acid sequence of Slack channels, the serine in position 1109 is preceded by two arginines (basic residues) in position 1107 (-2) and 1106 (-3) and followed by a leucine (hydrophobic residue) in position 1110 (+1), we could hypothesize that the serine in position 1109 could be a potential target of PKC kinases. The mutation found in the patient changes the basic arginine in position 1106 with a glutamine, which is a polar residue, leading us to speculate that this substitution could change the potential substrate consensus sequence, altering the possibility for PKC to phosphorylate the channel in this putative site. Indeed, our data suggest that the mutation make the channel insensitive PKC modulation.

Based on the results obtained so far, we believed that the investigation of mutant channels expression in cardiac myocytes could be potentially interesting. A commercially available cell line of cardiomyocytes derived from hIPSCs, that endogenously expressed *KCNT1* gene was selected, and a comparison of action potentials recorded in non transfected or WT or mutant Slack overexpressing CMs was carried on. No differences as far as concerned action potential frequency were observed, but their duration was significantly shorter in the transfected cells, probably due to the fact that with the overexpression, we were adding a potassium conductance. A significant increase in delayed afterdepolarization events, which are transient arrhythmogenesis-inducing depolarization following action potential [21], occurred in presence of R1106Q channel.

In conclusion, despite still more investigation are needed, following an increase in sodium intracellular concentration, the R1106Q mutation should induce modifications in the biophysical properties of Slack channel that could be positively related to BrS pathogenesis. Moreover the mutation seemed to be localize in a region important for the PKC-induced regulation of channel activity. Finally its overexpression in hIPSC derived cardiomyocytes seemed to generate a pro-arrhythmic substrate.

Fig. 1

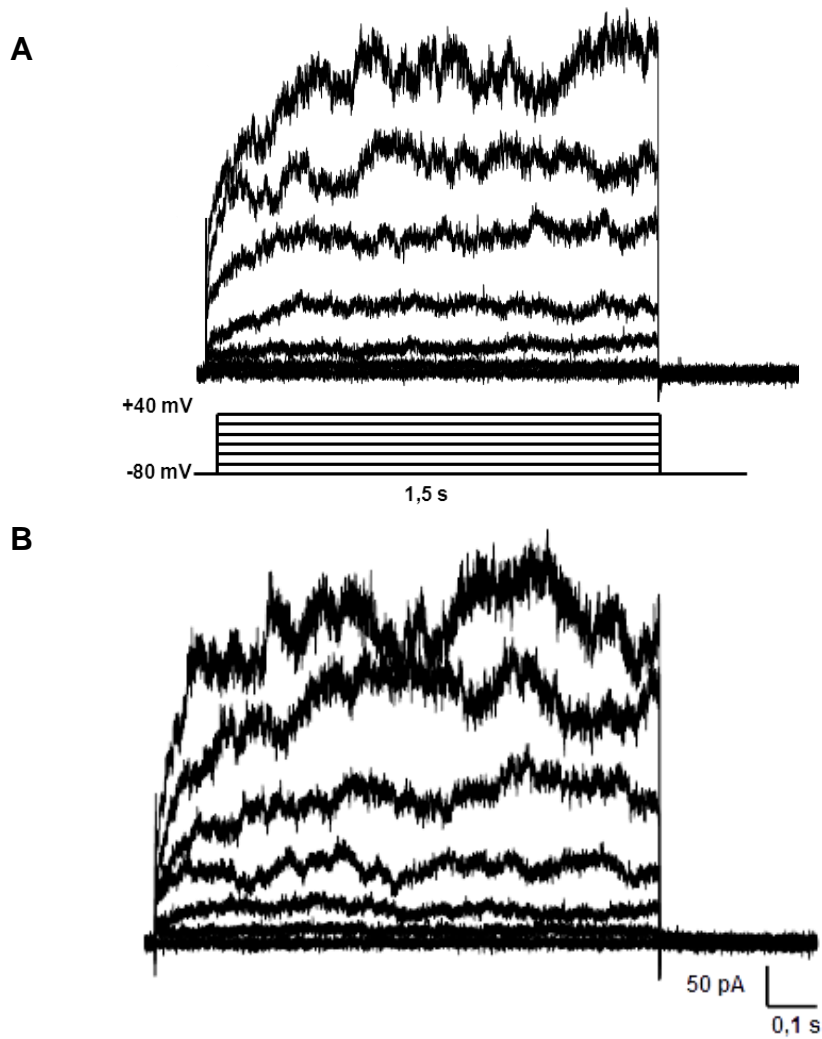


Fig. 1. Current density and kinetics of full activation in 10 mM basal sodium concentration. A-B. Representative families of whole cell current traces evoked in tsA201 cells expressing WT (A) or R1106Q mutant (B) KCNT1 channels by a protocol of voltage steps from -80 mV to +40 mV in 20 mV increments.

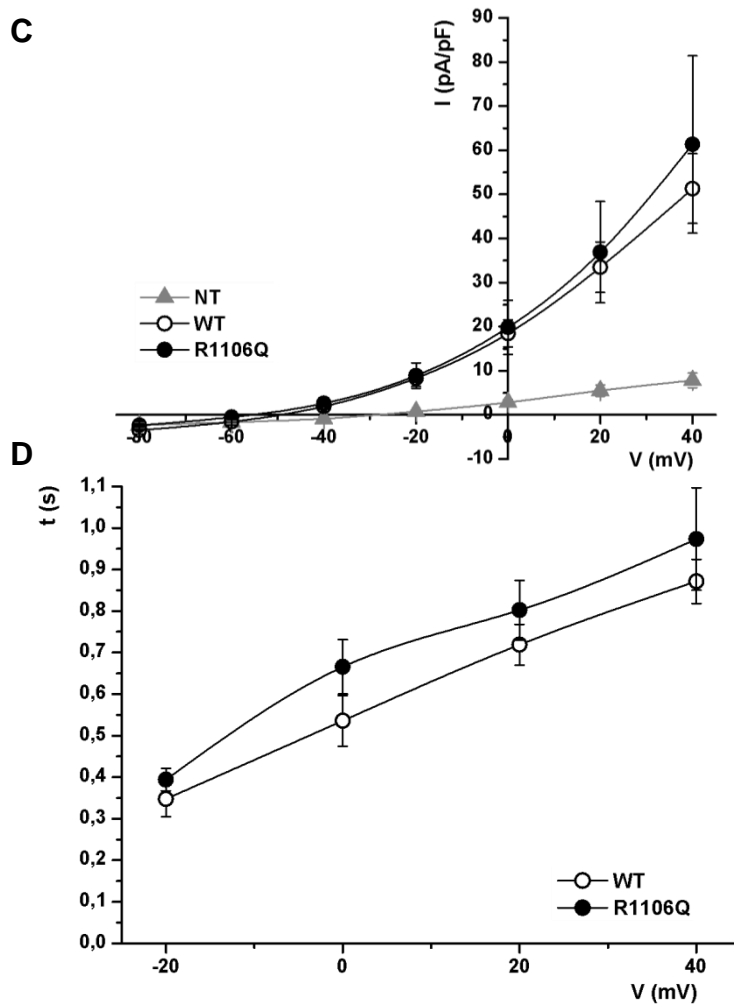


Fig. 1. Current density and kinetics of full activation in 10 mM basal sodium concentration. C. Current/voltage relationship showing current density recorded in non transfected cells (NT n=23) and cells expressing WT (n=8) and mutant channels (n=10). D. Kinetics of full activation (WT n=7; R1106Q n=7). This parameter was calculated as the time necessary for the current to reach a plateau and it was measured over a range of depolarizing potentials from -20 mV to +40 mV.

Fig. 2

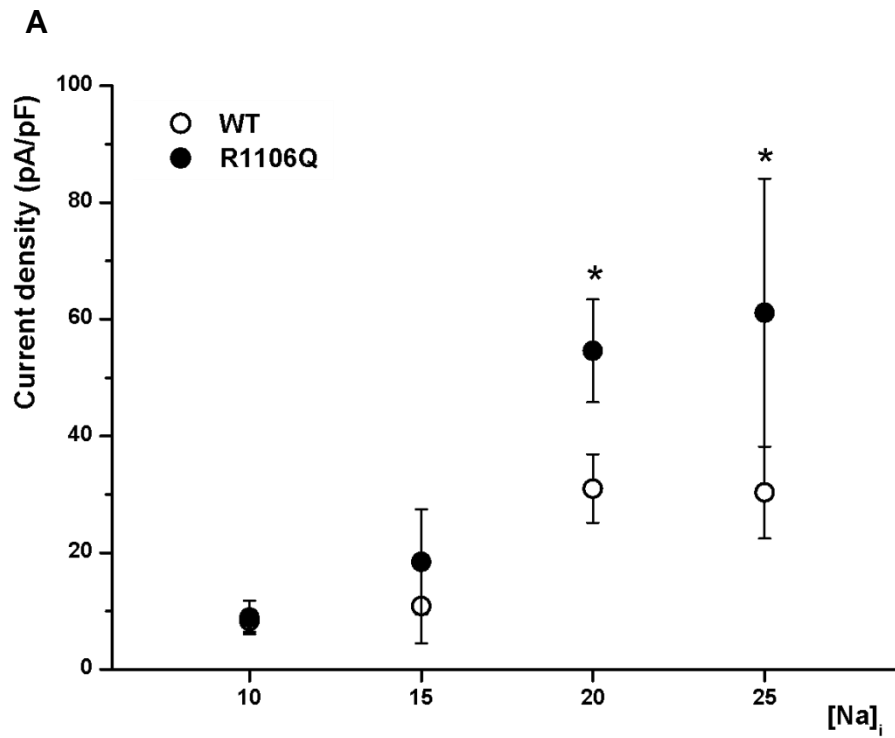


Fig. 2. Sodium sensitivity of WT and mutant Slack channels. Slack are sodium-dependent potassium channels, therefore, current density increased following intracellular sodium concentration elevation. R1106Q channels, as well as WT, showed a general increased current density, but in correspondence of 20 and 25 mM $[\text{Na}^+]_i$ the rise was significantly higher.

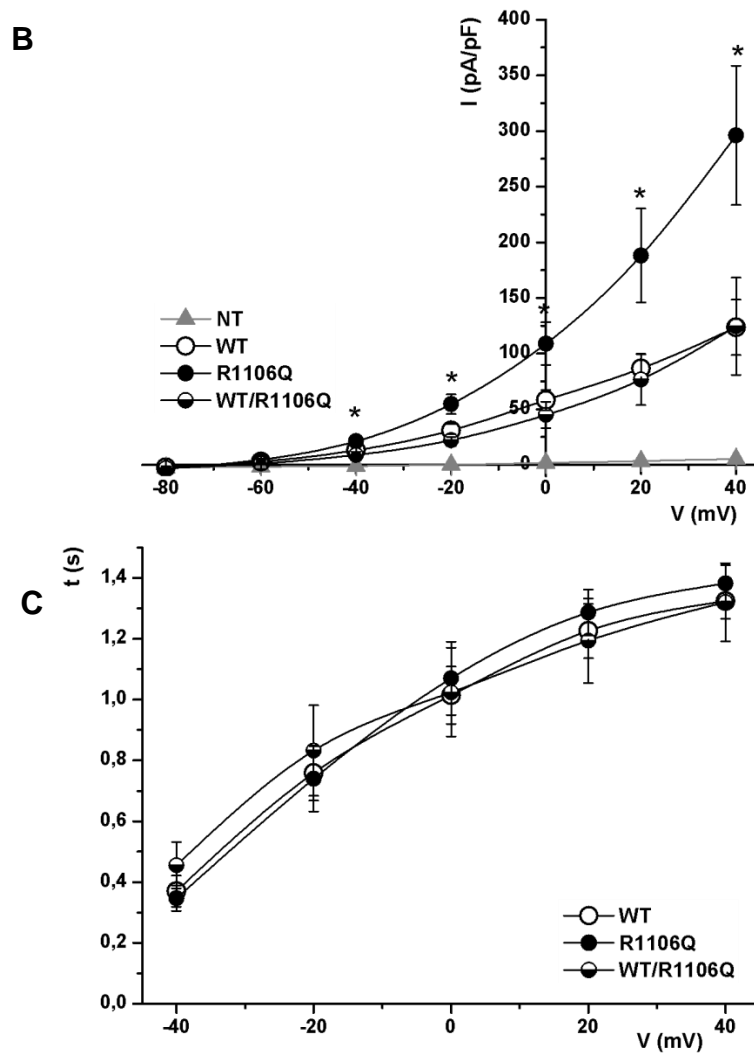


Fig. 2. Current density and kinetics of full activation of WT and mutant Slack channels in 20 mM $[Na^+]_i$. B. Current/voltage relationship showing that current density was significantly increased in R1106Q channels (n=19) compared to WT (n=14) and WT/R1106Q (n=8) (NT cells n=19). C. Kinetics of full activation were comparable between WT (n=19), WT/R1106Q (n=10) and R1106Q (n=25).

Fig. 3

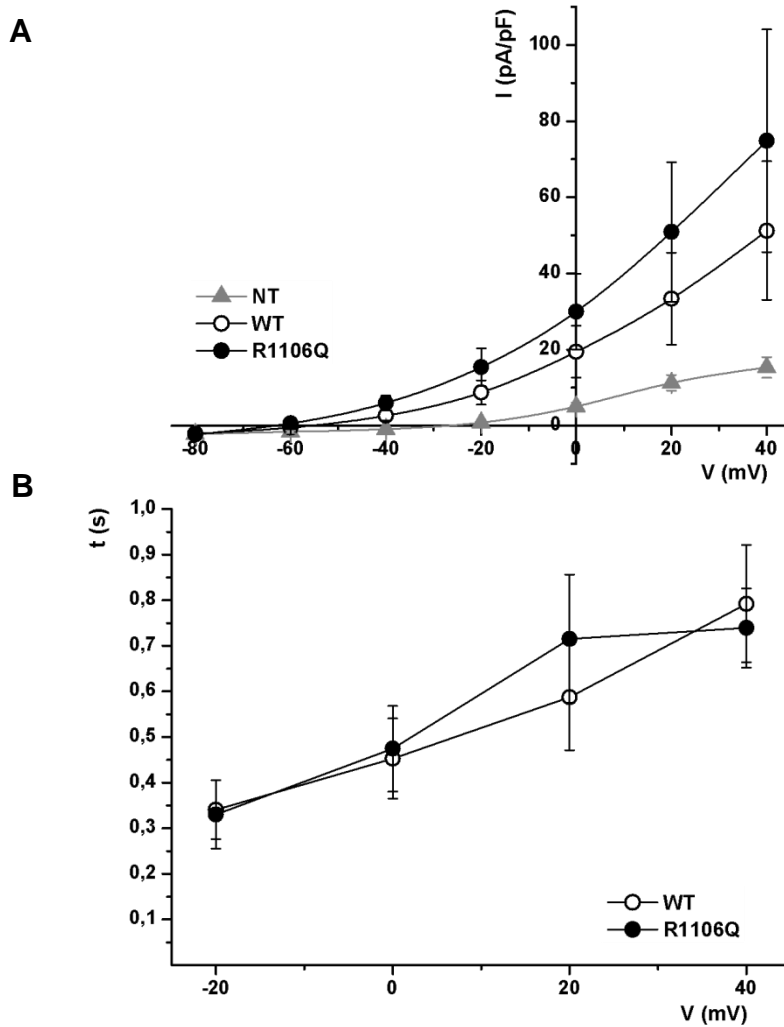


Fig. 3. Current density and kinetics of full activation in 10 mM $[\text{Na}^+]_i$ and 1 mM NAD^+ A. I/V relationship showing current density recorded in NT cells (n=50) and cells expressing WT (n=9) and mutant channels (n=12). The values did not differ from the ones reported in Fig. 1C. D. Kinetics of full activation were overlapping (WT n=8; RQ n=11), but faster compared to the ones obtained without NAD^+ .

Fig. 4

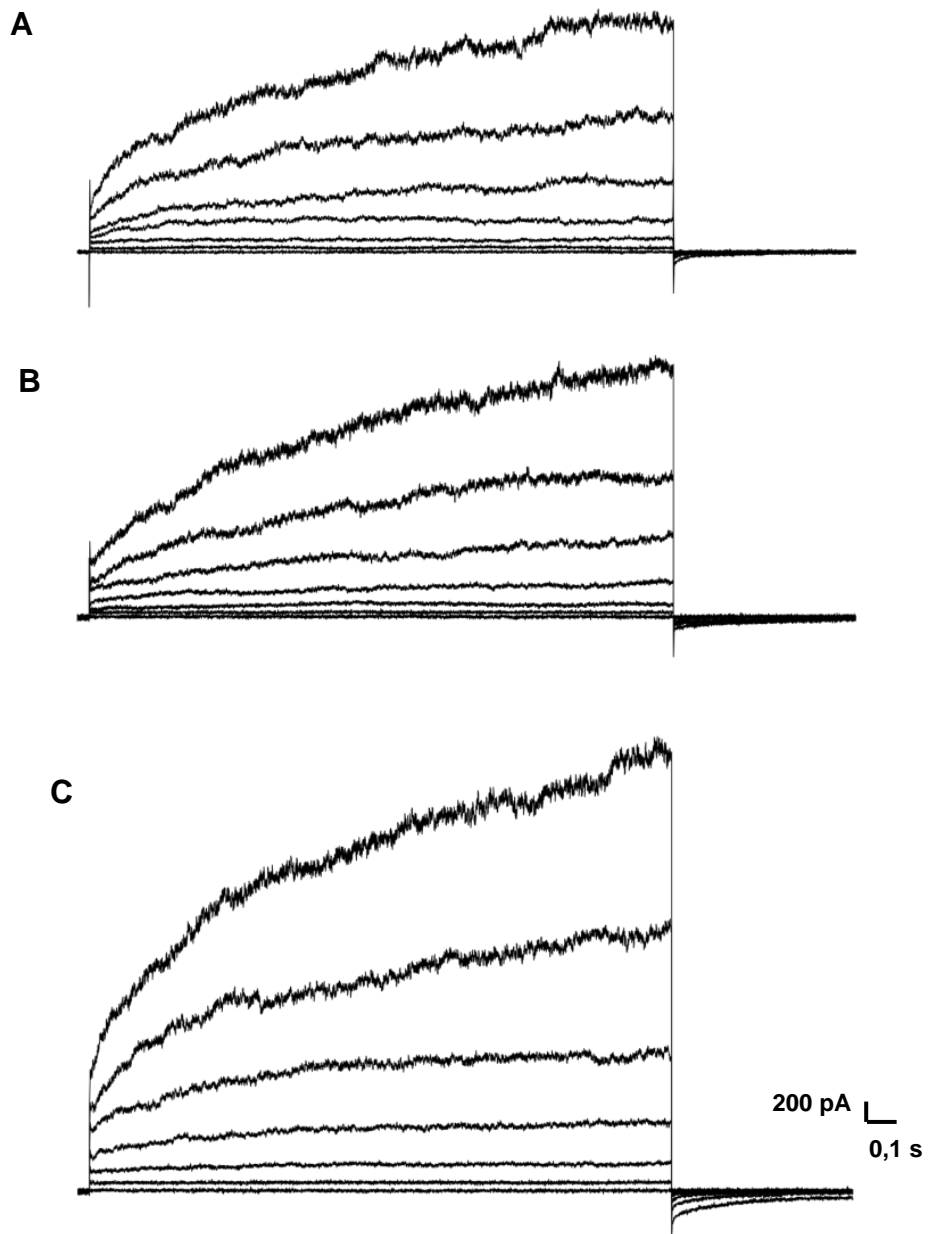


Fig. 4

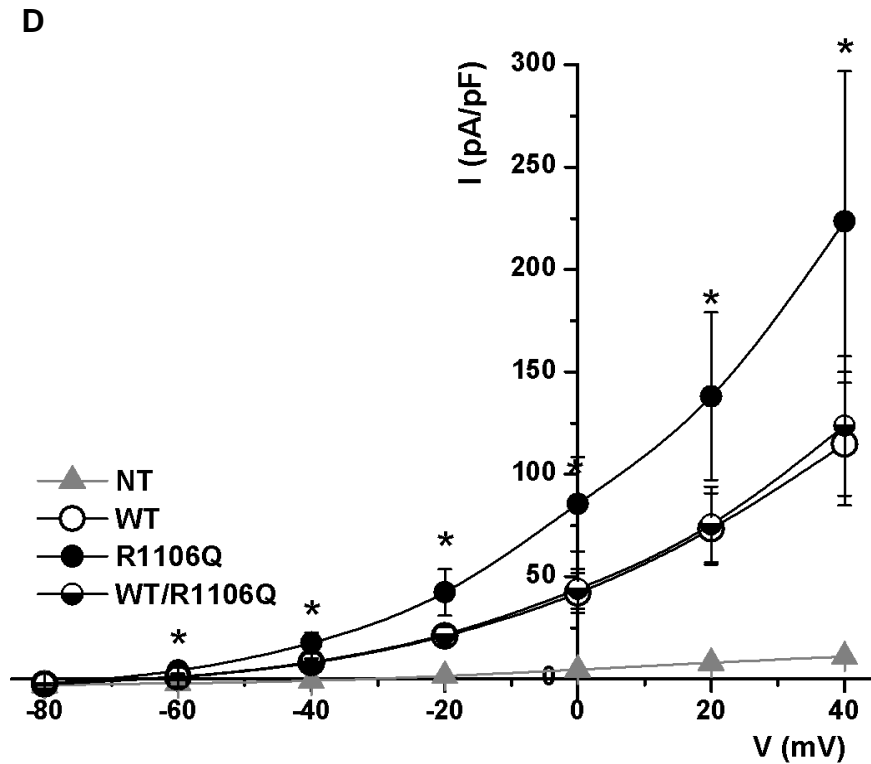


Fig. 4. Effect of NAD^+ in 20 mM $[\text{Na}^+]_i$ on Slack current . A-C. Representative families of whole currents evoked by a protocol of voltage steps from -80 mV to +40 mV in 20 mV increments in tsA201 cells expressing WT (A), WT/R1106Q (B) or R1106Q mutant (C) KCNT1 channels. D. Current/voltage relationship obtained from NT cells (n=29) and cells expressing WT (n=19), R1106Q (n=18) and WT/R1106Q (n=18) channels. The current density of the mutated channel was significantly higher compared to WT and WT/R1106Q channels.

Fig. 4

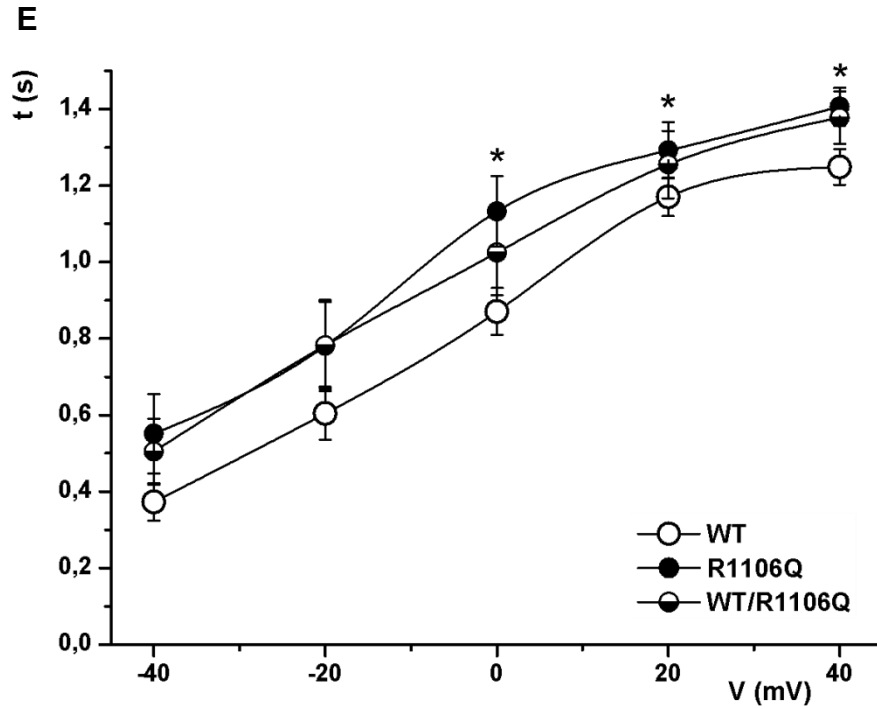


Fig. 4. Effect of NAD^+ in 20 mM $[\text{Na}^+]_i$ on Slack current. E. Kinetics of full activation of the Slack current (WT n=18; R1106Q n=18; WT/R1106Q n=18). At positive voltages, only the kinetics of activation of the WT was significantly speeded when compared to the mutated form of the channel ($p < 0.05$ WT vs R1106Q). Data suggested that despite no changes in the current density, the kinetics of activation of the heterozygous channel exhibited an intermediate behavior compared to WT channels ($p < 0.05$ in correspondence of +40 mV stimulus WT vs WT/R1106Q).

Fig. 5

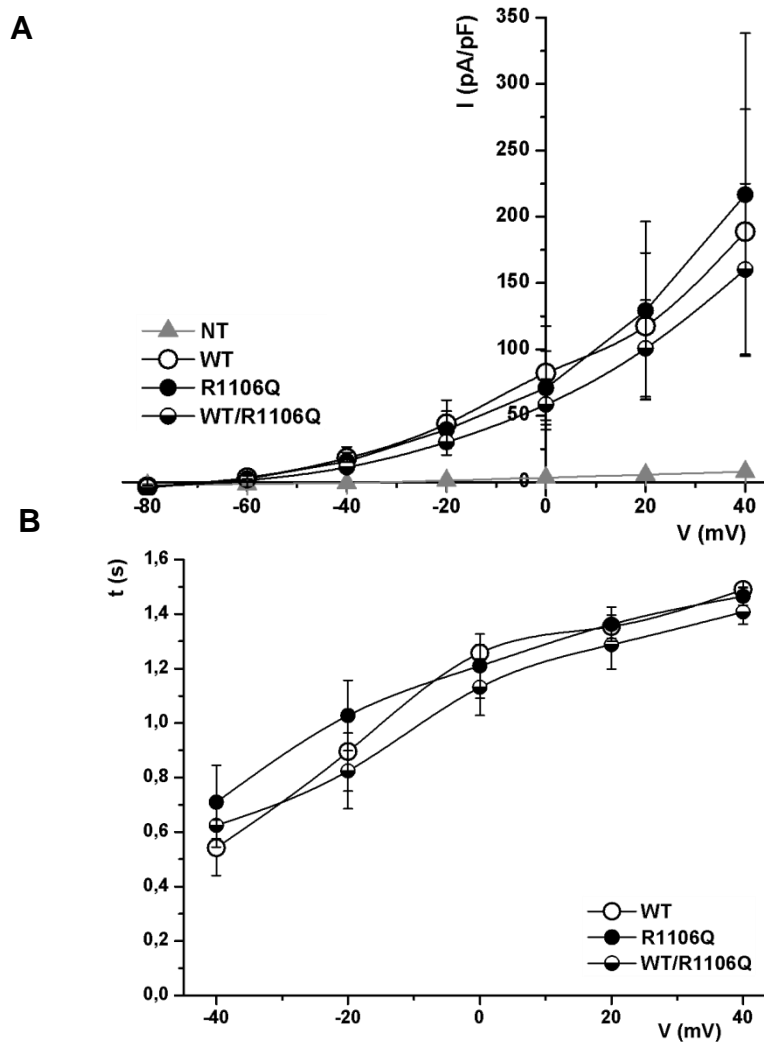


Fig. 5. Effect of PMA in 20 mM $[Na^+]_i$. A. Current/voltage relationship. Current density of WT (n=11) and WT/R1106Q (n=16) channels was overall increased due to PKC phosphorylation, however, R1106Q channel seemed to be insensitive to PKC modification (n=16) (NT cells n=21). B. Kinetics of full activation showed no sensitivity to PMA (WT n=11; R1106Q n=11; WT/R1106Q n=14).

Fig. 6

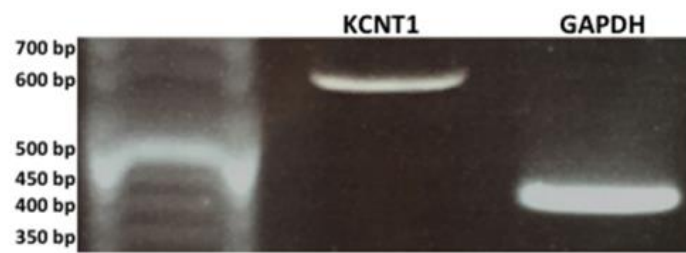


Fig. 6. Human cardiomyocytes derived from induced pluripotent stem cells expressed detectable levels of *KCNT1* gene (GAPDH was use as control of the PCR experiment).

Fig. 7

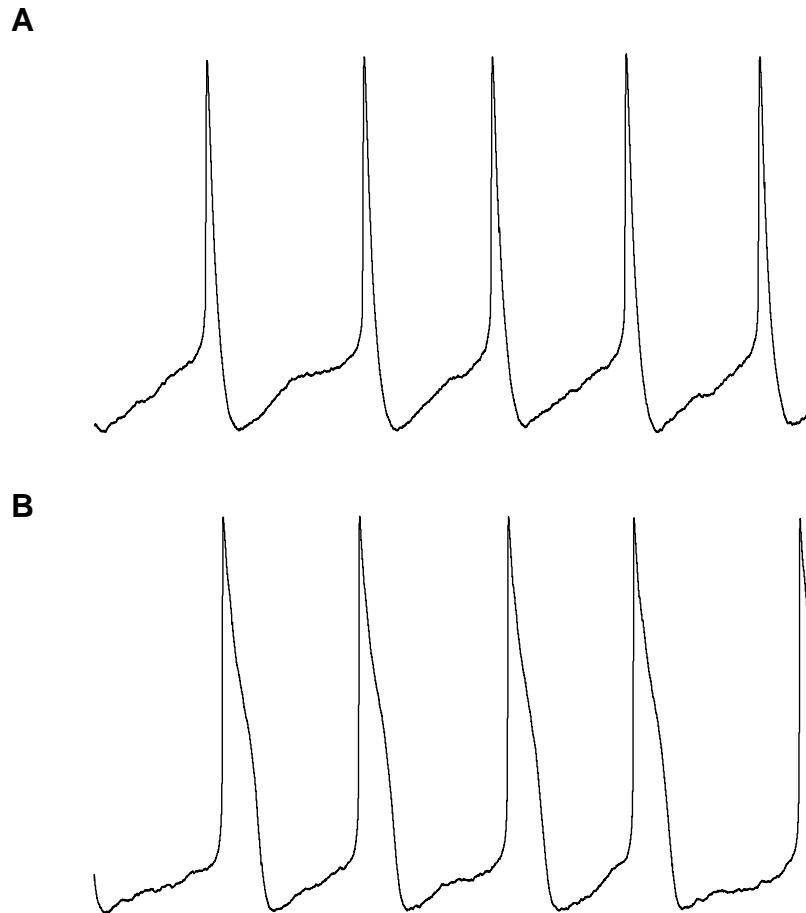


Fig. 7. Action potentials recorded in non transfected hiPSC-CMs. Cardiomyocytes cell population was heterogeneously composed, therefore action potentials could be divided based on their different phenotypes in atrial-like (A) or ventricular-like (B).

Tab. 1

A

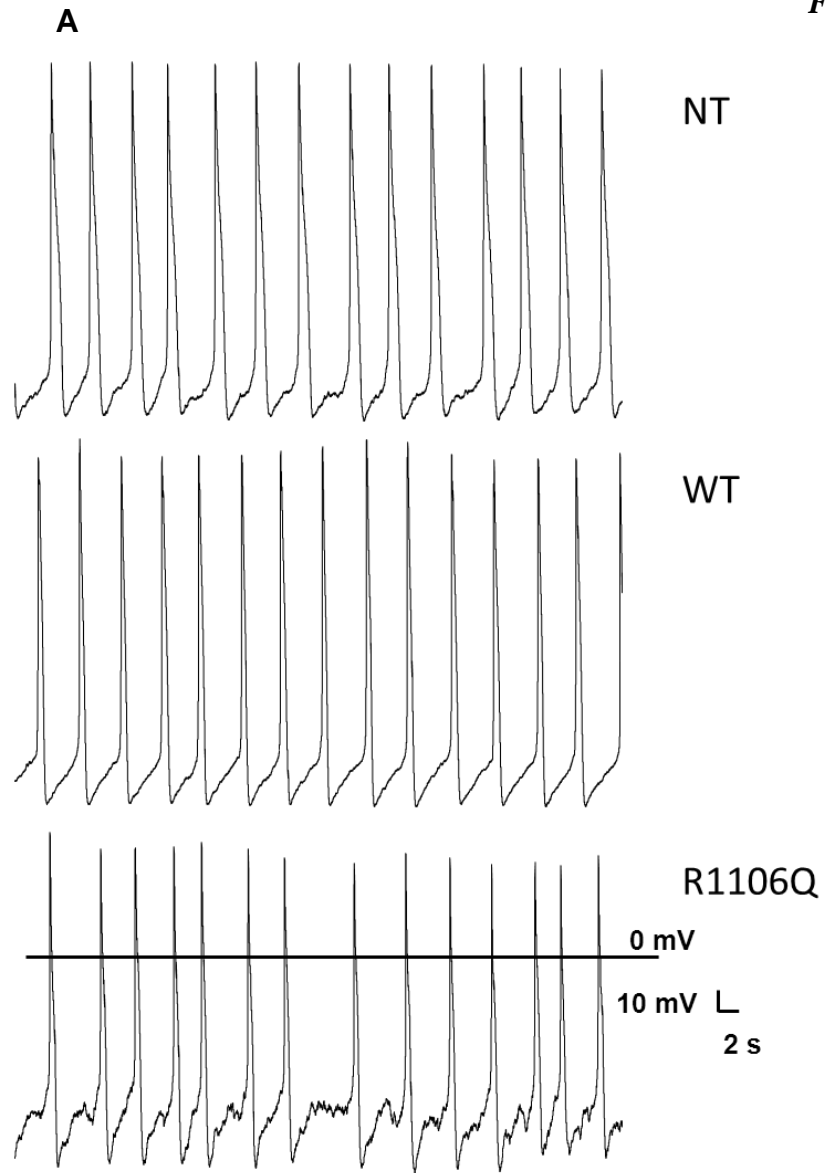
atrial-like APs	NT	WT	R1106Q
FREQUENCY (Hz)	0.36±0.08	0.26±0.08	0.33±0.05
APD90 (s)	0.45±0.05	0.37±0.04*	0.39±0.07*
DADs (#/100 s)	6.50±1.29	7.29±2.68	17.63±2.75*

B

ventricular-like APs	NT	WT	R1106Q
FREQUENCY (Hz)	0.22±0.06	0.20±0.05	0.19±0.06
APD90 (s)	0.71±0.09	0.53±0.05*	0.52±0.08*
DADs (#/100 s)	2.33±1.66	3.58±1.11	12.25±2.03*

Tab. 1. Action potentials characteristics. Slack overexpression did not influence action potential frequency, while, as expected, the overexpression of a potassium channel reduced action potential duration at 90% of repolarization ($p<0.001$). Interestingly mutant channel overexpression increased the number of delayed after depolarizations (DADs), which are usually considered as a common arrhythmogenic event both in atrial-like and in ventricular-like action potentials ($p<0.001$). (NT n=7 and n=7; WT n=10 and n=6; R1106Q n=8 and n=6 atrial- and ventricular-like respectively).

Fig. 8



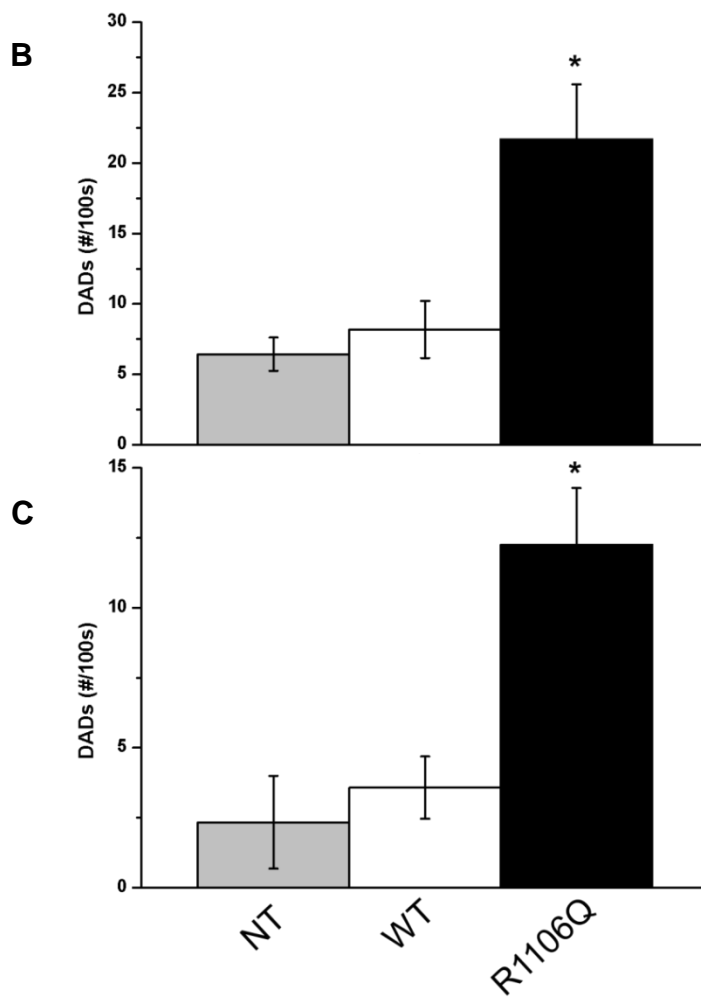


Fig. 8. A. Ventricular-like action potentials recorded in non-transfected and WT or R1106Q overexpressing hIPSC-CMs. Bar graph showing that mutant channel overexpression in hIPSC-CMs significantly increased the number of delayed after depolarization events compared to non transfected and to WT overexpressing cardiomyocytes considering both atrial- (B) and ventricular-like (C) action potentials.

References

- [1] Kaczmarek L.K., Slack, Slick, and Sodium-Activated Potassium Channels. *ISRN Neurosci*. 2013 Apr 18;2013.
- [2] Kim G.E. et al., Emerging role of the KCNT1 Slack channel in intellectual disability. *Front Cell Neurosci*. 2014 Jul 28;8:209.
- [3] Heron S.E. et al., Missense mutations in the sodium-gated potassium channel gene KCNT1 cause severe autosomal dominant nocturnal frontal lobe epilepsy. *Nat Genet*. 2012 Nov;44(11):1188-90.
- [4] Møller R.S. et al., Mutations in KCNT1 cause a spectrum of focal epilepsies. *Epilepsia*. 2015 Sep;56(9):e114-20.
- [5] Martin H.C. et al., Clinical whole-genome sequencing in severe early-onset epilepsy reveals new genes and improves molecular diagnosis. *Hum Mol Genet*. 2014 Jun 15;23(12):3200-11.
- [6] Allen N.M. et al., Unexplained early onset epileptic encephalopathy: Exome screening and phenotype expansion. *Epilepsia*. 2016 Jan;57(1):e12-7.
- [7] Fukuoka M. et al., Quinidine therapy for West syndrome with KCNT1 mutation: A case report. *Brain Dev*. 2016 Aug 28. pii: S0387-7604(16)30106-1.
- [8] Barcia G. et al., De novo gain of function KCNT1 channel mutations cause malignant migrating partial seizures of infancy. *Nat Genet*. 2012 Nov;44(11):1255-9.
- [9] Arai-Ichinoi N. et al., Genetic heterogeneity in 26 infants with a hypomyelinating leukodystrophy. *Hum Genet*. 2016 Jan;135(1):89-98.
- [10] Juang J.M. et al., Disease-Targeted Sequencing of Ion Channel Genes identifies de novo mutations in Patients with Non-Familial

Brugada Syndrome. *Sci Rep*. 2014 Oct 23;4:6733.

[11] Sarquella-Brugada G. et al., Brugada syndrome: clinical and genetic findings. *Genet Med*. 2016 Jan;18(1):3-12.

[12] Tamsett T.J. et al., NAD⁺ activates KNa channels in dorsal root ganglion neurons. *J Neurosci*.

2009 Apr 22;29(16):5127-34.

[13] Bellet M.M. et al., The time of metabolism: NAD⁺, SIRT1, and the circadian clock. *Cold Spring Harb Symp Quant Biol*. 2011;76:31-8.

[14] Badri M. et al., Cellular and ionic basis of J-wave syndromes. *Trends Cardiovasc Med*. 2015 Jan;25(1):12-21.

[15] Mackay K. et al., Localization, anchoring, and functions of protein kinase C isozymes in the heart. *J Mol Cell Cardiol*. 2001 Jul;33(7):1301-7.

[16] Santi C.M et al., Opposite regulation of Slick and Slack K⁺ channels by neuromodulators. *J Neurosci*. 2006 May 10;26(19):5059-68.

[17] Milligan C.J. et al., KCNT1 Gain of Function in 2 Epilepsy Phenotypes is Reversed by Quinidine. *Ann Neurol*. 2014 Apr;75(4):581-90.

[18] Rizzo F. et al., Characterization of two *De novo* Kcnt1 mutations in children with malignant migrating partial seizures in infancy. *Mol Cell Neurosci*. 2016 Apr;72:54-63.

- [19] Kang J.-H. et al., Protein kinase C (PKC) isozyme-specific substrates and their design. *Biotechnol Adv.* 2012 Nov-Dec;30(6):1662-72.
- [20] Nishikawa K. Determination of the Specific Substrate Sequence Motifs of Protein Kinase C Isozymes. *J Biol Chem.* 1997 Jan 10;272(2):952-60.
- [21] Liu M.B. et al., Delayed afterdepolarizations generate both triggers and a vulnerable substrate promoting reentry in cardiac tissue. *Heart Rhythm.* 2015 Oct;12(10):2115-24.

Chapter 6:

summary, conclusions
and future perspectives

Channelopathies are a huge heterogeneous group of disorders generally characterized by defective ion channel functions. Since ion channels are expressed and control activities not only in excitable tissues but also in non-excitable tissues, their dysfunctions could be associated to various pathological phenotypes affecting almost every human system [1]. Gain-of or loss-of-function mutations in genes encoding ion channels could have either mild or dramatic life-threatening consequences because aberrations could result in the codification of a non-functional protein, could cause incorrect protein folding, could lead to an altered trafficking or could induce modification of ion channel biophysical properties, such as conductance, gating or ionic selectivity. Besides overall rare familial forms, channelopathies are more commonly acquired, therefore ion channel dysregulation could depend on an imbalanced cellular environment that might derive from an altered cellular metabolism, an injury of the involved tissue, the administration of a pharmacological agent or a specific disease state [2]. Furthermore, mutations on gene encoding proteins that control expression, localization and regulation of ion channels could also result in ion channel dysfunctions. Indeed, ion channels are retained on the plasma membrane within a proper cellular membrane microdomain in which a macromolecular signaling complex of ion channel and auxiliary proteins ensure a rapid response to specific stimuli [3].

Among their different applications, the recent progresses of DNA sequencing technologies considerably improved diagnosis of channelopathies, moreover genetic tests could now sometimes allow

the detection of pre-symptomatic individuals carrying genetic variants [4]. Considering channelopathies, it is not infrequent that different pathological phenotypes could result from different mutations on the same gene and also the opposite situation could happen, thus mutations on different genes could cause a single pathological phenotype. In this second case, it is possible to use Sanger sequencing, the “first generation” of sequencing techniques, to identify and validate mutations found in various patients affected by the same disease and then create panel of genes exploitable through Next-Generation Sequencing (NGS) diagnostic protocols. NGS ensures the possibility to test many genes in a relatively short time. Novel identified variants are accepted only whether confirmed by Sanger sequencing [4]. The possibility to identify genetic alterations in more than one gene it is not unusual: beside mutations in the causative gene, the phenotype of a disease could be worsen or ameliorated by mutations in genes acting as modifying factors. NGS is continuously improving but, despite costs associated with genome-scale sequencing are progressively falling, these techniques are still very expensive. Furthermore obtained data need long analysis times and their translation into diagnostic information often requires further validation through functional assays [5].

Nevertheless the identification of new genetic variants could be the first step in the study of an aberrant protein in a patient affected by a channelopathy. Once the mutated gene is identified, it is possible to electrophysiologically characterize the effect of the mutant protein in order to evaluate its functional consequences in terms of ion channel

biophysical properties, such as ion selectivity, conductance, activation/inactivation and voltage-dependency. Biomolecular studies could explain an eventual defective protein trafficking or an altered plasma membrane expression of the aberrant ion channel.

Genetic and functional studies are aimed to identify the most appropriate therapy to each patient, showing how basic science could translate to clinical strategies. The idea of “personalized medicine” was introduced in the 1990s by the pharmaceutical company Roche and it refers to the possibility that the best therapeutic strategy for each patient should be individualized, thus chosen considering not only the disease of the patient but also his/her genetic background. Indeed the effects of one specific drug could be various based on genetic differences, ranging from high effectiveness to ineffectiveness. The first concept of “personalized medicine” has now been extended to “P4 medicine”: personalized, predictive, preventive and participatory. Predictive medicine refers to the evaluation of the patient's risk to develop a disease or complications, therefore therapeutic approach should avoid disease appearance, progression or both. Preventive medicine is the idea of a proactive strategy based on the overall state of health and well-being. Finally participative medicine tends to involve the patient in the therapeutic strategy, allowing the patient to take informed decisions and be responsible for his/her own health [6].

In order to guarantee a personalized therapy for those patients affected by a channelopathy, novel drug target are now in evaluation and novel molecules are currently under development. The use of human cell-

based approaches, such as primary cell culture derived from patients' biopsies, are an interesting opportunity not only to better understand the disease but also to design tailored therapies. Unfortunately biopsies are poorly available but somatic cells of a patient could be reprogrammed into induced pluripotent stem cells (iPSCs) and used for *in vitro* studies aimed to pharmaceutically characterize mutant ion channels in order to predict *in vivo* drug responses [7]. Some pharmacological agents could not only influence expression or functions of the aberrant ion channel causing the channelopathy but also have multiple unwanted unspecific effects. The more the drugs are specific against the mutant ion channel, the less side effects arise. Notably, RNA interference technology may represent a novel therapeutic strategy [8].

In conclusion, a molecular and biophysical characterization of ion channels encoded by mutant gene identified in patients affected by channelopathies is a useful strategy to achieve the best possible understanding of the pathological mechanisms of the disease and to suggest the better therapeutic approach.

References.

- [1] Kim J.B., Channelopathies. *Korean J Pediatr.* 2014 Jan;57(1):1-18.
- [2] Curran J. et al., Alternative Paradigms for Ion Channelopathies: Disorders of Ion Channel Membrane Trafficking and Posttranslational Modification. *Annu Rev Physiol.* 2015;77:505-24.
- [3] Kline C.F. et al., Defective interactions of protein partner with ion channels and transporters as alternative mechanisms of membrane channelopathies. *Biochim Biophys Acta.* 2014 Feb;1838(2):723-30.
- [4] Morini E. et al., Application of Next Generation Sequencing for personalized medicine for sudden cardiac death. *Front Genet.* 2015 Mar 2;6:55.
- [5] Pellacani S. et al., The Revolution in Migraine Genetics: From Aching Channels Disorders to a Next-Generation Medicine. *Front Cell Neurosci.* 2016 Jun 13;10:156.
- [6] Corvol H. et al., Translating the genetics of cystic fibrosis to personalized medicine. *Transl Res.* 2016 Feb;168:40-9.
- [7] Imbrici P. et al., Therapeutic Approaches to Genetic Ion Channelopathies and Perspectives in Drug Discovery. *Front Pharmacol.* 2016 May 10;7:121.
- [8] Ohya S. et al., Recent advances in therapeutic strategies that focus on the regulation of ion channel expression. *Pharmacol Ther.* 2016 Apr;160:11-43.

Publications

- *Bugiardini E, Rivolta I, Binda A, Soriano Caminero A, Cirillo F, Cinti A, Giovannoni R, Botta A, Cardani R, Wicklund MP, Meola G.* SCN4A mutation as modifying factor of Myotonic Dystrophy Type 2 phenotype. *Neuromuscular Disorders* (2015), doi:10.1016/j.nmd.2015.01.006
- *Meraviglia V, Azzimato V, Colussi C, Florio MC, Binda A, Panariti A, Qanud K, Suffredini S, Gennaccaro L, Miragoli M, Barbuti A, Lampe PD, Gaetano C, Pramstaller PP, Capogrossi MC, Recchia FA, Pompilio G, Rivolta I, Rossini A.* Acetylation mediates Cx43 reduction caused by electrical stimulation. *Journal of Molecular and Cellular Cardiology* 87 (2015), doi:10.1016/j.yjmcc.2015.08.001
- *Rivolta I**, *Binda A**, *Villa C, Chisci E, Beghi M, Cornaggia CM, Giovannoni R, Combi R.* Functional characterization of a novel KCNJ2 mutation identified in an Autistic proband. (* equally contributing authors) Submitted to PLOS One.
- *Juang J-MJ, Rivolta I, Lu T-P, Lee S-J, Lai L-C, Su Y-Y, Liu Y-B, Lin L-Y, Chen W-J, Binda A, Yu C-C, Hsiao Y-C, Chiang F-T, Tsai C-T, Yeh S-F S, Lai L-P, Hwang J-J, Chuang E Y, Lin J-L.* A Novel Copy Number Variant of GSTM3 in Patients with Brugada Syndrome. Manuscript in preparation.

- *Binda A, Juang J-MJ Cilibrasi C, Bentivegna A, Rivolta I.*
Functional characterization of a mutation in KCNT1 gene related to non-familial Brugada Syndrome. Manuscript in preparation.